1-1-2013

Characterization and Targeting of Thromboxane Receptor Dimerization: A Gateway to Novel Therapeutic Developments

Alexander Jack Frey
University of Pennsylvania, alex.frey.08@gmail.com

Characterization and Targeting of Thromboxane Receptor Dimerization: A Gateway to Novel Therapeutic Developments

Abstract
Thromboxane A_2 (TXA_2) contributes to cardiovascular disease (CVD) by activating platelets and vascular smooth muscle cell constriction and proliferation. Despite their preclinical efficacy, pharmacological antagonists of the TXA2 receptor (the TP), a G protein-coupled receptor (GPCR), have not been clinically successful, raising interest in novel approaches to modifying TP function. We sought to examine molecular mechanisms underlying auto-upregulation of the TP in response to agonist activation. We first determined a lack of agonist-induced TP mRNA modulation, focusing our attention on post-translational TP regulation. GPCR dimerization contributes to post-translational regulation of receptor expression and function, therefore we characterized how TP forms dimers with itself (homodimerization) or other related receptors (heterodimerization) and defined the relative affinities. To determine how disruption of TP dimerization impacts its regulation and function, we targeted a GxxxGxxxL helical interaction motif, reportedly involved in transmembrane protein-protein interactions between other membrane proteins and GPCRs, that is located in the human TP's (α isoform) 5th transmembrane domain. We determined that disruption of this motif suppressed TP agonist-induced Gq signaling and TPα homodimerization, but not its cell surface expression, ligand affinity or Gq association. Heterodimerization of TPα with the functionally opposing receptor for prostacyclin (the IP) shifts TPα to signal via the IP-Gs cascade contributing to prostacyclin's restraint of TXA2 function. Interestingly, and in contrast to the TPα homodimer, disruption of the TPα-TM5 GxxxGxxxL motif did not modify either TPα-IP heterodimerization or its Gs-cAMP signaling. Our study indicates that distinct regions of the TPα receptor direct its homo- and hetero- dimerization and normal homodimerization appears necessary for efficient TPα-Gq activation. Targeting the TPα-TM5 GxxxGxxxL domain may allow development of biased TPα- homodimer antagonists that avoid suppression of TPα-IP heterodimer's predicted beneficial "IP-like" effects. Such novel therapeutics may prove superior in CVD compared to non-selective suppression of all TP functions with TXA2 biosynthesis inhibitors or traditional TP antagonists.

Degree Type
Dissertation

Degree Name
Doctor of Philosophy (PhD)

Graduate Group
Pharmacology

First Advisor
Emer M. Smyth

Keywords
dimerization, GGL motif, GPCR, thromboxane, thromboxane receptor

CHARACTERIZATION AND TARGETING OF THROMBOXANE RECEPTOR DIMERIZATION: A GATEWAY TO NOVEL THERAPEUTIC DEVELOPMENTS

Alexander Frey

A DISSERTATION

in

Pharmacology

Presented to the Faculties of the University of Pennsylvania

in

Partial Fulfillment of the Requirements for the

Degree of Doctor of Philosophy

2013

Supervisor of Dissertation

_____

Emer M. Smyth, Associate Research Professor of Pharmacology

Graduate Group Chairperson

_____

Julie Blendy, Professor of Pharmacology

Dissertation Committee

David R. Manning, Professor of Pharmacology, Committee Chair

Lawrence F. Brass, Professor of Medicine

Tilo Grosser, Research Assistant Professor of Pharmacology

Donna Woulfe, Assistant Professor of Pharmacology

CHARACTERIZATION AND TARGETING OF THROMBOXANE RECEPTOR DIMERIZATION: A GATEWAY TO NOVEL THERAPEUTIC DEVELOPMENTS

This work is dedicated to every person; friend, family, colleague, and acquaintance, who has touched my life and guided me to this place I find myself today. I would not be who I am, and this work would likely not exist, without those who helped me along the way.

ACKNOWLEDGMENTS

Thanks go out to Emer Smyth for being an amazing advisor and mentor even beyond what expectations I had upon arriving here at Penn. For my having been your first graduate student, it seems that it came naturally to you how to strike the ideal balance between knowing when to answer my questions and when to tell me to go find it myself, and how to keep encouraging me through it all – even the really tough parts.

Thanks go out to all the members of the Smyth Lab, past and present. Mazell for being so welcoming to a chemist joining a microbiology lab; Nune and Salam for not only helping me when I needed it, but being great role models of experienced scientists; Ed for being a great friend and labmate and walking along this graduate school road alongside me; and Vicky for always being there to help keep the lab moving but, more importantly, to always be so ready with a laugh and a smile. And thanks to the numerous members of the FitzGerald lab, for providing so much support over the years, which I couldn't hope to expound upon in such a small space here. And thanks to Garrett FitzGerald as well, for your guidance and contributions to my work.

Thanks go out to my thesis committee, for finding the right balance between guidance and challenge that allowed me to stay on track while still giving me room to grow as a scientist.

Thanks go out to the faculty of the Pharmacology Graduate Group, from whom I've learned so much during my years here at Penn, especially Vlad Muzykantov and Julie Blendy for their efforts as chairpersons of the graduate, and Dave Manning and Randy Pittman for all the work they've done to ensure that early-year students have the guidance they need to succeed.

Thanks go out to the pharmacology graduate students, especially the rest of the entering class of 2007. Gabe, Mike, Trisha, Rob, Graham, Bobby, and Obe, the times we shared as both friends and students have been invaluable to me.

Thanks go out to my family, for the time and effort they put into raising me to be the best that I could be, and the support that I've garnered from the love you show me. I know that without the freedom you granted me to grow and find my own way in life I couldn't have come to this amazing point.

And thanks go out to my amazing fiancé, Dustin Utt, for not only keeping me sane and smiling through all of this, but for managing to put up with everything and providing encouragement when I needed it most.

ABSTRACT

CHARACTERIZATION AND TARGETING OF THROMBOXANE RECEPTOR DIMERIZATION: A GATEWAY TO NOVEL THERAPEUTIC DEVELOPMENTS

Alexander J. Frey

Emer M. Smyth

Thromboxane A_2 (TXA_2) contributes to cardiovascular disease (CVD) by activating platelets and vascular smooth muscle cell constriction and proliferation. Despite their preclinical efficacy, pharmacological antagonists of the TXA_2 receptor (the TP), a G protein-coupled receptor (GPCR), have not been clinically successful, raising interest in novel approaches to modifying TP function. We sought to examine molecular mechanisms underlying auto-upregulation of the TP in response to agonist activation. We first determined a lack of agonist-induced TP mRNA modulation, focusing our attention on post-translational TP regulation. GPCR dimerization contributes to post-translational regulation of receptor expression and function, therefore we characterized how TP forms dimers with itself (homodimerization) or other related receptors (heterodimerization) and defined the relative affinities. To determine how disruption of TP dimerization impacts its regulation and function, we targeted a GxxxGxxxL helical interaction motif, reportedly involved in transmembrane protein-protein interactions between other membrane proteins and GPCRs, that is located in the human TP's (α isoform) 5^{th} transmembrane domain. We

determined that disruption of this motif suppressed TP agonist-induced Gq signaling and TPα homodimerization, but not its cell surface expression, ligand affinity or Gq association. Heterodimerization of TPα with the functionally opposing receptor for prostacyclin (the IP) shifts TPα to signal via the IP-Gs cascade contributing to prostacyclin's restraint of TXA_2 function. Interestingly, and in contrast to the TPα homodimer, disruption of the TPα-TM5 GxxxGxxxL motif did not modify either TPα-IP heterodimerization or its Gs-cAMP signaling. Our study indicates that distinct regions of the TPα receptor direct its homo- and hetero- dimerization and normal homodimerization appears necessary for efficient TPα-Gq activation. Targeting the TPα-TM5 GxxxGxxxL domain may allow development of biased TPα- homodimer antagonists that avoid suppression of TPα-IP heterodimer's predicted beneficial "IP-like" effects. Such novel therapeutics may prove superior in CVD compared to non-selective suppression of all TP functions with TXA_2 biosynthesis inhibitors or traditional TP antagonists.

TABLE OF CONTENTS

LIST OF TABLES

LIST OF FIGURES

Chapter 1: INTRODUCTION

Thromboxane A_2 biosynthesis

Thromboxane (TxA_2) is generated by thromboxane synthase (TS) metabolism of prostaglandin H_2, the immediate product of cyclooxygenase (COX) action on arachidonic acid (1–3). It has a half-life of about 30s prior to non-enzymatic degradation into the inactive thromboxane B_2 metabolite (4). Platelet COX-1, the only COX isoform expressed in mature platelets, is the dominant source of TxA_2 synthesis under normal conditions (5). Other cells, including macrophages and monocytes, contribute to TxA_2 generation via both COX-1 and COX-2 with the latter isozyme being particularly relevant during inflammation (2, 6). COX and TS also act on 5,8,11,14,17-eicosapentaenoic acid (EPA) to form TxA_3, a less potent relative of TxA_2 believed to play a role in the cardioprotective effects of n-3 polyunsaturated fatty acids consumption, most frequently found in fish oils.

Physiological and pathophysiological actions of thromboxane A_2

Actions in the vasculature

TxA_2 acts as a local autocrine or paracrine mediator to mediate a range of physiological and pathophysiological responses that include platelet activation, vasoconstriction, and smooth muscle cell proliferation (3, 7–11). TxA_2 acts in a paracrine manner activating adjacent platelets to generate more TxA_2 and amplify the action of other, more potent, platelet agonists (12, 13). These

processes are of particular relevance to cardiovascular disease (CVD) in which TXA_2 generation is markedly elevated and expression of its receptor, the TP, is increased (14–16). In humans inhibition of platelet COX-1 with low-dose aspirin is widely used for prevention of heart attack and stroke (17–20), while in mouse models of atherogenesis and injury-induced vascular proliferation or remodeling, disease severity was blunted by antagonism or deletion of the TP (8, 21, 22). Interestingly, in hyperlipidemic mice TP antagonist was more effective in reducing atherogenesis that COX inhibition (23). This may reflect antagonism of COX-independent TP ligands, such as the isoprostanes, free-radical derived metabolites of arachidonic acid that can activate the TP *in vivo* (24). These and other studies have placed significant emphasis on the TP as a therapeutic target in CVD(8, 12, 23). Despite their potential, however, pharmacological antagonists of the TP have been clinically disappointing compared to low-dose aspirin, in large part because none replicate aspirin's irreversible inhibitory effect on platelets (12, 25–27).

Actions in the nervous system

Within the central nervous system, TxA_2 acts to promote proliferation and survival of oligodendricytes (28) as well as increased secretion of interleukin 6 (29) and peripheral adrenal catecholamine (30). It is also involved in astrogliosis in astrocytes and astrocytoma cells (31) as well as the dipsogenic response to angiotensin II (32). In the peripheral nervous system, TxA_2 can elicit pulmonary and cardiovascular reflexes via stimulation of peripheral sensory neurons (33–

35) and has been implicated in transduction of allergic itching responses in a murine model (36).

Other actions

In the kidney, TxA_2 acts on mesangial cells to cause cell contraction and proliferation (37, 38), modulate cellular ion fluxes (39), and has been implicated in the progression of nephritis and nephrotic disease (40, 41). Within the immune system, TxA_2 stimulates apoptosis and DNA fragmentation of $CD4^+/CD8^+$ cells (42) and modulates acquired immunity through various effects upon native T cells (43). Additionally, studies report a role for TxA_2 in inflammation in the lung (44), heart (45), and liver (46), and in the pathophysiological development of asthma, rhinitis, and atopic dermatitis (47–49). During carcinogenesis, TxA_2 may contribute to angiotensin II-induced neovascularization (50) and to metastasis (11).

The thromboxane receptor

Structure

The TP is a class A cell-surface G protein-coupled receptor (GPCR) exhibiting the typical seven-transmembrane domain structure characteristic of this class of receptors (Figure 1). In humans, but not in other species, there are two splice variants, the TPα and TPβ, which differ structurally only in their C termini. As ligand binding domains for the receptor are considered to be located on extracellular loops or transmembrane sites near the extracellular domain, the two

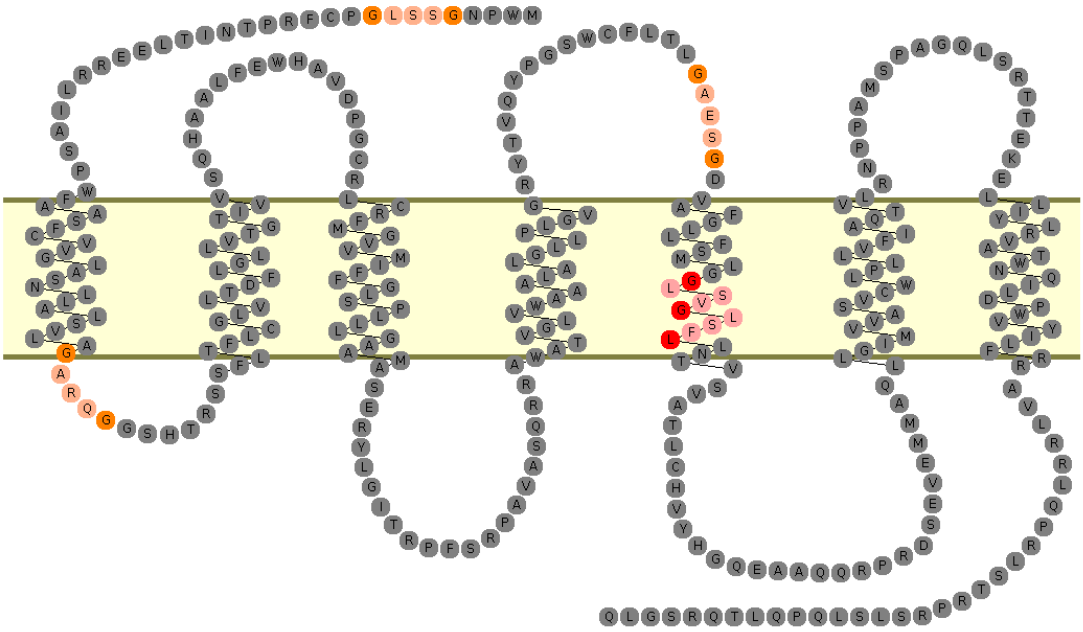

Figure 1: Snake plot of the human TPα. GxxxG motifs in the N terminal, first intracellular second extracellular domains are indicated in orange. The TM5 GxxxGxxxL motif under investigation in the second section of this work our study is highlighted in red.

isoforms are thought to have identical ligand binding sites, an assumption that is supported experimentally (51).

Transcription of the α and ß TP variants is modulated by different upstream promoters (52, 53) and the isoforms both maintain differences in some of their post-translational modifications, interacting proteins, and agonist-induced regulation (54–59). In transfected CHO cells, for example, stimulation of cells expressing TPα led to an increase in cAMP levels, while similar activation of TPβ-transfected cells cause a decrease in cAMP, suggesting a preference for coupling with G_s and G_i, respectively; however, both receptor isoforms responded similarly to agonist in terms of inositol phosphate generation (56). In another study, activation of either TPα or TPβ led to ERK1/2 phosphorylation. For TPα-expressing cells, this action was inhibited by H89, an inhibitor of protein kinase A, whereas for TPβ-expressing cells it was abrogated through overexpression of p115-RGS, which has an inhibitory action towards $G_{12/13}$ (55). These and other examples suggest that the unique C-termini of each isoform may provide differential preferences of G protein association.

Despite these differences, studies have not established significant physiological or pathophysiological divergence between the two TP isoforms (12). As Smyth notes, however, the fact that only humans express both TP isoforms should be a principal consideration in the analysis of *in vivo* studies of the receptor in model organisms that lack TPβ (12). There is evidence for an anti-angiogenic role for TxA_2 via TPβ in the vasculature (60–62); at the same time, other studies have

shown that TxA_2 is a positive regulator of blood vessel growth, particularly in tumors, in murine models using SQ 29,548 to inhibit TP activation (11, 63).

Signaling

The TP is expressed in a wide variety of tissues and cells including platelets, smooth muscle cells, endothelial cells, lungs, kidneys, heart, thymus, and spleen (64–66). A number of tissues appear to express both splice variants (67, 68) although TPα is the only isoform expressed in platelets (69). This thesis work focused on the TP α isoform. Thus, unless otherwise noted, references made in this thesis to "TP" refer to TPα. Research from our group and others has defined the TP's functional and regulatory pathways (51, 54, 69–72) (Figure 2). Signaling via the TP can be transduced through multiple G protein pathways, including G_q, G_{11}, $G_{12/13}$, G_{15}, G_{16}, G_i, G_s and G_h (51), though some of these associations have only been reported in isolated studies.

The two signaling pathways that appear most relevant to the biological actions of TP are G_q and $G_{12/13}$ (73), which stimulate the phospholipase-C pathway of inositol phosphate/intracellular calcium elevation and RhoA activation, respectively (74). TP-mediated signaling via G_q causes activation of phospholiase C (75) and, through phosphoinositide hydrolysis, generation of 1,4,5-trisphosphate (IP_3) and diacylglycerol (DAG), thereby mobilizing intracellular Ca^{2+} and activating protein kinase C (PKC)(76–78). Signal transduction via $G_{12/13}$ follows the activation of RhoGEF (79) and the associated

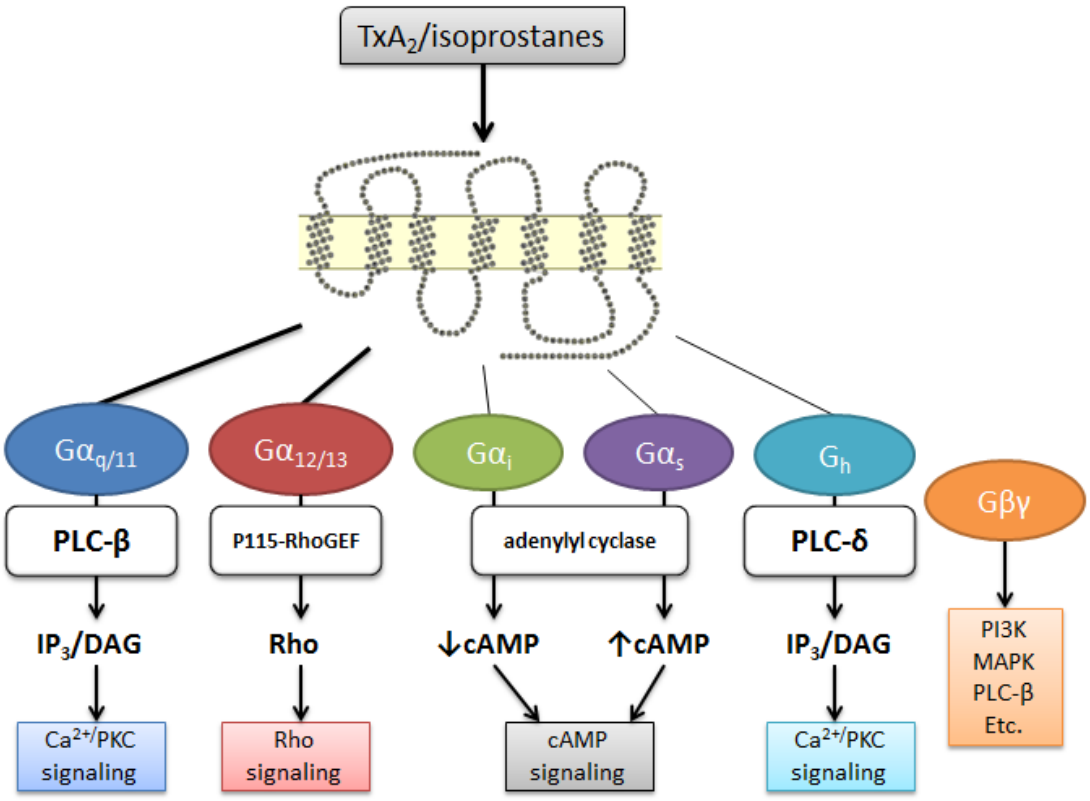

Figure 2: Summary of the reported major and minor signaling pathways of TP activation. TP primarily acts through activation of $G\alpha_{q/11}$ and $G\alpha_{12/13}$, with additional signaling having been reported through activation of $G\alpha_s$, $G\alpha_i$, and G_h. Downstream effectors vary based on tissue or cells of interest. Additionally, dissociation of the Gβγ subunit can lead to concurrent activation of other signaling pathways.

Rho signaling cascade, modulating such responses as regulation of the actin cytoskeleton, cytokinesis, cell motility, contraction, cell proliferation, apoptosis, thymic cellularity, Na^+/H^+ exchanger and myosin light chain kinase (51).

These systems both appear to contribute to platelet function - $G_{12/13}$-mediated stimulation of RhoA signaling induces myosin light chain phosphorylation leading to platelet shape change, with subsequent activation of G_q-PLCβ signaling causing aggregation (80). In mice, platelets lacking G_q or G_{13} are completely unresponsive to TxA_2, showing that G_q and G_{13} are required for platelet activation (74). It is also interesting to note that low concentrations of the TP agonist U46619 are sufficient to cause platelet shape change, while high concentrations are necessary to induce aggregation (81).

In addition to signaling through Gα subunits, studies have reported Gβγ-mediated activation of phosphatidylinositol 3-kinase (PI3K), phospholipase C-β2 and p44/42 mitogen-activated protein kinase (p44/42 MAPK)/extracellular signal-regulated kinase 1/2 (ERK1/2), though the precise role in TP function and biology has not been clearly defined (73, 82).

Regulation: Desensitization

The TP undergoes both homologous (following its own activation) and heterologous (following activation of another receptor) desensitization (58, 83–86) via phosphorylation of residues in the C-terminus. Here distinctions between the unique C-termini of the two TP isoforms have been reported. For the TPα

isoform, Ser^{329} is a phosphorylation site for protein kinase A (PKA) activated by cAMP, allowing heterologous desensitization by G_s-coupled receptors like the prostacyclin receptor (86). Ser^{331} is a target for protein kinase G (PKG)/cGMP-mediated desensitization, and Thr^{337} is a site for protein kinase C (PKC) phosphorylation (51).

The TPß, on the other hand, undergoes phosphorylation at Thr^{299} and Ser^{145} by PKC (87), and at Ser^{357} (in tandem with Ser^{239}) by G protein-coupled receptor kinase (predominantly GRK2; lesser effects seen with GRK3, GRK5, or GRK6) (88). GRK-mediated phosphorylation leads to recruitment of β-arrestin and subsequent decoupling of G proteins from the receptor followed by internalization (89). Arrestin-mediated internalization has been implicated in regulation of the TPß contributing to lower basal surface expression levels of the receptor (54), and its more ready internalization, compared to TPα, following activation (88).

Of noteworthy relevance to the discussion of TP is an autoupregulation system downstream of TP activation. Work by Wilson et al. uncovered a reactive oxygen species (ROS)-dependent mechanism through which stimulation of the TP leads to activation of NADPH oxidase, in turn leading to increased TP protein stability in early biogenesis and, ultimately, increased receptor expression at the cell surface (70). Though the mechanism underlying this pathway is as yet ill-defined, exogenous ROS can also increase in TP protein stability and expression, which may be particularly relevant in cardiovascular disease where ROS levels are elevated (12).

Regulation: Intracellular trafficking

As previously noted, TPα has been seen to be generally expressed at higher levels at the cell surface compared to TPβ, at least in the transfected cell models found in the literature, likely because the latter binds to protosomal subunit α7 and proteasome activator PA28γ through the unique TPβ the C-terminal domain, leading to TPβ degradation by PA28γ-dependent protease activity (90). TPβ endocytosis also occurs in a Rac-1-dependent manner through interaction with Nm23-H2 (91), a process that requires interaction with the actin cytoskeleton (92). TPβ that has been thus internalized may be recycled to the cell surface through an interaction with Rab11 and the its GTPase-positive recycling endosome (57, 93). Studies disagree on whether or not TPα is internalized suggesting that internalization of TPα may cell- or context- specific (88, 94). Successful trafficking to the TP to the cell surface appears to be strictly dependent on glycosylation of Asn^{4} and Asn^{16} at the N-terminus, a process common to both isoforms. Treatment of TPα and TPβ with tunicamycin (a specific inhibitor of N-linked glycosylation) significantly reduced the binding of SQ 29,548, a TP antagonist, in both isolated cell membranes (95) and whole stably receptor-expressing cells (96). Further, targeted mutation of either of these sites resulted in a reduction by half of the B_{max} for SQ 29,548 binding, while mutation of both lead to near-complete retention of the receptor within the endoplasmic reticulum and failure to couple with G proteins (71).

Interplay between thromboxane and prostacyclin and their receptors

The actions of TxA_2 are generally opposed by prostacyclin (PGI_2), another short-lived prostanoid that is generated from arachidonic acid predominantly through COX-2 and prostacyclin synthase in the vascular endothelium (97). Acting though the prostacyclin receptor (IP), PGI_2 inhibits platelet activation, reduces vascular proliferation, and causes vasodilation (98). The IP is coupled to G_s, thus activation leads to increased intracellular cyclic AMP generation. Mice lacking the IP display heightened thrombotic responses (99) and accelerated development of atherosclerosis (8). A critical function of the IP is to restrain TP function – mice that lack the IP show increased platelet and proliferative responses to vascular injury *in vivo* with the opposite phenotype in TP deficient mice and normalization of both phenotypes in double receptor knock out animals (21). With their opposing roles, the interplay between TxA_2 and PGI_2 is an important component of cardiovascular function and disease and is particularly relevant in later parts of this work.

G protein-Coupled Receptor Dimerization

Substantial evidence has emerged in the field of GPCR research that these seven-transmembrane proteins do not function only as monomeric receptors in physiological systems, but rather as dimeric, and possibly oligomeric, units (100–103). Receptor dimerization appears necessary for normal physiological signaling of some receptors (104, 105) and dimeric forms of GCPRs have

become a novel target for therapeutic research, with the goal of modifying dimerization through the use of small molecules. Both homodimer and heterodimer formation has been noted for a variety of GPCRs. For the $GABA_B$ receptor, dimerization has been described as “obligatory”, with the pairing necessary for proper biogenesis and receptor function (106, 107). In comparison, dimer formation does not appear essential for other receptors, like the dopamine receptor, but does modulate the receptor’s signaling response to agonist (108, 109). In addition, “‘non-obligatory’ GPCR heterodimer” formation has been noted for a number of GPCRs (100), including the TPα (see below) with significant changes in downstream signaling of a given receptor when it forms a heterodimer as compared to its homodimer (110, 111).

Dimerization may contribute early in GPRC biosynthesis (112) at certain quality-control checkpoints (100). Homodimerization can occur early in the biosyntetic pathway, most likely in the endoplasmic reticulum (112, 113), and is a prerequisite for receptor trafficking to the cell surface for a number of other GPCRs including the $GABA_B$ receptor (107), α_{1D}- and α_{1B}-adrenoceptors (114), and β2-adrenergic receptor (115). Mutations that cause GCPR retention in the ER/Golgi can act in a dominant-negative manner to block cell surface expression of wild-type receptor (116, 117), as the mutants remain able to dimerize, yet cannot pass through quality control checkpoints to exit the ER and continue through biogenesis to be transported to the cell surface. These studies further support the model that dimerization occurs early in the posttranslational biogenic

pathway, and have raised interest in developing ways to disrupt dimer formation as a novel approach to modifying receptor function. For example, a small molecule that prevents dimerization would also prevent cell surface expression, an alternative approach to antagonism to reduce receptor function. If the target receptor were one involved in disease pathophysiology, such as the TP in CVD, then disease could be prevented or ameliorated.

Across the GPCR superfamily, there is substantial evidence for receptor dimerization (118, 119) and a significant contribution therein to receptor trafficking, ligand recognition, signaling and regulation (100, 102, 115, 120). As mentioned above, previous work in our lab reported that the TP forms dimeric receptor complexes (94, 121–123). In addition to homodimerization, TPα can heterodimerize with TPβ, leading to enhanced isoprostane responsiveness (122). Further, as part of the work outlined in this thesis, we observed equal propensity for TPα to heterodimerize with the receptor for PGI_2, the IP (123). As mentioned above, the PGI_2, a predominantly COX-2-derived mediator, acts via the IP to activate the G_s-adenylyl cyclase signaling pathway causing vasodilation and inhibition of platelet activation (98). In mice, the restraint placed by the PGI_2-IP system on TxA_2-TP function limits the proliferative and platelet response to vascular injury (21) demonstrating the *in vivo* relevance of this interplay. Further, the elevated cardiovascular hazard in patients treated with COX-2 inhibitors can be explained by selective suppression of COX-2-derived PGI_2 without alteration of COX-1-derived TXA_2 levels (124). We determined that heterodimerization of

the TP with the IP contributes to the PGI_2-TXA_2 interplay - dimerization with the IP dramatically shifts TP function from a lipid raft-excluded G_q-coupled receptor to a raft-associated G_s-coupled receptor that yields a robust G_s-cAMP response, concomitant with reduced G_q-inositol phosphate signaling, to TP agonists (121, 123). In effect therefore, the IP can bias the response of TXA_2-TP toward a PGI_2-IP "like" signal predicted as beneficial in CVD. Loss of this shift in TP function in individuals heterozygous for a signaling deficient IP mutant, IP^{R212C}, may contribute to their accelerated CVD (125).

Dimerization motifs as mediators of GPCR pairing

The importance of transmembrane (TM) helical interactions to protein structure and function is evident across multiple diverse integral membrane protein families (126, 127). Consequently, there is significant interest targeting TM domains to modulate the function of membrane-spanning proteins, including GPCRs (107, 118, 120, 128–130). Various studies, include those resolving GPCR crystal structures (131), have shown that dimerization interfaces are predominantly found in the TM domains (132–134).

Among all TM domains, a GxxxG motif, in which two glycines are separated by any three other residues, is strongly over-represented (135), highly conserved across species (136, 137) and can direct homologous or heterologous helical interactions (126, 127, 138). Neighboring residues, especially the large aliphatic residues isoleucine, valine and leucine, appear critical to GxxxG-mediated helix-

helix interactions (136, 137). In a number of proteins (139–142), including at least two GPCRs (104, 115), placement of a leucine three residues after the second glycine, to create a GxxxGxxxL motif, directs protein-protein interaction and function. We identified a GxxxGxxxL motif within the 5th transmembrane of the TPα (Figure 3) and, as part of this thesis research, examined its relevance for TP function.

Current Therapeutics Targeting TXS and TP

Therapeutics that interfere with TP signaling generally act in one of three ways: inhibition of COX-1/2 conversion of arachidonic acid to PGH_2, inhibition of TXS conversion of PGH_2 to TxA_2, or antagonism of the TP itself. Low-dose aspirin which inhibits platelet COX-1-derived TxA_2 is used widely to protection against heart attack and stroke. Although true aspirin resistance is likely extremely rare (143), heterogeneity in the beneficial response and weak benefit in some pathophysiologies (e.g., diabetes, peripheral artery disease (144, 145), as well as possible gender differences (146)) underscore the need for greater mechanistic understanding to advance new therapeutic TXA_2-TP approaches in CVD.

Over the past decade, attempts to use therapeutics that targeted TxA_2 synthase or the TP itself have generally met with limited to no clinical success. Most recently, the selective TP receptor antagonist terutroban showed comparable, but not superior, efficacy as low-dose aspirin in preventing recurrent ischemic stroke in clinical trials (147). Other thromboxane receptor agonists include

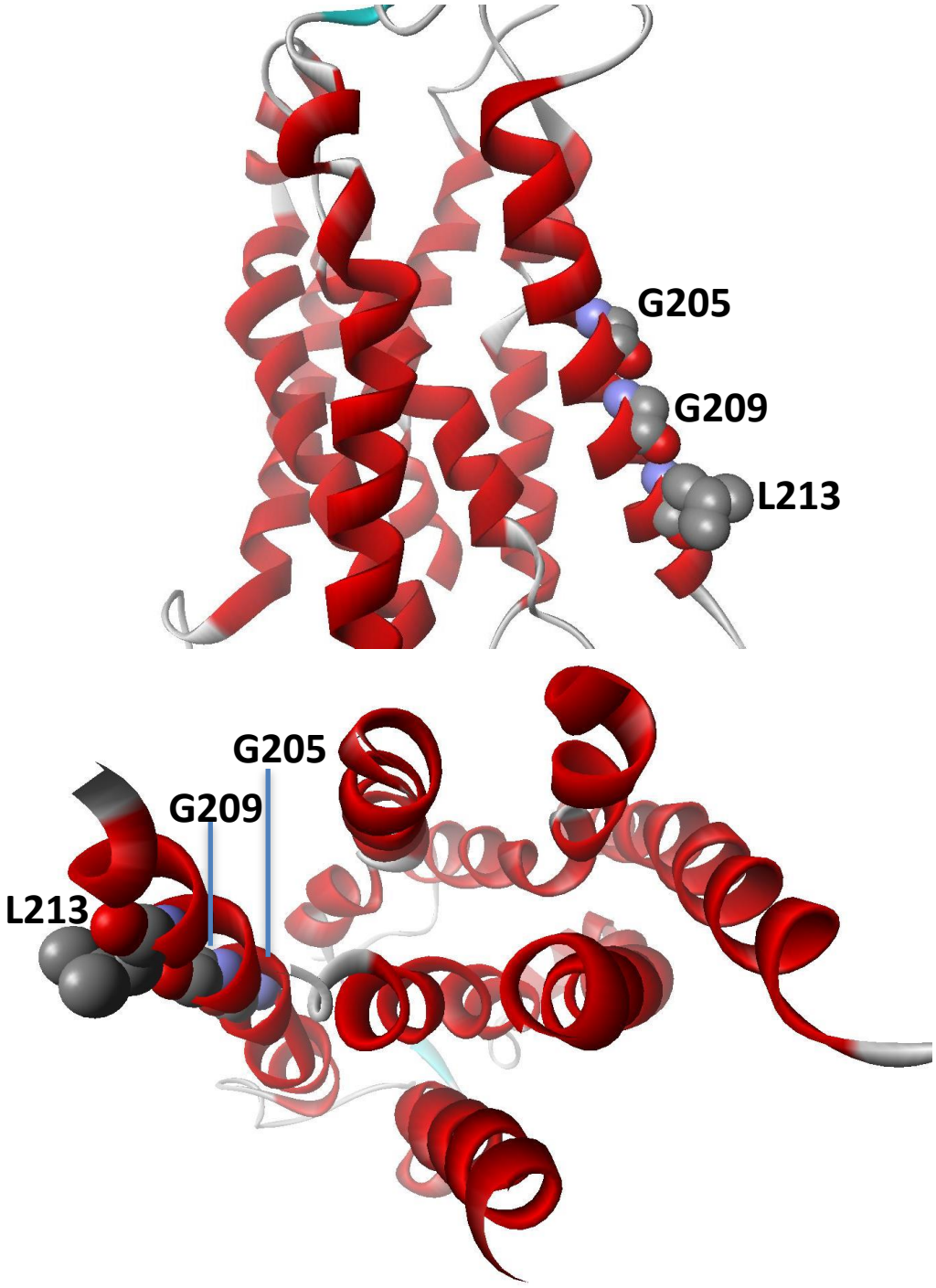

Figure 3: Location and positioning of the GxxxGxxxL motif within the TP. Homology modeling (SWISS-MODEL) of the human TPα based on a 2.8Å crystallographic bovine rhodopsin template. Relative positions of G_{205}, G_{209} and L_{213} are highlighted. Each appeared to face the lipid bi-layer aligned on one side of TM5. (Credit: Scott Gleim/Hwa Lab, Yale University School of Medicine)

ifetroban (148), seratrodast (used for treatment of asthma) (149), and sulotroban (150).

A number of other drugs act as tandem TP antagonists/TxA_2 synthesis inhibitors. Dipyridamole has been shown to be effective in adjunctive therapy with aspirin for secondary prevention following stroke (151). Picotamide is a platelet aggregation inhibitor that has shown antiplatelet efficacy in some studies (152). Ridogrel has been tested for use in helping to treat Crohn's disease and ulcerative colitis, but without promising results (153, 154).

Furegrelate is a potent inhibitor of thromboxane synthase with little effect on other enzymes essential for arachidonate metabolism, and has been investigated for use in treatment of pulmonary arterial hypertension with promising early results in model animals (155). Ozagrel also acts to inhibit synthesis, and has been seen to reduce neurological impairment suffered with stroke, though without improving long-term morbidity or other endpoints (156).

Project aims

While previous work by Wilson established the presence of the ROS-dependent auto-upregulation paradigm, the underlying mechanisms of TP regulation within the cell remained ill-defined. As such, one aim of my thesis work sought to explore the mechanism(s) for the increase in cell surface TP expression in response to activation. One possibility was that stimulation of the receptor was leading to an increase in mRNA levels, thus increasing TP protein levels.

However, quantitative real-time PCR analysis did not strongly support this hypothesis.

In light of emerging evidence for dimerization as a mode of GPCR regulation, I also sought to confirm TP homodimerization, which was apparent in co-immunoprecipitation studies previously performed in the laboratory. Not only was I able to confirm TP homodimerization, I also characterized the relative efficiency of TP interaction with other prostanoid receptors, including the IP and the DP1 receptor for prostaglandin D_2.

The findings from dimerization studies in this first aim, taken together with research in the literature describing the significance of the GxxxGxxxL helical interaction motif, a motif we identified within the TPs 5^{th} TM, led to the development of the second aim. The second aim sought to determine if the GxxxGxxxL motif contributed to TP dimerization and, if so, whether or not targeting of this motif would be a novel therapeutic approach to suppress TP function. We determined that the TP TM5 GxxxGxxxL motif does contribute to TP dimer formation. Further, using mutant forms of the TP, we demonstrated that this motif was selectively involved in TP homodimer formation and signaling but not TP-IP heterodimerization or signaling by the TP-IP heterodimer. These studies provided the first proof-of-principle that the homo- and hetero-dimeric functions of the TP and TP-IP can be discriminated to suppress the CVD-deleterious TP function and preserve the CVD-beneficial TP-IP function.

Targeting of the TP GxxxGxxxL motif with a peptide, which was designed against

a similar transmembrane domain in the αII integrin (128), provided an exciting initial indication of the potential for targeting this region to develop a biased therapeutic directed against the deleterious side of TP signaling. Full analysis of these results and their implications follow.

CHAPTER 2: Materials and Methods

Constructs

Hemagglutinin- (HA) tagged human IP and TPα cloned into the mammalian expression vector pcDNA3 (Invitrogen, CA) were previously created in the lab (123). QuikChange site-directed mutagenesis (Stragagene, CA) was used to replace G_{205} and G_{209} with leucines, a small-to-large replacement that disrupts helix-helix interaction (139, 141, 142). We replaced L_{213} with a tyrosine based on the studies of the GxxxGxxxL motif in the ß2-adrenergic receptor(115). The resulting mutant was termed $TP_{L205,L209,Y213}$. Similar mutations were made at the partial GxxxG motif at the beginning of the first intracellular loop to create the $TP_{L51,L55}$ mutant. See Table 1 for the list of primers designed for mutagenesis. HA-tagged IP, TPα, and $TP_{L205,L209,Y213}$ were fused at their C-termini to either Renilla luciferase (rLuc) or yellow fluorescent protein (YFP), via restriction enzyme cutting and reassembly after purification of DNA segments (157). Briefly, the stop codon was removed by PCR and each stop-less construct cloned into pRLuc-N3(h) (Perkin-Elmer, MA) and pEYFP-N1 (Clontech, CA) plasmids in frame with the fusion protein start site. All sequences were verified by DNA sequencing.

The TP first transmembrane domain (TM1) interacting peptide was created through PCR amplification of the TP sequences between residues R_{23} and T_{59}, containing the entirety of TM1. This amplification product was inserted via

Table 1: Sequences of primers used in the generation of mutants employed in this work. Note that some primers must be used following the introduction of a prior mutation due to overlap in the sequences.

Target Mutation	Primer Sequence
$G_{205}xxxG_{209}xxxL_{213} \rightarrow G_{205}xxxG_{209}xxxY_{213}$	
Sense	5'- CTG TCC TTC TAC CTG AAC ACG GTC -3'
Antisense	5'- GAC AGG AAG ATG GAC TTG TGC CAG -3'
$G_{205}xxxG_{209}xxxY_{213} \rightarrow G_{205}xxxL_{209}xxxY_{213}$	
Sense	5'- CC ATG CTG GGC GGC CTC TCG GTC TTG CTG TCC TTC -3'
Antisense	5'- GAA GGA CAG CAA GAC CGA GAG GCC GCC CAG CAT GG -3'
$G_{205}xxxL_{209}xxxY_{213} \rightarrow L_{205}xxxL_{209}xxxY_{213}$	
Sense	5'- GG CTG CTC TTC TCC ATG CTG GGC CTC CTC TCG GTC -3'
Antisense	5'- GAC CGA GAG GAG GCC CAG CAT GGA GAA GAG CAG CC -3'
$G_{51}xxxG_{55} \rightarrow G_{51}xxxL_{55}$	
Sense	5'- CGC GCG GCA GTT GGG TTC GCA CAC GCG CTC -3'
Antisense	5'- GAG CGC GTG TGC GAA CCC AAC TGC CGC GCG -3'
$G_{51}xxxL_{55} \rightarrow L_{51}xxxL_{55}$	
Sense	5'- CTG AGC GTG CTG GCG CTC GCG CGG CAT TG -3'
Antisense	5'- CAA TGC CGC GCG AGC GCC AGC ACG CTC AG -3'

restriction enzyme digestion and religation, into the pNTAP vector obtained as part of the InterPlay N-terminal Mammalian TAP System (Stratagene, LaJolla, CA) to provide necessary the constitutive cytomegalovirus promoter and SV40/poly-adenosine tail for stability (Figure 4).

Cell culture

HEK 293 and Meg-01 cell lines were from the American Type Tissue Culture Collection (ATTC; Rockville, MD). HEK 293 cells were maintained following established and published protocol in the lab (48); HEK cells were grown in DMEM High Glucose medium (Invitrogen) containing 10% fetal bovine serum, 1% penicillin-strepomycin, 2mM L-glutamine, and 25mM HEPES buffer. Cells were grown in 75 cm^2 surface area flasks and passaged in a 1:4 ratio upon reaching 80-90% confluency by allowing cells to lift in 37°C Hank's Balanced Salt Solution containing 0.02% EDTA prior to collection and redistribution into new plates.

Meg-01 cells were grown in RPMI-1640 (Invitrogen) containing 10% fetal bovine serum and 1% penicillin-strepomycin. Cells were grown in 20 mL of medium in 75 cm^2 surface area flasks. Passaging was performed according to ATTC literature that accompanied the cells, every 2-3 days by scraping the bottom of the flask with a disposable cell scraper and addition of 5 mL of this cell suspension to 15 mL of fresh medium in each new flask.

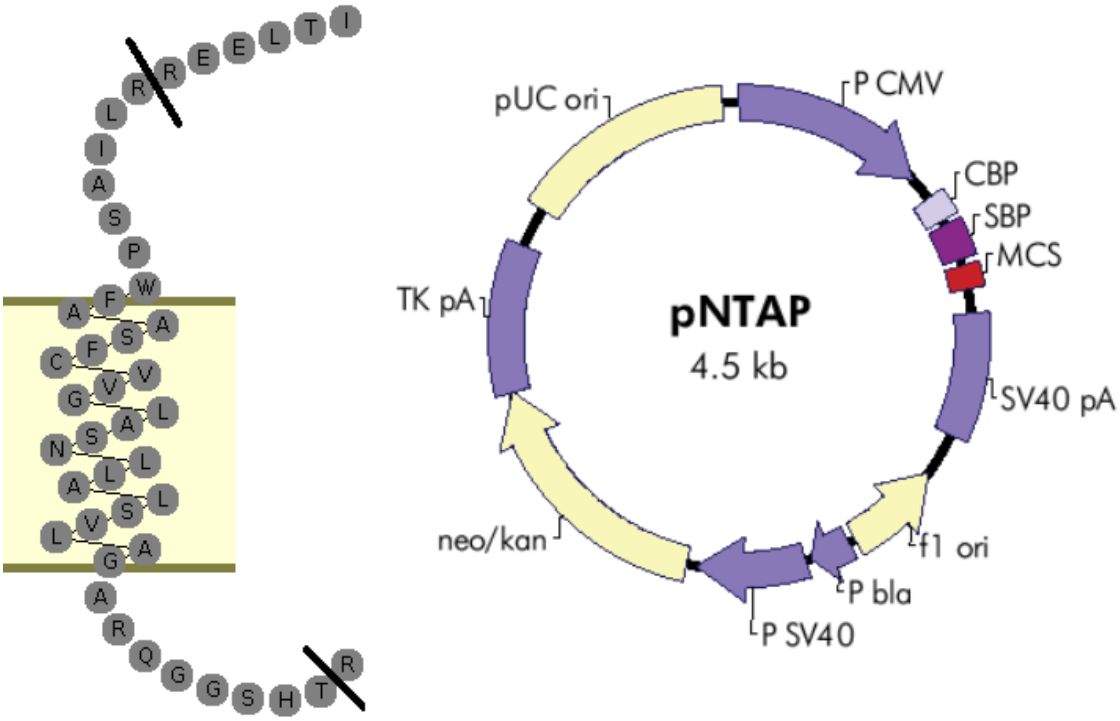

Figure 4: Design of the TP TM1 interacting peptide. Sequence excerpted from the TP sequence for creation of the TP TM1 peptide (A). Excerpted fragment runs from residues R_{23} through T_{59} to ensure inclusion of full TM1 domain. The fragment was inserted into a pNTAP vector (B) for introduction of cytomegalovirus promoter and poly-adenosine stabilization sequence.

Human aortic smooth muscle cells (HuAoSMCs, Biowhittaker Inc., Walkersville, MD) were cultured in smooth muscle cell basal medium supplemented with fetal bovine serum (5%), human recombinant epidermal growth factor (hEGF; 0.5 ng/ml), insulin (5 g/ml), human recombinant fibroblast growth factor (hFGF; 2 ng/ml) plus gentamicin (50 g/ml), and amphotericin-B (50 ng/ml) (all supplies via Lonza, Allendale, NJ). HuAoSMCs of passages 5–9 were used in experiments.

Transient transfection of cell lines

Transient transfections of HEK 293 cells were initially performed using FuGENE 6 (Roche Applied Science, IN) following manufacturer's instructions (123). After discontinuation of FuGENE 6 production, transfections were performed using X-tremeGENE 9 (Roche Applied Science, IN), following manufacturer's instructions. This replacement reagent was created by Roche as an improved form of FuGENE 6 with reduced cytotoxicity and the need for less reagent per transfection. The serum-free medium used in transfections was Opti-MEM medium (Invitrogen). DNA transfected ranged widely, based on the needs of the given experiments, but always following the proscribed DNA:transfection reagent:Opti-MEM medium ratio provided in the literature from the manufacturer. Exact amounts of DNA transfected varied, based on the assay to be performed and quantity of cells needed, and are noted in subsequent sections below. Transient transfections of Meg-01s were performed by nucleofection using an Amaxa Nucleofector™ II and Nucleofector™ Kit C (Lonza, NJ), per the

manufacturer's instructions, introducing a total of 3 µg of DNA to the cells as instructed. The range of DNA quantities used in HEK 293 transfection was not possible given the constraints of the nucleofection system. Experimental design with transfected Meg-01 cells was adjusted based on this constraint, dictating how many duplicate measurements or treatment groups were possible in a given replicate.

In all cases, DNA levels were equalized in all transfections using empty pcDNA3 vector. Assays were performed 48 hours after transfection.

Bioluminescence Resonance Energy Transfer (BRET) assay: original protocol.

Dimerization of rLuc and YFP fused receptors was examined by measuring bioluminescence resonance energy transfer (BRET) from an energy donor (rLuc fused) receptor to an energy acceptor (YFP-fused) receptor following addition of substrate for rLuc (coelenterazine h; Molecular Probes, Life Technologies, NY) (Figure 5). Coelenterazine h was supplied solid, 250 µg, and stored at -20°C. A stock vial, in which the compound was resuspended to a 2.5 mM solution in 200-proof ethanol, was maintained for further dilution into a working solution (50 µM) for the assay.

In BRET saturation experiments, cells were transfected with a fixed amount of rLuc-receptor (0.25µg) together with increasing amounts of YFP receptor (0.125µg to 1.75µg). Experiments in which the two receptors were capable of

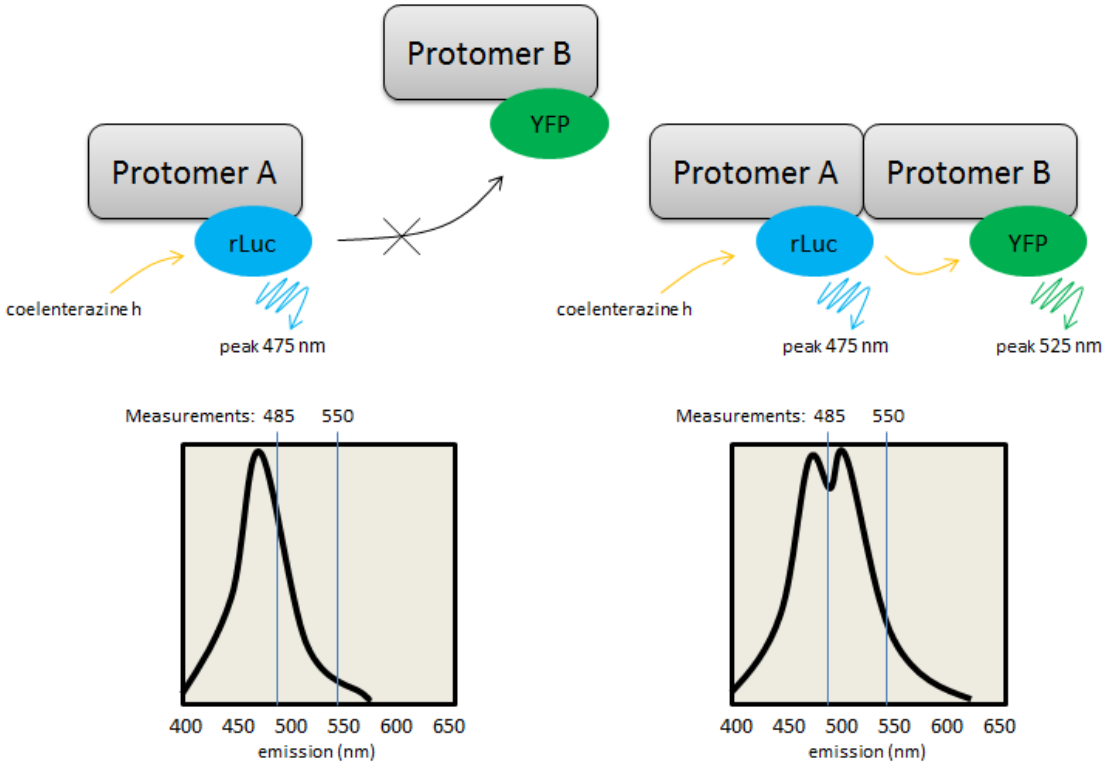

$$\text{BRET (mBu)} = \left(\frac{550nm}{485nm} - \frac{550nm}{485nm}\right) \times 1000$$

transfected sample — untransfected control

Figure 5: Illustrated summary of Bioluminescent Resonance Energy Transformation (BRET) methodology. The underlying mechanism of the BRET assay rests on the short distance between the two protomers (A and B, above) of a dimeric pair, which brings the donor, *Renilla* luciferase (rLuc), and receptor, yellow fluorescent protein (YFP), tags into close proximity. Coelenterazine activates the rLuc enzyme, producing light with a peak emission of 475 nm. When no dimerization occurs (left), the distance between rLuc and YFP is too great to initiate resonance energy transfer, producing a spectrum as shown. However, when the A and B interact closely, such as during dimer formation, then energy emitted by rLuc is transfered to YFP, which emits light at a peak of 525 nm, generating the combined spectrum pictured on the right. Measurement of emissions at 485nm and 550nm (as shown) allows for quantification of BRET, calculated as the ratio of the emission at 550 over the emission at 485 corrected for BRET signal background as calculated from untransfected cells.

dimerization resulted in a characteristic saturation curve (Figure 6A) that allowed for calculation of the $BRET_{50}$ - the level of acceptor receptor YFP-rLuc tagged receptor (expressed as fold over basal total YFP, excited with an external light source; see details below) at which half of the maximal BRET signal was detected.

The $BRET_{50}$ served as a quantitative measurement of affinity for dimerization, with a lower $BRET_{50}$ indicating a higher affinity for dimerization. This allows for comparison of affinities between receptor pairings. Changes in the maximal BRET values may reflect absolute levels of dimer formed. However, the absolute BRET value also can be influenced by the distance and orientation of the donor and acceptor molecules, which are variable based on the molecular arrangement of a particular dimer, rather than simply the number of dimers formed. Similarly, binding of a ligand to either protomer can change the three-dimensional structure of a receptor, potentially changing the distance between the rLuc donor and YFP acceptor molecules and, thus, the absolute BRET values. This possibility is discussed further in the relevant section of the results. Thus, the $BRET_{50}$ is particularly useful as a readout of dimerization affinity that is independent of changes in donor-acceptor distance.

In BRET competition assays, increasing amounts of a competitor receptor (without a donor or acceptor moiety) were co-transfected together with a fixed ratio (1:7) of receptor-rLuc + receptor-YFP (and hence a fixed BRET value). A reduction in BRET signal as the competing receptor levels are increased

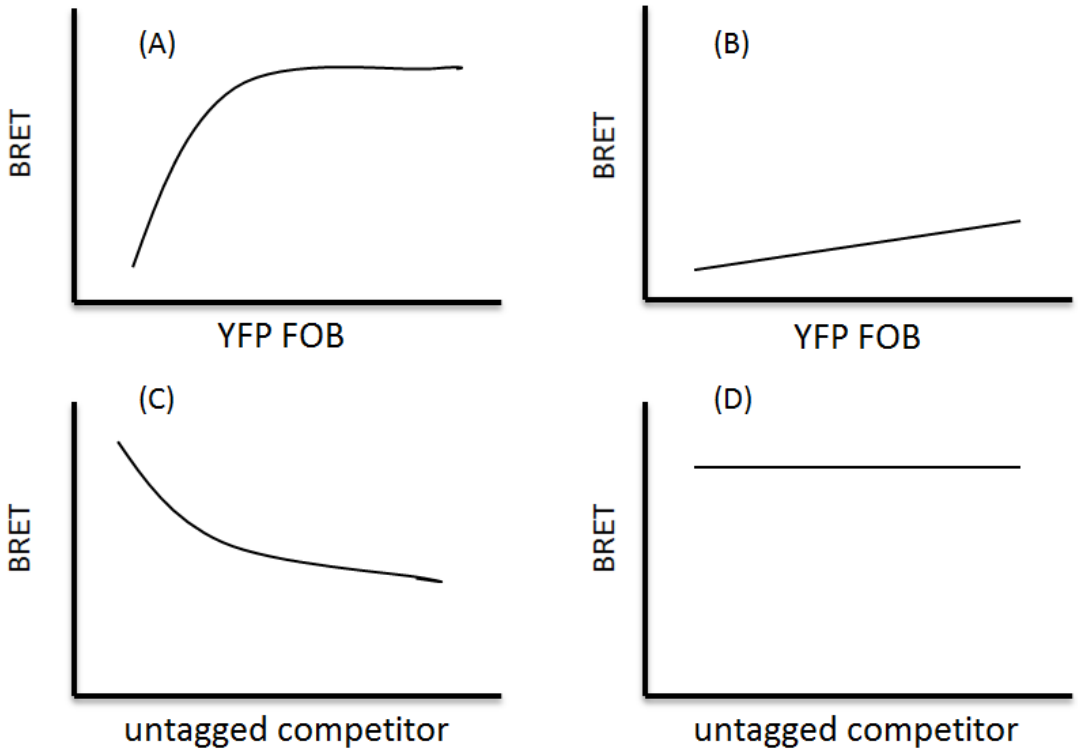

Figure 6: Indicative responses from BRET assays. Simulated responses from the BRET assays. (A) A robust, saturable response seen in the BRET saturation assay in response to increasing concentration of acceptor-tagged receptor indicates a dimerization between the two receptors of interest. (B) A muted, linear response is obtained from BRET occurring through random, proximity-based interactions for non-dimerizing species. (C) Loss of BRET response upon introduction of increasing amounts of non-reporter-tagged receptor is indicative of dimerization between the untagged competitor and at least one of the reporter-tagged receptors while (D) no loss of BRET signal indicates that the untagged receptor lacks sufficient affinity for dimerization with either tagged receptor.

indicates that the competing receptor can interact with either (or both) protomer, allowing an initial characterization of dimerization affinity (Figure 6C). This assay is useful for initial screen of receptor pairings of interest, as it does not require the time-consuming work of stop codon removal generation of donor and acceptor fused proteins.

Initially, BRET measurements were performed following protocols published by Bouvier, et al. (121). Forty eight hours after transient transfection, cells were harvested (phenol red-free Hank's Balanced Salt Solution containing 0.02% EDTA), washed twice with phosphate-buffered saline and resuspended in DPBS containing 5.56 mM glucose (Invitrogen, 14287), then redistributed in two 96-well plates (first: black, clear-bottomed; second: white, opaque-bottomed; 100,000 cells/well) and maintained at 37°C. Total YFP (Ex485nm, Em555nm) was first collected using a luminescence multi-plate reader (VICTOR3, Perkin Elmer) with the black, clear-bottomed plate and acceptor expression calculated as fold over basal. Following this, coelenterazine h (Invitrogen, stock resuspended to 2.50 mM in ethanol for working solution) was diluted to 5μM in phosphate buffered saline containing Ca^{2+} and Mg^{2+}. A fresh solution was made each time, added to all cells in the white plate, and emission from the donor (485nm) and acceptor (555nm) were gathered sequentially from each well across the entire plate. Milli BRET units (mBU) were calculated as the ratio of Em555 over Em485 nm corrected for cells expressing the rLuc receptor alone, and arbitrarily multiplied by 1000.

BRET assay optimization

After several months of using this standard approach, concerns surfaced as to the stability of the BRET signal over the time taken to process a single plate (i.e. from the time of substrate addition to the time of the last BRET reading, typically 20 minutes). A simple experiment was designed to examine signal stability: a single population of HEK 293 cells were transiently transfected with a set ratio (1:7) of rLuc- and YFP-tagged TPα and the established protocol used to establish whether YFP and BRET readings were consistent across both plates. Total YFP values were stable across the black plate; however, the BRET signal was strikingly unstable (Figure 7, Figure 8), with a significant loss of signal. This loss of signal across a homogenous plate raised concerns for interpretation of the BRET assay going forward.

A variety of different experimental adjustments were made in attempts to minimize the loss of BRET signal observed with the original assay protocol: *[1]* the protocol was amended to take a reading of one sample set (6 replicates) from the black total YFP plate followed by one reading from the white BRET plate, alternating so as to more closely align the time of measurement of the two values for a given sample. *[2]* 2-hydroxypropyl-β-cyclodextrin, a ring-shaped compound that increases solubility and stability of compounds in water (158), was added to the coelenterazine solution in an attempt to stabilize the substrate over the time

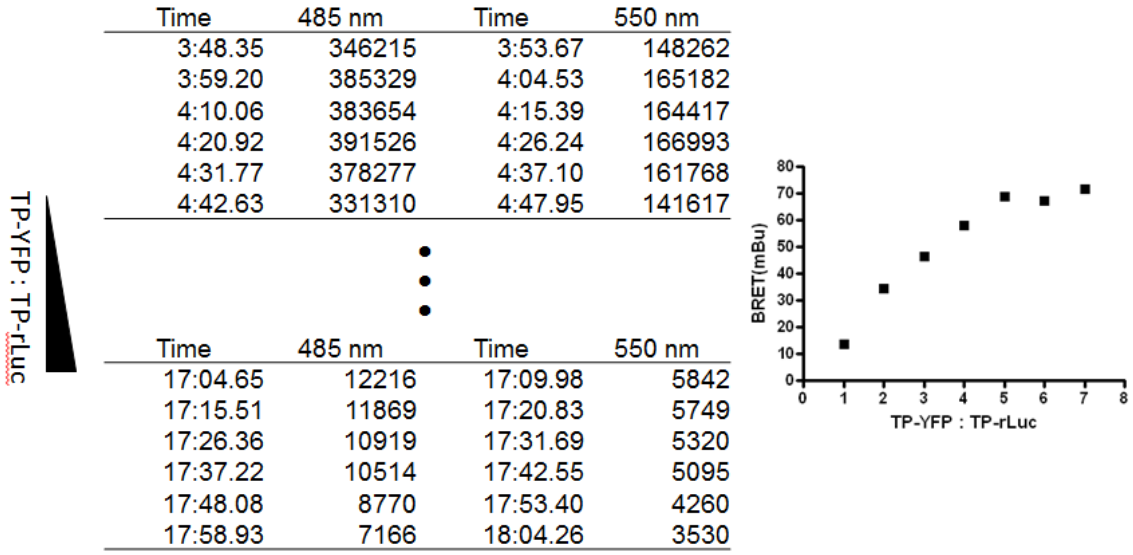

Figure 7: Signal loss inherent in the original BRET methodology. Over the course of the nearly 20 minutes required for sequential measurement of emissions at 485nm and 550nm, a steep drop in the raw values, by approximately two thirds, was noted. This raised significant concerns of increased noise as the signal drops towards the limit of detection.

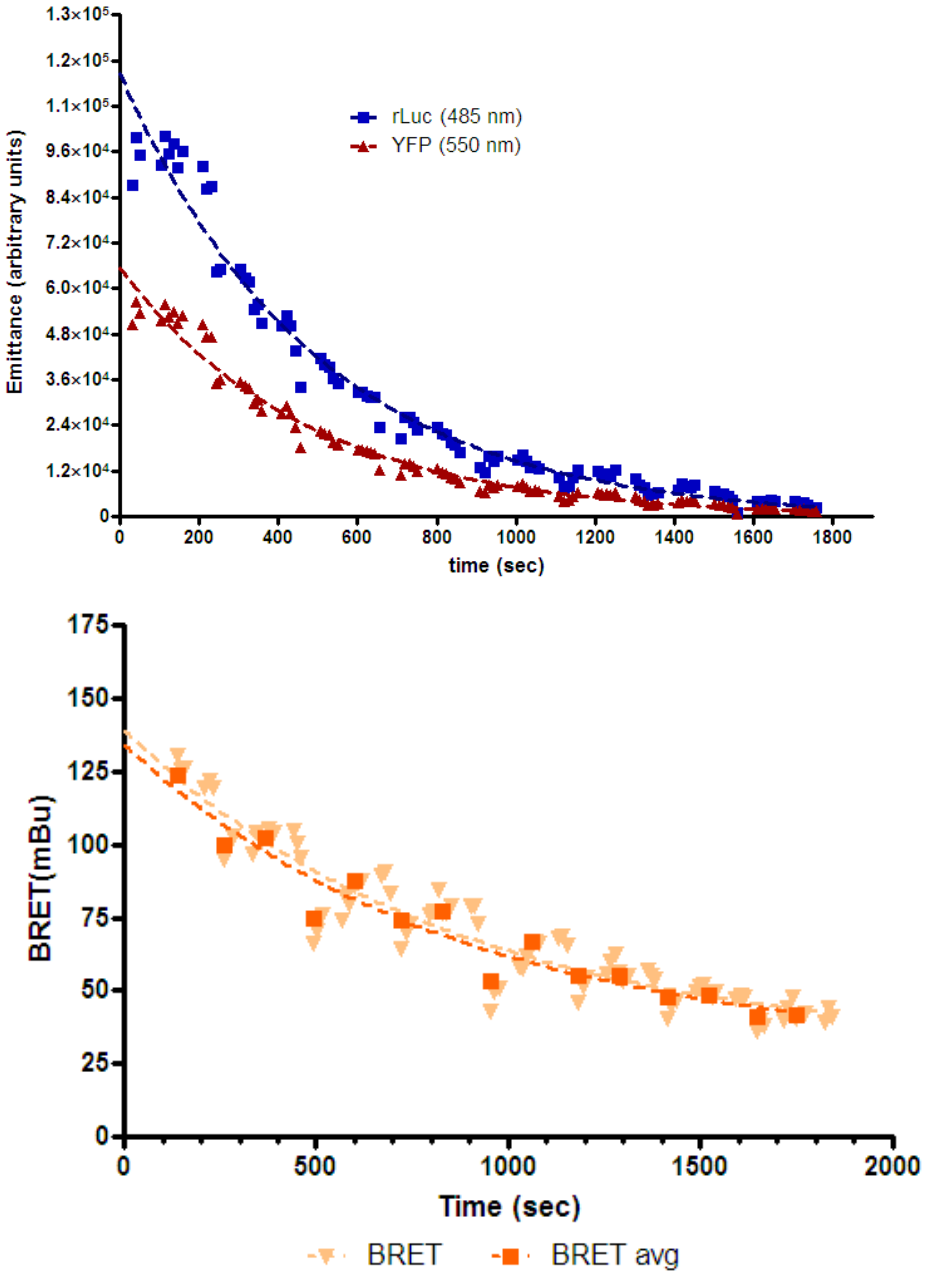

Figure 8: Decay in BRET and component emissions over time. HEK 293 cells were transfected with rLuc- TP_{WT} (donor, 0.25µg) + YFP- TP_{WT} (acceptor, 0.75µg). Two 96-well plates were prepared containing identical samples in each well (except for the control rLuc alone cells), and assayed following the original BRET protocol: coelenterazine was diluted to 50 µM in PBS containing Ca^{2+} immediately prior to distribution into all 96 wells, with the full plate (white opaque bottom) read at one sitting. Total.YFP emission was measured separately in the second plate (black, clear bottom). A representative experiment is shown. Emission at both 485nm and 550nm decreased over a full order of magnitude (top), while BRET values decayed from 125 mBu to 50 mBu (bottom).

taken to perform the readings. Neither adjustment improved the signal stability across a homogenous set of plates.

A search of data sheets and technical literature for coelenterazine h as a substrate for *Renilla* luciferase revealed (159) that coelenterazine undergoes a predictable deterioration upon introduction to aqueous solution with a 40-50% loss of functional capacity over the first 20 minutes. After this period has passed, however, the solution maintains a mostly linear functional response over the next four hours (Figure 9). Additionally, this decay appears to be caused in part by the presence of calcium cations in solution. Based on this information, the BRET assay was modified to include *[3]* a 20-minute waiting period at room temperature after addition of the coelenterazine into Ca^{2+}-free phosphate buffered saline before addition to the wells.

Because of the time taken from the first addition of colenterazine to the final reading of the 96^{th} well (20 min), loss of signal due simply to substrate catabolism by rLuc was a further issue. One approach to addressing this issue was imaging of the whole plate at one time through use of an IVIS imaging system. Luciferase and YFP activity was captured for the plate as a whole, and binning (manually overlaying a 96-square grid onto the image produced by the IVIS so as to allow quantitation of activity by well) was employed to measure the YFP and BRET signals given off by samples. This proved significantly less sensitive that the Victor multiwell plate reader. However, a significant observation was made in the course of the imaging trials: the white, opaque plate used in the BRET assay

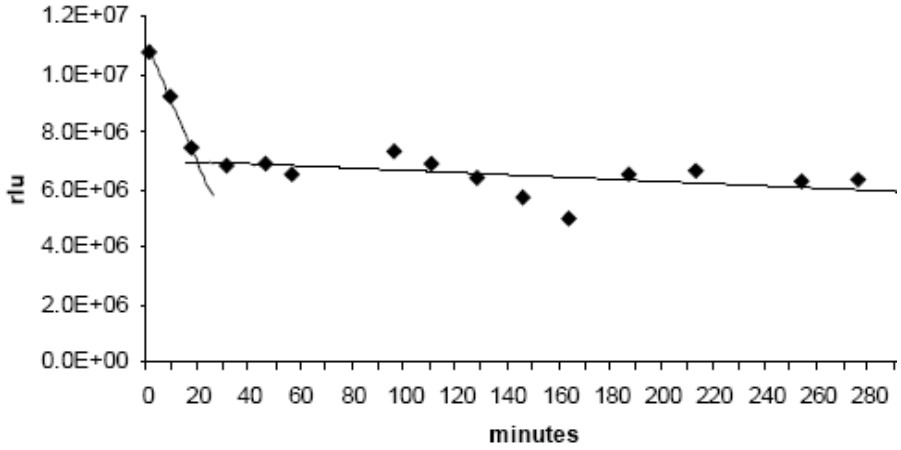

Figure 9: Decay of aqueous coelenterazine at 27 °C. Colenterazine ((10 mg/mL; 2.4mM in 200mM NaCl, 50mM Tris, 0.08% (v/v) Triton® X-100, pH 7.8). Measurements were made with EG&G Berthold LB 96V Microplate Luminometer and integrated over 10 seconds. The fast decay phase (~ 20 min) coincides with the window of time emissions are collected using the original BRET protocol, thus colenterazine emission will be significantly lower for wells read last compared to first. (Credit: FluoProbes® technical sheet)

itself emitted significant amounts of background light emission during the measurement. Thus, despite the established protocols calling for the use of two separate plates for the BRET assay – the clear bottomed black plate for total YFP and the opaque white plate for BRET, it appeared that it was preferential to avoid the white plate (hence reducing background) and instead to *[4]* use a single clear-bottomed black plate to measure first the YFP signal and then, after addition of coelenterazine h (rested in Ca^{2+}-free buffer for 20 mins), the BRET signal. This change to the method had the added benefit of taking paired YFP and BRET measurements from the exact same sample of cells, as opposed to two different distributions of the same cell mixed in two parallel plates, further improving precision (Figure 10).

To avoid loss of signal due to enzymatic substrate catabolism, *[5]* coelenterazine was added to one sample (six replicate wells) and the BRET signal was measured before moving to the next sample. This approach greatly reduced the time that the substrate sat in the well with the enzyme before the BRET reading. Altogether, these 5 changes to the assay resulted in a marked improvement in signal stability across a plate (Figure 11) as well as the following improved protocol that is now standard in the laboratory:

Coelenterazine h (Invitrogen, stock resuspended to 2.5 mM in 200-proof ethanol for working solution) was diluted to 5μM in Ca^{2+}- and Mg^{2+}-free phosphate buffered saline and allowed to rest at room temperature for 20 minutes. Cells transiently transfected 48 hours prior were harvested (phenol red-free Hank's

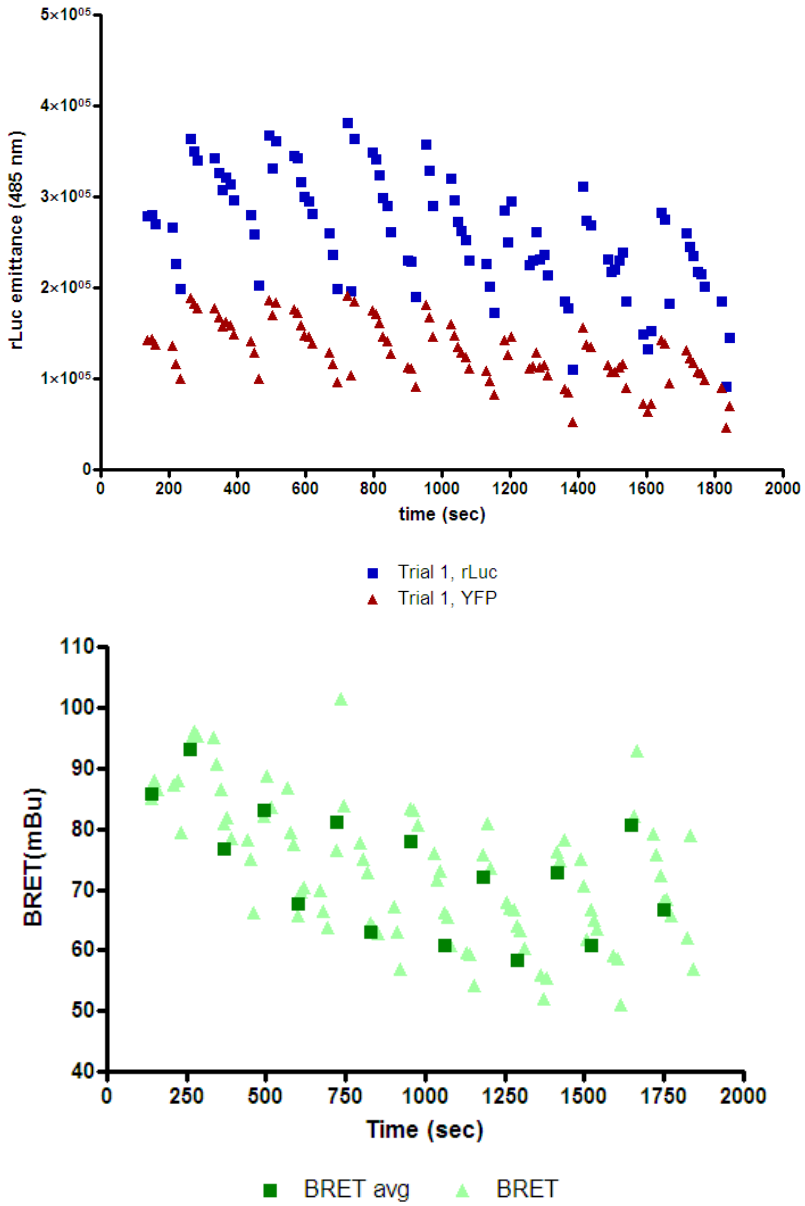

Figure 10: Decay in BRET and component emission measurements after initial modifications to BRET protocol. HEK 293 cells were transfected with rLuc- TP_{WT} (donor, 0.25µg) + YFP- TP_{WT} (acceptor, 0.75µg). Two 96-well plates were prepared containing identical samples in each well (except for the control rLuc alone cells) and assayed following a modified BRET protocol: coelenterazine was diluted to 50 µM in PBS without Ca^{2+} and allowed to sit for 20 minutes prior to use. Coelenterazine was distributed into each row separately, and emissions collected row by row immediately following coelenterazine addition (white opaque bottom). Total YFP emission was measured separately in a second plate (black, clear bottom). A representative experiment is shown. Although the drop in emission at 485nm and 550nm was less that with the original BRET protocol, there was a marked spread in values across each row (top); the decay in BRET values was also blunted (90 mBu to about 70 mBu; bottom) but similarly inconsistent across a single row.

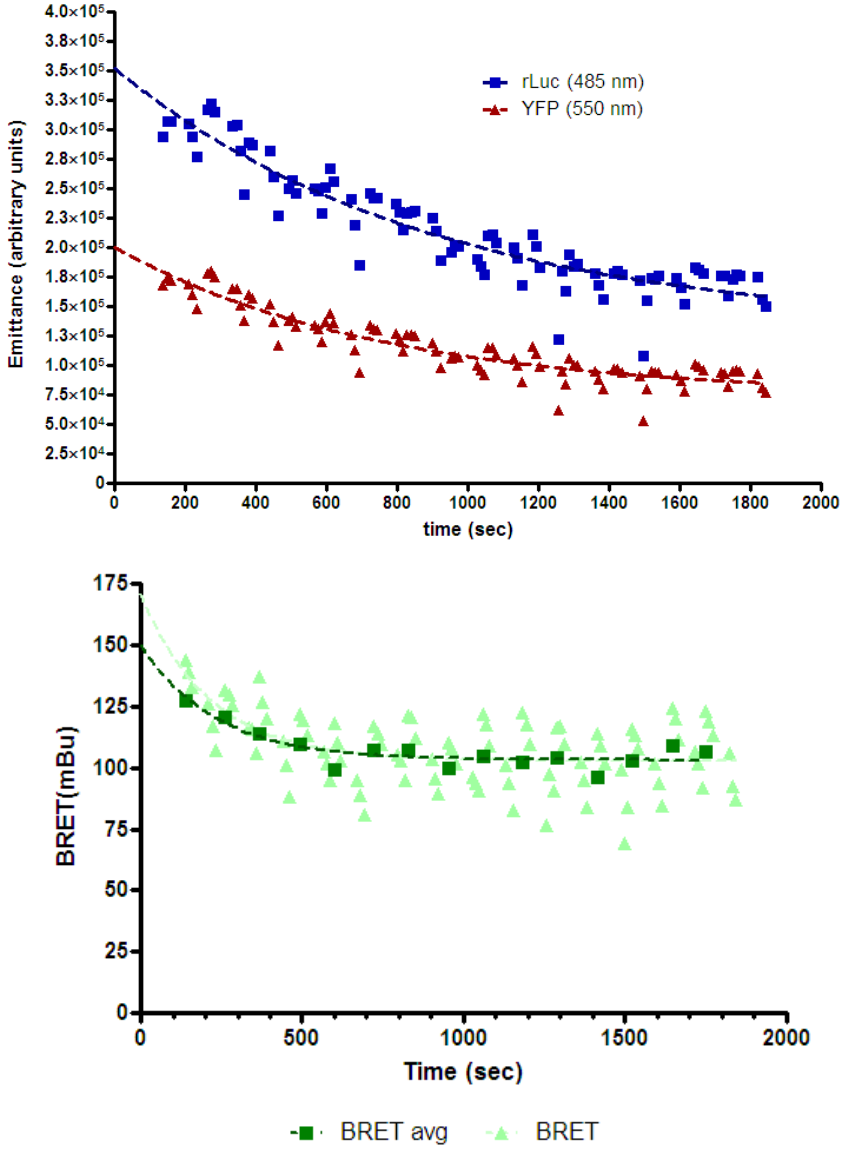

Figure 11: Decay in BRET and component emission measurements after final modifications to BRET protocol. HEK 293 cells were transfected with rLuc-TP_{WT} (donor, 0.25µg) + YFP- TP_{WT} (acceptor, 0.75µg) assayed following the a further modified BRET protocol: coelenterazine was diluted to 50 µM in PBS without Ca^{2+} and allowed to sit for 20 minutes prior to use. Cells were distributed into a black, clear-bottomed 96-well plate. Total YFP emission was measured. Coelenterazine was then added to each of the 6 replicate wells and emissions collected immediately. This process was repeated for each sample until all samples were read. A representative experiment is shown. Some drop in emission at 485 and 550 nm was evident, however this was to a much lesser degree that the original or mid-optimization and there was good agreement for replicate values from each sample (top). Further, BRET values decayed slightly from 125 mBu to about 110 mBu over the first 500 seconds but remained steady for the rest of the assay (bottom).

Balanced Salt Solution containing 0.02% EDTA), washed twice with phosphate-buffered saline and resuspended in DPBS containing 5.56 mM glucose (Invitrogen, 14287), then redistributed into a black, clear-bottomed 96-well plate (100,000 cells/well) and maintained at 37°C. Total YFP (Ex485nm, Em555nm) was first collected using a luminescence multi-plate reader (VICTOR3, Perkin Elmer) and calculated as fold over basal (no YFP-fused receptor present). Following this reading, coelenterazine h was added a set of six replicate wells and donor (485nm) and acceptor (555nm) emissions gathered sequentially for each sample. Colenterazine addition and BRET readings in sets of 6 replicate wells were repeated until all data was collected. Milli BRET units (mBU) were calculated as the ratio of Em555 over Em485 nm corrected for cells expressing the rLuc receptor alone, and multiplied by 1000.

Cell surface expression of the TP

HEK 293 and Meg-01 cells were transfected with HA-tagged TP_{WT} or HA-$TP_{L205,L209,Y213}$. Cells were harvested into ice-cold FACS buffer (DPBS containing 1% BSA and 0.1% sodium azide). Cell suspensions were stained with anti-HA mouse IgG1 (Monoclonal 16B12) conjugated to Alexa Fluor® 488 (Invitrogen, CA) for 30 minutes prior to washing. Median fluorescence intensity (MFI) was collected using a BD FACSCalibur flow cytometer (Becton Dickinson, Franklin Lakes, NJ, maintained by UPenn flow cytometry core). Cells were first gated to include only live cells of the proper size in the measurement via forward and side

scatter measurements, then gated on the FL1 filter (488nm excitation, 530/30nm filter emission) to obtain MFI values, which were corrected by subtraction of collected MFI values of non-transfected, antibody-stained HEK 203 of Meg-01 cells.

Measurement of second messenger generation

Measurement of intracellular inositol monophosphate (InosP) or cyclic AMP (cAMP) was performed using the IP-One Tb kit (Cisbio Bioassays, MA) or LANCE cAMP 384 kit (PerkinElmer, MA), respectively, according to the manufacturer's instructions. Both kits are based around the same principle of fluorescence resonance energy transfer (FRET) between two fluorophores. In the IP-One InosP assay, cells are treated with a mixture of [a] monoclonal anti-InosP antibody (Ab) tagged with crypate (a fluorophore) and [b] InosP tagged with the dye "d2", in addition to [c] LiCl, which inhibits inositol-phosphate phosphatase. The d2-InosP forms a complex with the crypate-Ab that allows for FRET from the crypate to the d2 upon excitation of the former. Unlabeled InosP, produced by the cell, competes for binding to the crypate-Ab. The more InosP is produced by the cell, the less FRET-capable complex is created, with the ratio of light emitted by the crypate to light emitted by the d2 dye as the quantitative readout of cellular InosP production after comparison to a standard curve of InosP concentrations. This same principle is employed by the LANCE cAMP assay, with europium-tagged streptavidin replacing the crypate-Ab, and AlexaFluor-tagged cAMP

replacing the d2-tagged InosP. IBMX (3-isobutyl-1-methylxanthine) is employed to inhibit cAMP degradation through phosphodiesterase inhibition. Cells were stimulated with or without the TP agonist U46619 (Cayman Chemicals, MI) over a range of concentrations, as noted in the respective results section, for one hour.

Radioligand binding and displacement

HEK 293 cells, transfected with HA-tagged TP_{WT} or $TP_{L205,L209,Y213}$ in poly-L lysine-coated 12 well plates, were washed with radioligand binding buffer (HBSS with 2% BSA). For saturation binding ^{3}H-SQ 29,548 (PerkinElmer, Waltham, MA or American Radiolabeled Chemicals, St. Louis, MO) was distributed to cells at concentrations ranging from 25 μM to 250 μM. After 60 minutes at 37°C, cells were washed with ice-cold binding buffer to remove unbound ligand, lysed with 1 M NaOH for 30 minutes at 37°C and radioactivity measured by scintillation counting.

For displacement analysis, ^{3}H-SQ 29,548 was held constant at 0.25 nM and competing ligands were added 5 minutes prior to the radioligand. Competing ligands I-BOP and cold SQ 29,548 were applied as treatments ranging from 5 nm to 500 nm, while U46619 and the isoprostane E_{2III} (iPE_{2III}) concentrations ranged from 25 nm to 2500 nm, due to lower affinity for the TP. In either experiment, non-specific binding was accounted for by the addition of a 100-fold excess of cold SQ 29,548. After 60 minutes at 37°C, cells were washed with ice-cold

binding buffer to remove unbound ligand, lysed with 1 M NaOH for 30 minutes at 37°C and radioactivity measured by scintillation counting.

Immunoprecipitation and immunoblotting

HA-tagged TP_{WT} or $TP_{L205,L209,Y213}$ were immunoprecipitated from transfected HEK 293 cells using Pierce HA Tag immunoprecipitation/Co-immunoprecipitation Kit (cat# 23610,Thermo Scientific, Waltham, MA), according the manufacturer's instructions. This kit uses anti-HA antibody conjugated to agarose beads for immunoprecipitation of HA-tagged proteins. Eluted proteins were resolved via NuPAGE electrophoresis (Invitrogen, CA) under reducing conditions. HA-tagged TP_{WT} or $TP_{L205,L209,Y213}$ were visualized with anti-TP (Cayman Chemicals, MI; 1:100) while immunoprecipitated $G_{q\alpha}$ was visualized with anti-$G_{q/11\alpha}$ (Millipore, CA; 1:1000). Antigen-antibody complexes were revealed using horseradish peroxidase conjugated anti-rabbit IgG (Jackson ImmunoResearch, PA; 1:10,000) and visualized by enhanced chemiluminesence (ECL Plus, GE Healthcare/Amersham, NJ). Quantification of proteins was by densitometry.

Treatment of cells with the CHAMP peptide

A computed helical anti-membrane protein (CHAMP) peptide (128, 142) was supplied by the lab of Dr. Joel Bennett (University of Pennsylvania School of Medicine) as 1 mM CHAMP in DMSO. As directed by members of the Bennet lab, the treatment concentration of 1 μM CHAMP was employed in BRET and

second messenger generation assays. To avoid vehicle effects, the total final concentration of DMSO in media did not exceed 0.1%.

Quantitative-PCR

RNA isolated from human aortic smooth muscle cells grown in culture was quantified (NanoDrop Spectrophotometer) and reverse transcribed into cDNA (MultiScribe Reverse Transcriptase, Applied Biosystems) according to manufacturer's instructions. Quantitative real-time polymerase chain reaction (Q-PCR) was carried out using inventoried primer/probe gene expression assays with TaqMan Universal PCR Master Mix (Applied Biosystems) for the human thromboxane receptor gene (TBXA2R, cat# 4331182). Q-PCR products were monitored using the ViiaTM 7 Real-Time PCR System (Applied Biosystems) and data was analyzed using the 2-ΔΔCt method of relative quantification (RQ) using 18S for normalization (160).

Receptor modeling

Working with the Hwa Laboratory (Yale Medical School), the human hTPα sequence was aligned with solved crystal structures, bovine rhodopsin (OPSD, UniProt identifier P02699) and the human ß2-adrenergic receptor (ADRB2, UniProt identifier P0755) in ClustalW [http://www.clustal.org]. Both the PAM250 and BLOSUM evolution matrix modeling algorithms (161) indicated closer alignment of hTPα to align more closely with OPSD (similarity score 30.16) than

with ADRB2 (33.48). Each bundle of seven transmembrane α-helices was therefore based on a 2.8Å crystallographic bovine rhodopsin template (1HZX) (162) using the internet-based protein-modeling server, SWISS-MODEL [http://swissmodel.expasy.org] (GlaxoSmithKline, Geneva, Switzerland), and energy minimized using the Gromos96 force field in DeepView [http://spdbv.vital-it.ch]. Extracellular and cytoplasmic loop regions were manually constructed, built according to JPred consensus, and energy-minimized using the NAMD molecular dynamics simulator (163).

Fluorescence microscopy

HEK 293 cells were grown to 80-90% confluency in 60 mm dishes, then lifted in 1 mL 0.25% trypsin, then added to 8 mL HEK growth medium. Cells were transfected in 0.4 mL aliquots by 0.25 µg of either myc-TP_{WT} or myc-$TP_{L205,L209,Y213}$, with each aliquot being dispensed into one well of an 8-well poly-D-lysine-coated slide (Becton Dickinson, Franklin Lakes, NJ) and allowed to grown for 48 hours. Cells were then fixed with 4% paraformaldehyde for 10 minutes at room temperature, followed by permeabilization with 0.2% Triton X-100 in PBS. Staining was performed with 1:800 diulted anti-myc AlexFluor 555 conjugate (Millipore, Billerica, Massachusetts) for one hour with gentle shaking. Cells were then mounted with Vectashield + DAPI (VectorLabs, Burlingame, CA) and cover slips were sealed with clear nail polish. Imaging was performed on a Zeiss Widefield Microscope at 40x magnification.

CHAPTER 3: Characterization of Thromboxane Receptor Regulation.

TPα auto-upregulation is not driven by increases in mRNA levels

The first possibility explored as a mechanistic explanation for auto-upregulation of the TP following agonist activation (70) was increased receptor biogenesis resulting from elevated levels of mRNA. If one downstream effect of TP activation was to increase TP mRNA levels this could contribute to the increase in TP protein and cell surface TP levels observed. To examine whether TP activation leads to increases in mRNA levels TPα-transfected HEK 293 cells or human aortic smooth muscle cells (HuAoSMCs), which endogenously express TP, were treated with either 100 nM IBOP, 1 μM SQ 29,548 (a TP antagonist), or a combination of both for 2 hours. Cells were harvested and TP mRNA quantified by real-time PCR. IP mRNA was also measured as a negative control since IP is not stimulated by IBOP. Quantitative comparisons made to mRNA levels at pre-treatment showed no significant change in mRNA levels for cells with any treatment (Figure 12). Thus, upregulation of TP transcription in response to short-term agonist treatment did not appear to contribute to auto-upregulation. Additional studies were performed to query whether a longer-term agonist treatment could lead to changes in mRNA levels that might explain that auto-upregulation paradigm. In both transiently transfected HEK 293 cells as well as natively expressing HuAoSMCs, 6- or 12-hour treatment with 100 nM IBOP lead to no significant change in TPα mRNA levels (Figure 13A, B). Nor did we see any change in mRNA levels in HuAoSMCs treated with 1 μM IBOP over a time

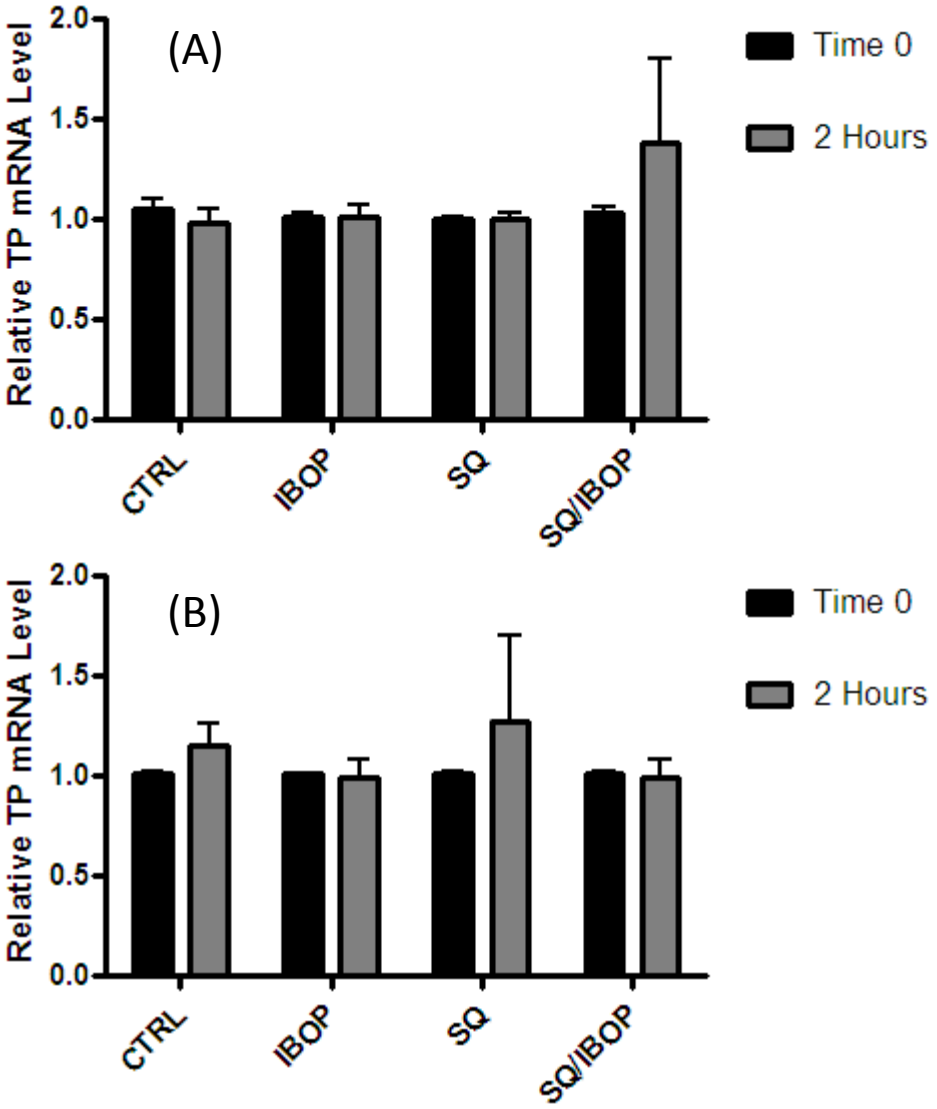

Figure 12: Levels of TP and IP mRNA after a 2-hour IBOP treatment. TP mRNA levels were measured by real time PCR. Human aortic smooth muscle cells were treated 100 nM IBOP, 1 μM SQ 29,548 (a TP antagonist), or a combination of the two, for 2 hours prior to harvest and quantification of TP, IP, and 18S mRNA. mRNA expression for both TP and IP is reported as a ratio of receptor mRNA present at the given time to mRNA at time zero, corrected for 18S. No significant difference was evident for any treatment in either TP or IP mRNA levels. Data are mean ± standard error of n=3.

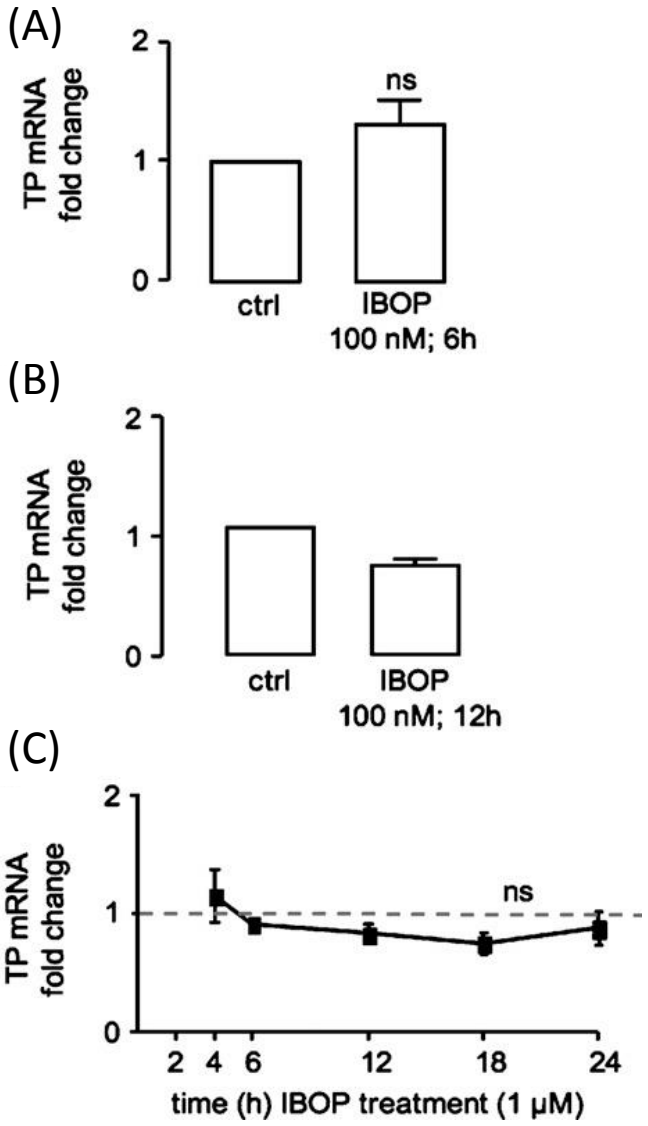

Figure 13: Activation of the TP does not alter TP transcription. HEK 293 cells transiently transfected with TPα (A) or HuAoSMCs (B, C) were serum starved for 24 hours before IBOP treatment. Total RNA was extracted and reverse transcribed into cDNA, and TP expression was examined by real-time PCR. Values were normalized to either β-actin or 18S levels and are expressed as the fold change compared with control (no IBOP). Data are mean ± SEM (n = 3–5). ns, nonsignificant compared to control.

course of up to 24 hours (Figure 13C). Thus, agonist activation in both and the long and short terms did not cause any noticeable changes in mRNA levels that could explain the auto up-regulation seen for the TPα.

A modified version of the BRET assay provides greatly increased sensitivity

Preliminary co-immunoprecipitation studies carried out previously in the lab suggested that, similar to other GPCRs (100–103, 107, 114, 115), the TP formed homodimers within the cell. To address the question of dimerization in live cells (as compared to the cell homogenates used in co-immunoprecipitation assays), we used the bioluminescence resonance energy transfer (BRET) assay, which measures transfer of energy from a donor (rLuc-fused receptor) to acceptor (YFP-fused receptor) as their physical interaction (for details see *Chapter 2, Methods, Pages 26-30* and Figure 6). As outlined in Chapter 2 (*Pages 31-39*), while establishing the BRET assay, we noticed a large decline in the raw values for the emission readings from the beginning to end of reading the BRET plates. We considered whether this decline in signal was a real reflection of changing dimerization events or indicative of potential problems with the design of the BRET assay itself. To examine this, one large, homogenous batch of cells were transfected with a set amount of TP-rLuc and TP-YFP. These cells were harvested, then resuspended in DPBS with glucose and sodium pyruvate, then plated in all 96 wells of the plate, as per the original BRET protocol.

Coelenterazine h (rLuc substrate) was added to all wells, and the plate was read as a whole (approximately 20 min from start to finish). Rather than the expected equivalent signals from all wells, the rLuc emission signal (read at 485 nm) decreased dramatically from 10,000 to less than 1,000 (arbitrary units), while the YFP emission signal decreased from approximately 5,000 to under 500 (arbitrary units). Of particular concern, the BRET signal itself decreased from 120 to 50. As described above (Chapter 2, Figure 11), the BRET assay was rigorously assessed and optimized to avoid these possible confounding issues with the original protocol. First, we discovered that coelenterazine decomposes significantly during the first 20 minutes after introduction to aqueous solution, particularly in solutions containing calcium. Thus the protocol was changed to used Ca^{2+}- and Mg^{2+}-free DPBS for coelenterazine dilution and to include a 20 minutes rest period prior to use. Second, to minimize loss of substrate by rLuc metabolism during the significant “down-time” between coelenterazine addition and emission collection, samples were stimulated and read immediately as separate 6-well groups (a single sample with 6 replicate measurements). With these modifications, signal loss was significantly improved to 30,000 to 20,000 for rLuc and 18,000 to 11,000 for YFP across a representative plate. Additionally, BRET signal only decayed from 130 to 110 across the plate and was steady after the first 500 seconds.

Dimerization of the TP occurs with TP, IP, and DP1, but not CCR5

HEK 293 cells were transiently transfected with rLuc- (donor, 0.25µg) plus YFP- (acceptor, 0.125µg – 0.75µg) fused pairings of TP-TP. We confirmed that the TPα does undergo homodimer formation within living cells with an affinity that suggests physiological occurrence of dimerization (Figure 14). Previous work in the lab also demonstrated co-immunoprecipitation of TPα with the IP, thus we also examined this association by BRET. In HEK 293 cells transiently transfected with rLuc- (donor, 0.25µg) plus YFP- (acceptor, 0.125µg – 0.75µg) fused pairings of TP-IP BRET was saturable and occurred at a similar affinity to TP-TP indicating equal propensity for the TPα homodimer and TPα-IP heterodimer to form (Figure 15A). A concern in the field of GPCR dimerization is that over-expression of any two GPCRs will lead to some level of interaction providing a "false positive" for dimerization. Thus, it is important to define a negative control (a non-interacting receptor). We examined two GPCRs as non-interacting receptor controls, the PGD_2 receptor DP1 (121) and chemokine receptor CCR5. TP-DP1 or TP-CCR5 dimerization was assessed using the BRET assay. Interestingly, TPα formed a heterodimer with DP1, but this was at a significantly lower affinity compared to TP-TP and TP-IP (Figure 15B). This suggests that, in a physiological setting, the TP could dimerize with the DP1, potentially modifying the function of either or both partners, but the TP-TP and TP-IP dimers are likely to out-compete the TP-DP1 dimer. It is possible that the TP-DP1 heterodimer is more relevant in situations where DP1 is present at a higher relative concentration compared to the TP and/or IP, or under conditions of agonist

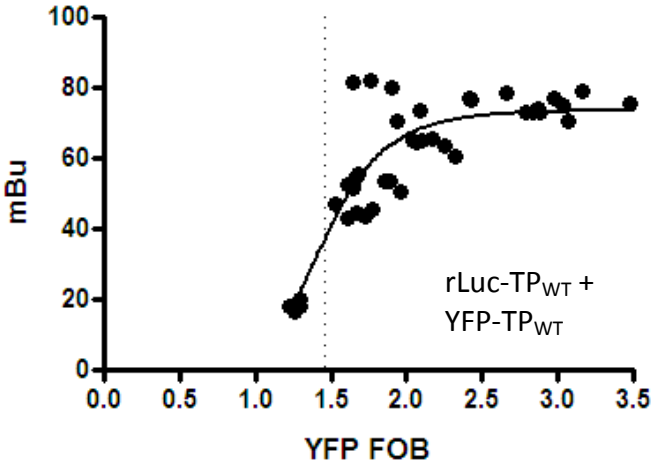

Figure 14: Homodimerization of TP_{WT} by BRET. Saturable BRET was observed for rLuc- (donor, 0.25µg) + YFP- (acceptor, 0.125µg – 0.75µg) fused pairings of TP_{WT}-TP_{WT} in transiently transfected HEK 293 cells. Representative experiment is shown. Data are milli BRET units plotted against fold over basal total YFP emission (a measure of YFP-fused acceptor receptor expression). The $BRET_{50}$ value for this experiment is indicated by the dotted gray line.

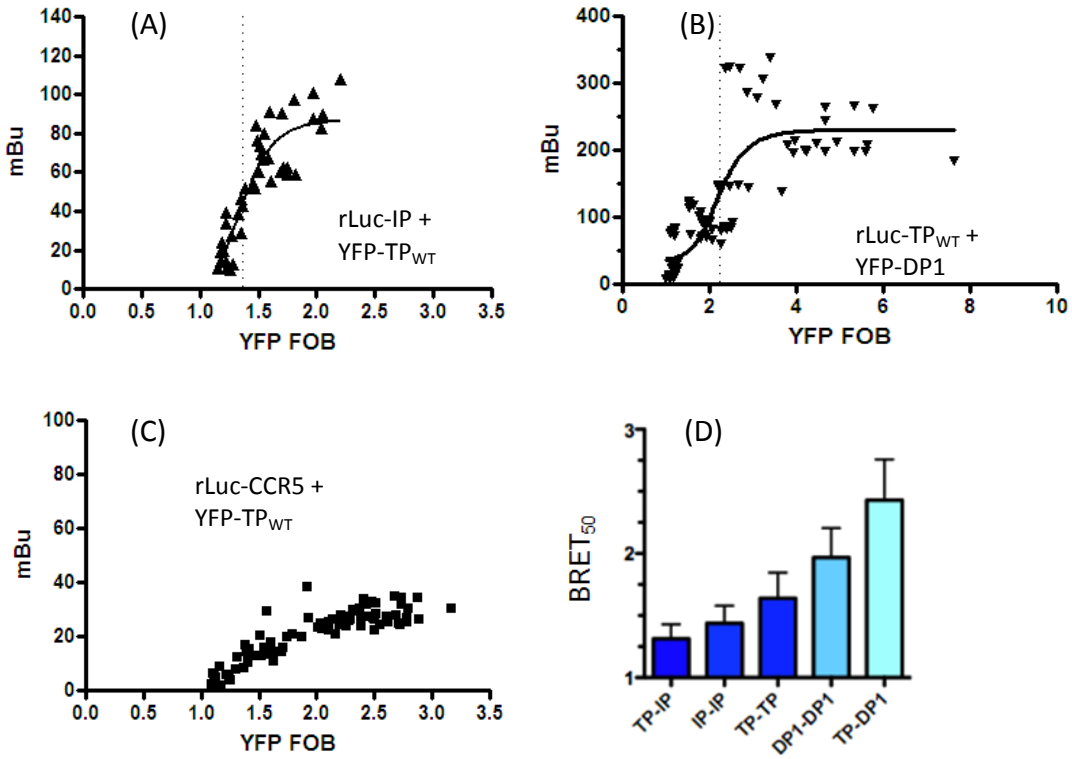

Figure 15: Heterodimerization of TP_{WT} by BRET. Saturable BRET was observed for rLuc- (donor, 0.25µg) + YFP- (acceptor, 0.125µg – 0.75µg) fused pairings of (A) TP_{WT}-IP and (B) TP_{WT}-DP1 in transiently transfected HEK 293 cells. No saturable BRET was observed for (C) rLuc- TP_{WT} (donor, 0.25µg) + YFP- CCR5 (acceptor, 0.125µg – 0.75µg) in transiently transfected HEK 293 cells. Representative experiments are shown. Data are milli BRET units plotted against fold over basal total YFP emission (a measure of YFP-fused acceptor receptor expression). Individual $BRET_{50}$ values for each representative experiment are indicated by the dotted gray lines. (D) $BRET_{50}$ values were calculated from 4-6 individual BRET saturation experiments. Data are mean $BRET_{50}$ values ± SEM from n=4-6.

activation or other cell or context-specific settings. These are intriguing questions that remain to be experimentally examined. Importantly, there was no evidence for dimerization of the TP with CCR5, arguing against a non-specific interaction between any two GCPRs expressed in the same cell (Figure 15C).

Dimerization does not contribute to auto-upregulation of the TP following agonist activation.

Studies report that dimerization is essential for normal biogenesis of GCPRs (109, 114, 115, 164). Thus, having shown that TP homodimerization does occur, we considered whether agonist-induced modulation of TPα homodimerization might contribute to augmented receptor stability and membrane expression, providing a post-translational mechanistic explanation for auto-upregulation of the agonist-stimulated TP. To examine this possibility, cells were treated with IBOP, a TxA_2 mimetic, prior to analysis of TPα homodimerization by BRET. However, there was no significant change in maximal BRET or $BRET_{50}$ (Figure 16A). We and others reported that auto-upregulation of TPα is dependent on a reactive-oxygen species mechanism and replicated by treatment of cells with H_2O_2 (70, 165). Thus we examined whether H_2O_2 treatment modified TPα homodimerization. Similar to IBOP treatment, however, there was no significant effect of H_2O_2 on TPα homodimerization by BRET assay (Figure 16B).

These experiments that were designed to address how agonist activation of a receptor modifies its dimerization raised interesting questions that have been

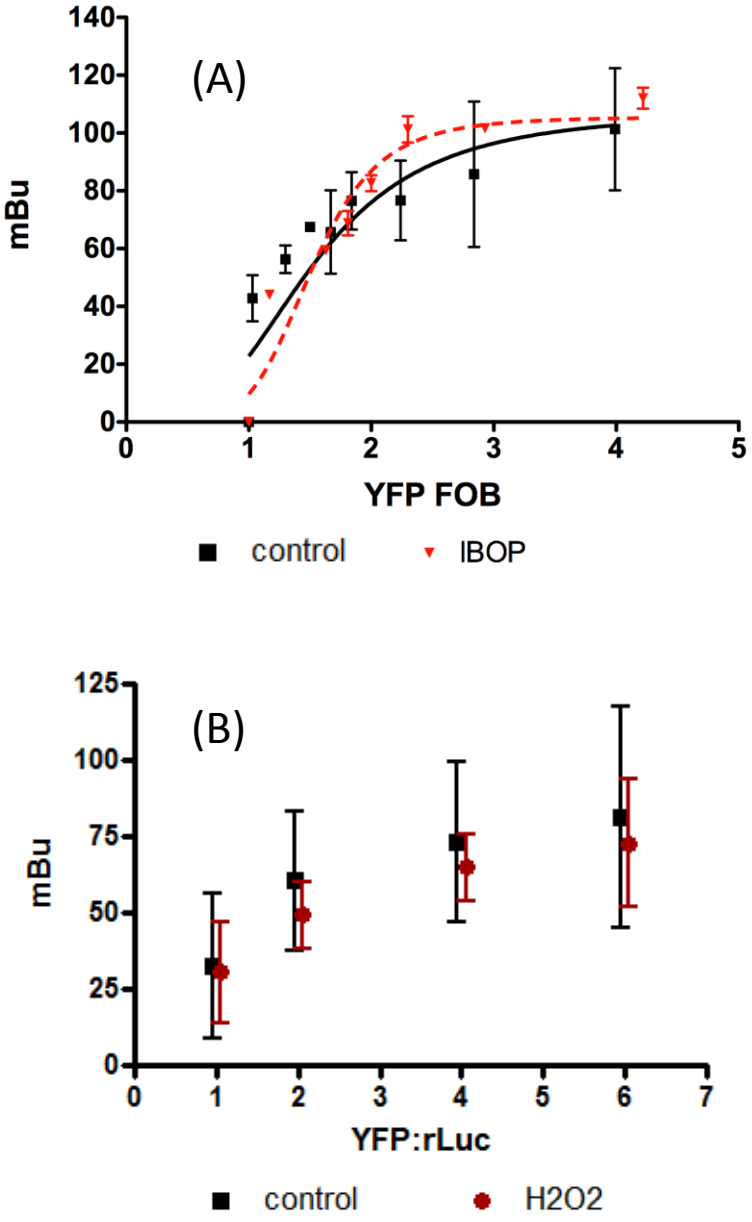

Figure 16: Impact of agonist treatment on TPα homodimerization. Saturable BRET was observed for rLuc- TP_{WT} (donor, 0.25µg) + YFP-TP_{WT} (acceptor, 0.125µg – 0.75µg), with or without (A) 100 nM IBOP (6hr) or (B) 1uM H_2O_2. No significant change was seen in either $BRET_{max}$ or $BRET_{50}$. Data are mean ± standard error of n=3.

considered by other GPCR labs but not formally addressed: does ligand treatment modify BRET independent of true changes in absolute dimer levels? Since resonance energy transfer is dependent on the close proximity of the donor and acceptor molecules, and the magnitude of this distance determines the efficacy of the energy transfer, then it stands to reason that shifts in the conformation of the partners in a dimeric arrangement could induce a change in the distance or orientation between the pair of signaling molecules. Such a conformational change is commonly accepted as necessary for propagation of agonist-induced signaling to downstream effector molecules. Thus, the treatment of a dimer with an agonist (or any other ligand that causes conformational changes) to either or both of the protomers could impact the BRET signal but not reflect a change in dimerization per se, leading to a false positive for ligand-dependent dimerization. To study the possibility of this occurring in the TP dimerization assay, HEK 293 cells were transfected with rLuc- (donor, 0.50µg) + YFP- (acceptor, 1.00µg) fused pairings of TP_{WT}-TP_{WT}, then treated with either agonist (100 nM IBOP), 1uM SQ 29,548 (antagonist), or both for 10 minutes prior to BRET analysis. Maximal BRET after treatment with combined SQ 29,548 and IBOP was significantly lower than that of untreated cells (*$p<0.05$) (Figure 17). While the change seen in this assay was small, it suggests that ligand and conformational changes binding can impact assay readout making the BRET assay less suitable to study agonist-induced modulation of TPα dimerization. Thus, although our studies did not support the hypothesis that TP dimerization

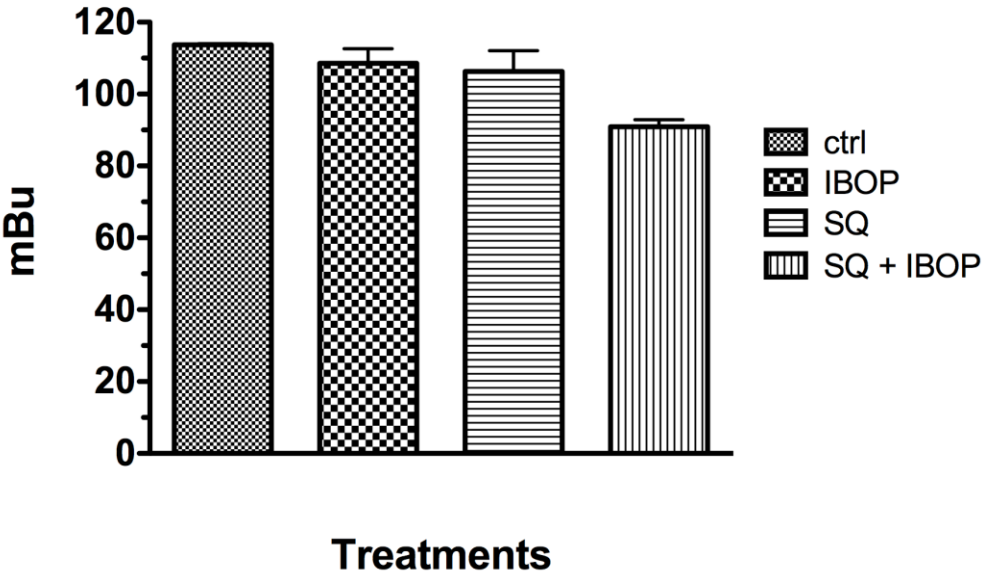

Figure 17: Effect of ligand treatment on maximal BRET values in TPWT homodimerization. HEK 293 cells were transfected with rLuc- TP_{WT} (donor, 0.50µg) + YFP- TP_{WT} (acceptor, 1.00µg) then treated with either 100 nM IBOP, 1uM SQ 29,548, or both for 10 minutes prior to BRET analysis. Maximal BRET after treatment with combined SQ 29,548 and IBOP was significantly lower compared to untreated cells (*$p<0.05$). Data are mean ± standard error of n=3.

contributes to its auto-upregulation, this possibility still exists and could be examined through use of an assay that lacks these potential limitations of the BRET assay.

CHAPTER 4: Targeting the Specific GGL Motif of the TP as a Means of Receptor Regulation

Identification and mutation of a GxxxGxxxL motif in the 5th transmembrane of the TPα

Analysis of the TPα amino acid sequence revealed a GxxxGxxxL motif in TM5: $G_{205}LSVG_{209}LSFL_{213}$ (see Figure 1). Additional GxxxG motifs were identified toward the N-terminus (G_5SSLG_9), within the 1st intracellular loop ($G_{51}ARQG_{55}$) and 2nd extracellular loop ($G_{188}AESG_{192}$). Given that a TM GxxxGxxxL motif has been implicated in the functioning of at least two GPCRs (104, 115), and that transmembrane domains have been noted for their involvement in dimerization (126, 127), we chose to focus further on the $G_{205}LSVG_{209}LSFL_{213}$ domain. Three-dimensional homology modeling of the TP revealed an outward-facing orientation of G_{205}, G_{209} and L_{213} (see Figure 3) in TM5 indicating that this domain is appropriately positioned for protein-protein interaction within the membrane. To define the functional relevance of the TM5 GxxxGxxxL motif in the TP we employed site-directed mutagenesis to replace G_{205} and G_{209} with leucines and L_{213} with a tyrosine to generate $TP_{L205,L209,Y213}$. As outlined previously (Chapter 2, C*onstructs, Pages 21-22*), we replaced G_{205} and G_{209} with leucines, a small-to-large replacement that disrupts helix-helix interaction (139, 141, 142), and replaced L_{213} with a tyrosine based on the studies of the GxxxGxxxL motif in the ß2-adrenergic receptor (115). Mutagenesis was carried out via polymerase chain

reaction and using primers designed with a modified sequence for the residues of interest (Table 1). The mutations were added sequentially, with verification of the target sequence prior to introduction of the next mutation.

Disruption of the TM5 GGL motif suppressed TP function

Having successfully introduced mutations into the $G_{205}xxxG_{209}xxxL_{213}$ motif, we examined the impact on TP function. We first measured the ability of the wild type TP_{WT} and $TP_{L205,\ L209,\ Y213}$ to transduce a signal via the canonical phospholipase C/inositol phosphate pathway in response to the thromboxane mimetic U46619. In transiently transfected HEK 293 cells, the maximal signaling capacity of $TP_{L205,\ L209,\ Y213}$ was significantly reduced by ≈25% compared to TP_{WT} transfected cells, although there was no significant change in EC_{50} (Figure 18A). We also examined signaling of the mutant receptor in the Meg-01 cell line. Meg-01 cells are megakaryoblasts derived from a chronic myelogenous leukemia line (166). When grown in culture, adherent Meg-01s can be nucleofected leading to the release of daughter cells into suspension that express the construct of interest. These daughter cells are platelet-like cells, thereby serving as a closer approximation to the TP's native environment. Depressed signaling via the $TP_{L205,\ L209,\ Y213}$ was also evident in Meg-01 cells (Figure 18B), with a ≈50% reduction in inositol phosphate generation and a significant rightward EC_{50} shift. Thus, disruption of the TM5 GxxxGxxxL motif markedly suppressed TP response to agonist.

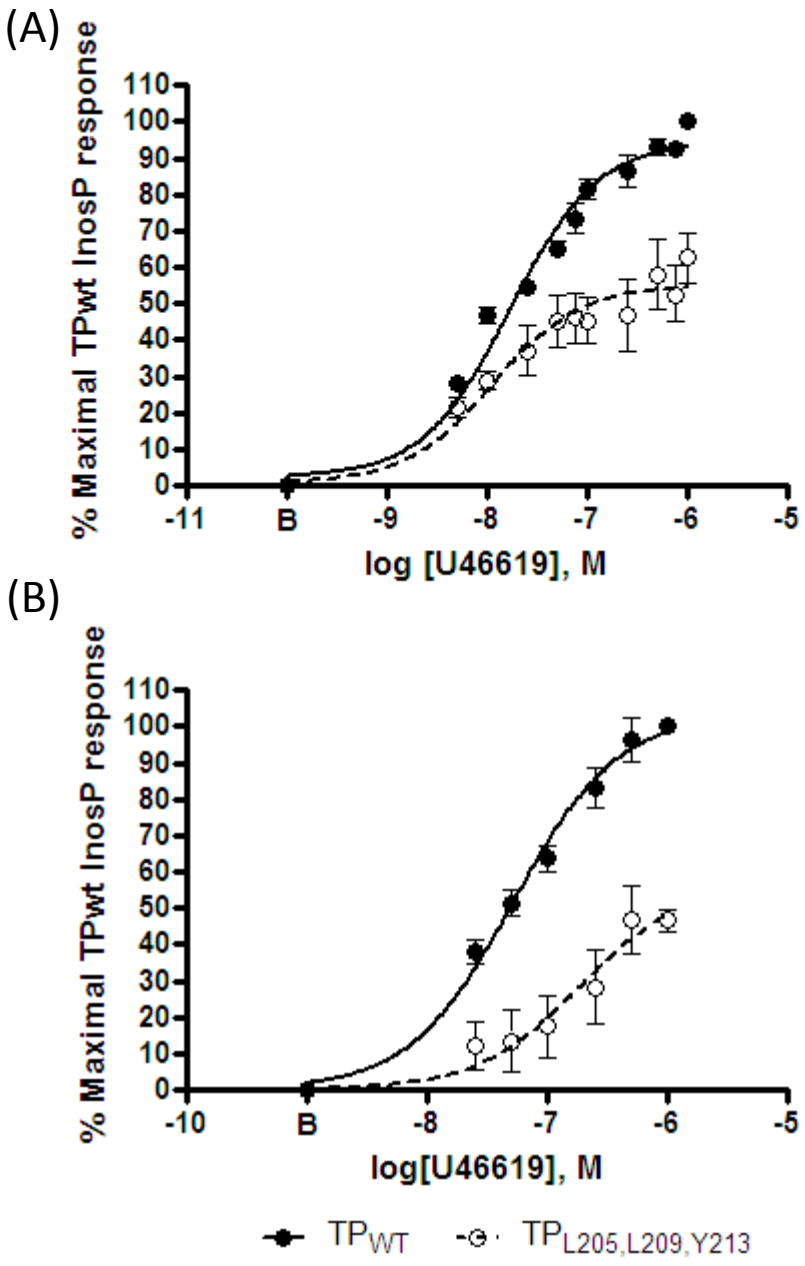

Figure 18: Inositol Phosphate Signaling through WT and mutant TP. (A) Maximal inositol phosphate (InosP) generation was reduced by 25 ± 5% ($p<0.0001$) in $TP_{L205,L209,Y213}$ (open circles) compared to TP_{WT} (closed circles) transfected HEK 293 cells. There was no significant change in EC_{50}. (B) Maximal InosP generation was reduced by 50 ± 7% ($p<0.01$) with a significant rightward shift in EC_{50} ($p<0.05$), in $TP_{L205,L209,Y213}$ (open circles) compared to TP_{WT} (closed circles) transfected Meg-01 cells. Data are % of maximum response (in TP_{WT}) and are mean ± sem; n=4-6.

We next sought to define how mutation of the $G_{205}xxxG_{209}xxxL_{213}$ motif reduced TP signaling. We considered the various stages along the biogenic and signaling pathways that could be impacted by the introduction of such a mutation. For example, disruption of this motif could lead to protein misfolding in the ER, possibly causing ER retention through failure at a dimerization-dependent checkpoint (115). Alternatively, the mutant receptor may be processed and expressed normally but disruption of helical interactions via the TM5 GxxxGxxxL motif could lead to loss of ligand binding, because of possible changes to the ligand-binding pocket or G protein interaction, thereby disrupting signal transduction in response to agonist. Finally, even if the receptor maintained normal ligand binding and normal communication with downstream effectors, disruption of the TM5 GxxxGxxxL helical interaction motif may interfere with normal dimerization with a consequent failure of proper interaction between the protomers and suppressed signaling. These possibilities were examined in turn.

Disruption of the TM5 GGL motif did not reduce TP cell surface expression

First, we examined whether the loss of $TP_{L205,\ L209,\ Y213}$ signaling reflected simply reduced cell surface expression of the mutant receptor. By confocal microscopy of HEK 293 cells transiently transfected with HA-tagged TP_{WT} or $TP_{L205,L209,Y213,}$ we observed qualitatively similar subcellular distribution of the mutant compared to WT (Figure 19), suggesting that loss of the TM5 GxxxGxxxL motif does not cause a change in retention of the receptor in the ER, or altered distribution in

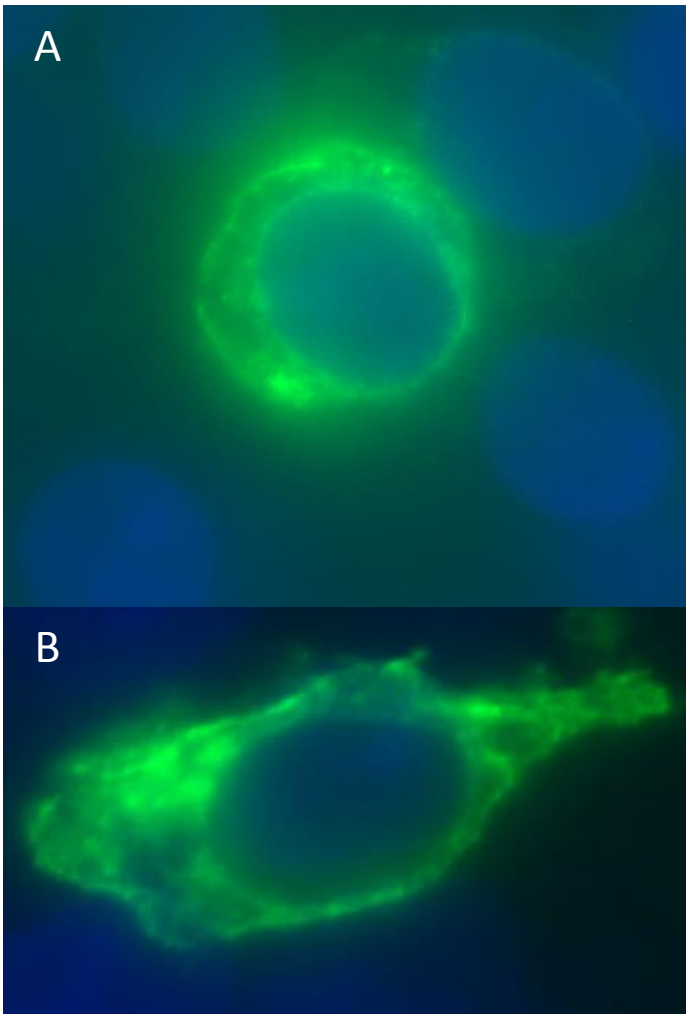

Figure 19: Cellular localization of TP_{WT} or $TP_{L205, L209, Y213}$ mutant. HEK 293 cells were transiently transfected with either TP_{WT} or $TP_{L205, L209, Y213}$, tagged at the amino terminus with a c-myc epitope tag. Receptor localization was examined by immunofluorescence microscopy in cells stained with fluorophore-tagged antibody against the relevant epitope tag [AlexaFluor 555-anti-myc] and nuclei stain [4,6-diamidino-2-phenylindole (DAPI), blue stain], 40x magnification. Images are from a representative experiment that was repeated with similar results.

other areas of the cell. As is typical for transiently transfected GPCRs expressed under a constitutively active promoter, plasma membrane receptor expression was not clearly distinguished by immune fluorescence microscopy. To quantitatively establish disruption of the TM5 GxxxGxxxL motif altered membrane localization of receptor we examined cell surface expression of the TP_{WT} or $TP_{L205,\ L209,\ Y213}$, both tagged at their N terminus with the HA epitope tag, by flow cytometry. In both transfected HEK 293 or Meg-01 cells there was no significant difference in cell surface receptor levels, as measured by median surface HA fluorescence intensity, between TP_{WT} and $TP_{L205,\ L209,\ Y213}$ transfectants in either cell type (Figure 20). Thus, disruption of the TM5 GxxxGxxxL motif did not appear to substantially modify receptor processing to the surface, indicating that the signaling deficit we observed could not be explained by quantitative changes in the receptor population on the plasma membrane leading to reduced exposure to ligand.

Ligand affinity and is not modified by mutation of the TM5 GxxxGxxxL motif

Second, we addressed the possibility that loss of the TM5 GxxxGxxxL motif might cause a conformational shift changing the TP ligand-binding domain thereby reducing agonist affinity for $TP_{L205,\ L209,\ Y213}$ and suppressing signal. Intact HEK293 cells expressing either TP_{WT} or $TP_{L205,\ L209,\ Y213}$ were labeled with a single concentration of ^{3}H-SQ 29,548 and displacement examined for two TP

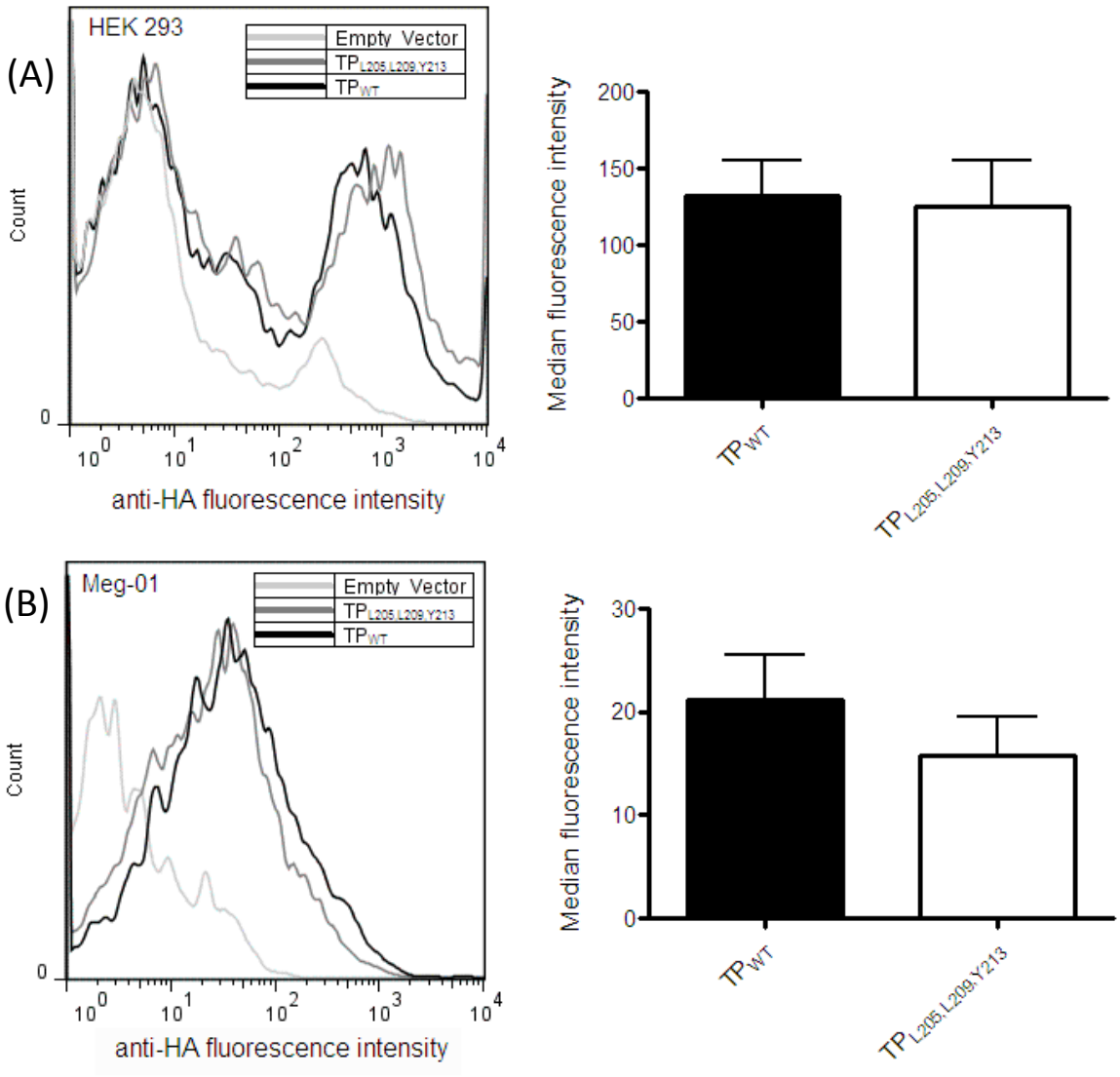

Figure 20: Surface Expression of Wild Type and Mutant TP. (A) HEK 293 cells or (B) Meg-01 cells were transfected with N-terminal hemagglutinin (HA)-tagged TP_{WT} or $TP_{L205,L209,Y213}$ and surface HA quantified by flow cytometry as a measure of surface receptor expression. Left panels show representative histograms, taken at one sitting using identical settings; right panels show the median fluorescent intensities (mean ± SEM, n=7). There was no significant difference in surface expression of TP_{WT} vs $TP_{L205,L209,Y213}$ in either cell model.

agonists, U46619 (K_i=90nM for TP_{WT} vs. 52nM for $TP_{L205, L209, Y213}$) and IBOP (K_i=1.8nM for TP_{WT} vs. 2.5nM for $TP_{L205, L209, Y213}$), or by unlabelled SQ 29,548 (K_i=4nM for both TP_{WT} and $TP_{L205, L209, Y213}$) as a reference. No significant difference in displacement was evident between the wild type and mutant receptors. We also examined an isoprostane, iPE_2III (K_i=334nM for TP_{WT} vs. 403nM for $TP_{L205, L209, Y213}$), a free radical-generated metabolite of arachidonic acid that can activate the TP in vivo (24), and again saw no difference in radioligand displacement (Figure 21). Further, in ^{3}H-SQ 29,548 in saturation binding analysis (Figure 22), although saturation was not reached because of issues with ^{3}H-SQ 29, 548 solubility, there was no apparent different between the TP_{WT} and $TP_{L205, L209, Y213}$. Thus, disruption of the TM5 GxxxGxxxL motif did not appear to alter the receptor's ligand binding properties and reduced affinity of agonist could not explain suppressed signaling.

Association of TP with G_q is not modified by mutation of the TM5 GxxxGxxxL motif

Third, we considered whether disruption of the TM5 GxxxGxxxL motif interferes with the association of the TP to its effector, G_q, leading to suppressed signaling. Previous studies of GPCRs, particularly with G_s coupled receptors, have noted that association of the G protein with the receptor in the inactive, non-ligand-bound conformation provides a high affinity state for agonist (167, 168). Such in-depth studies have not been reported for G_q- coupled receptors, like the TP,

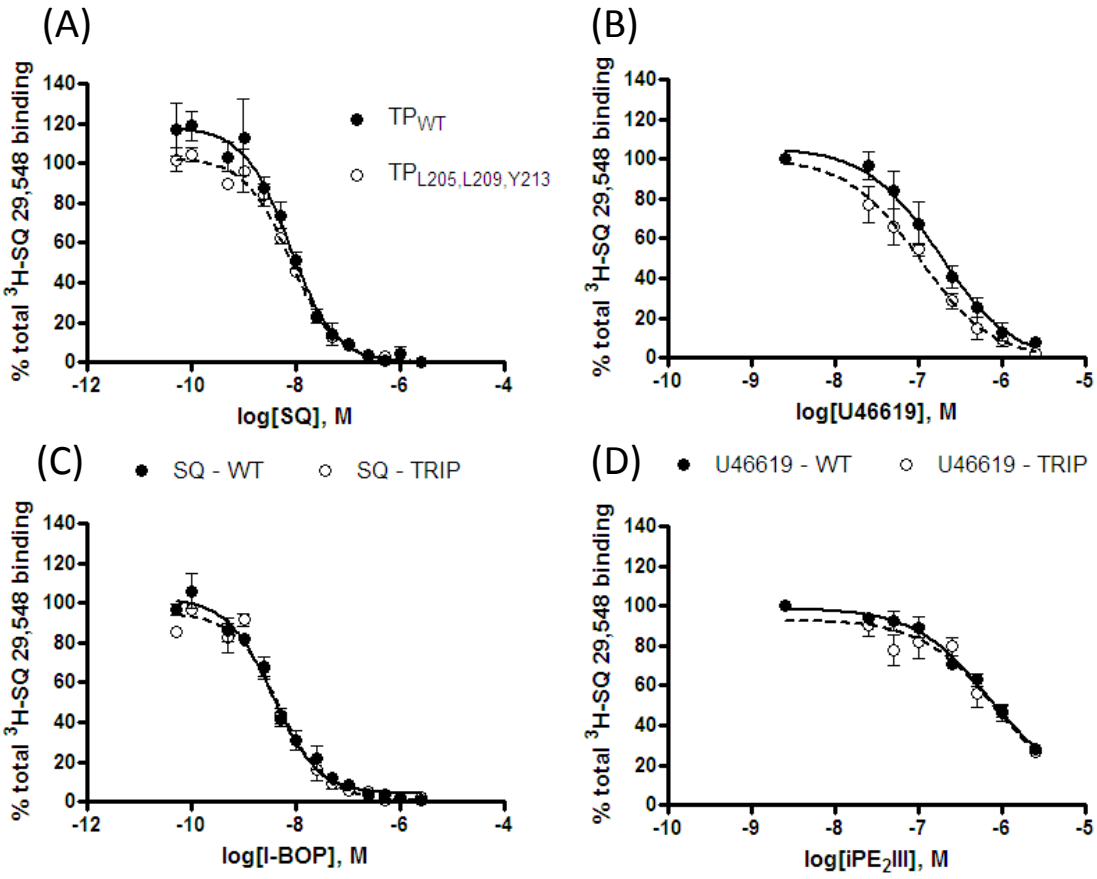

Figure 21: Displacement of ^{3}H-SQ 29,548 by Various Ligands. Displacement of ^{3}H-SQ 29,458 (TP antagonist) by SQ 29,548, the TP agonists U46619 or I-BOP or the isoprostane iPE$_2$III in HEK 293 cells transiently transfected with TP$_{WT}$ (closed circles) or TP$_{L205,L209,Y213}$ (open circles). Data are expressed as % of total binding (no displacer) and are mean ± SEM (n=3-8). No significant change in Ki values for displacement between TP$_{WT}$ and TP$_{L205,L209,Y213}$ was seen for any TP ligands used.

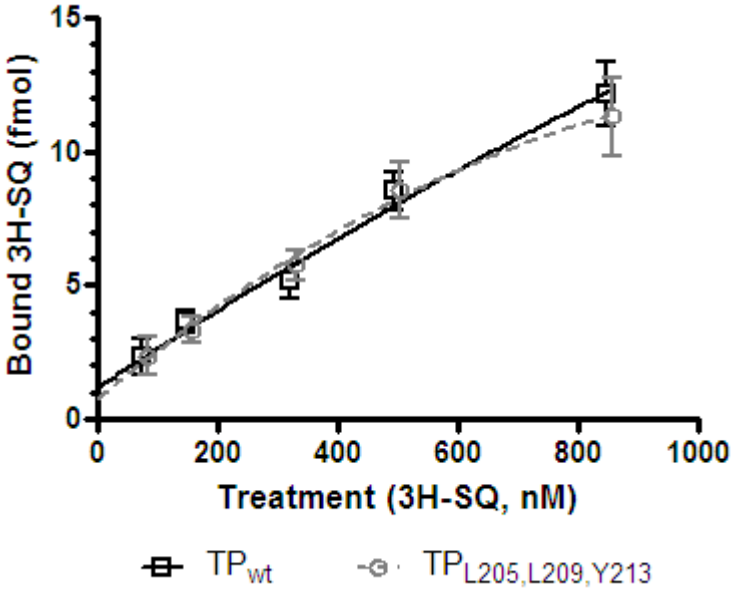

Figure 22: Binding of ^{3}H-SQ 29,548 to whole cells. Binding of ^{3}H-SQ 29,458 (TP antagonist) to whole HEK 293 cells transiently transfected with TP_{WT} (black squares) or $TP_{L205,L209,Y213}$ (grey circles). Data are expressed as fmol of bound antagonist and are mean ± SEM (n=5). No change seen in SQ 29,548 binding between TP_{WT} and $TP_{L205,L209,Y213}$ was seen up to maximum possible concentration (based upon solubility constraints).

however it is likely that a similar paradigm for the high affinity receptor state applies. In the radioligand displacement analyses discussed above, we included two TP agonists: U46619 and IBOP. The lack of difference in the K_i's for both agonists argues against a reduction in the affinity state of $TP_{L205,L209,Y213}$ for agonist, and thus against modified G_q as an explanation for suppressed signaling of the mutant.

To confirm normal G_q association of the $TP_{L205, L209, Y213}$, we performed co-immunoprecipitations in HEK 293 cells transiently transfected with either HA-tagged TP_{WT} or HA-tagged $TP_{L205,L209,Y213}$. Cells were lysed and passed over anti-HA tagged agarose beads, then probed with either anti-G_q antibody, or anti-TP antibody to determine the relative levels of TP within the samples. We observed that comparable levels of G_q co-immunoprecipitated with either TP_{WT} or $TP_{L205,L209,Y213}$ (Figure 23). Taken together with the radioligand displacement assay, these analyses indicate that mutation of the TM5 GxxxGxxxL motif in TP allows normal formation of the high affinity receptor-G_q complex at the cell surface.

Disruption of the TM5 GxxxGxxxL motif modifies TP homodimerization

As outlined in Chapter 1, and in previous reports from the laboratory, the TP physically associates to form homodimers (70, 122, 123). The molecular determinants of TP homodimerization have not been defined, nor has the precise role contribution homodimerization to TPα expression and function. However

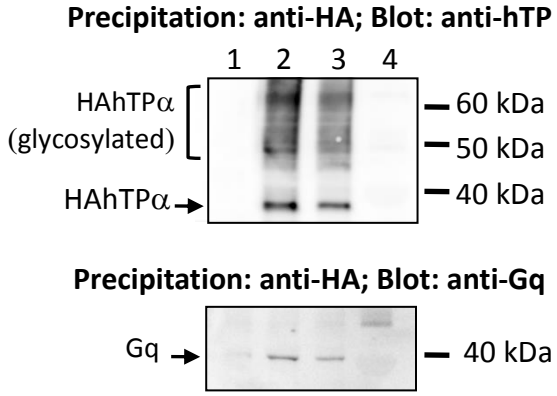

Figure 23: Co-immunoprecipitation of G_q with HA-TP_{WT} or HA-$TP_{L205,L209,Y213}$. Lysates from HEK 293 cells transfected with empty pcDNA3 (lane 1), HA-TP_{WT} (lane 2) or HA-$TP_{L205,L209,Y213}$ (lane 3) were subjected to immunoprecipitation with anti-HA. In lane 4 lysate is from E Coli expressing an unrelated HA-tagged control (HA-GST-PI3 kinase-SH2 domain; supplied by the manufacturer). The upper blot was stained with anti-TP antibody. Molecular species corresponding to unglycosylated TP and differentially glycosylated TP are indicated. The lower blot was probed with an anti-Gq antibody. A representative experiment, which was repeated with similar results, is shown. Densitometric quantification of Gq relative to HA-TP showed no difference between TP_{WT} and $TP_{L205,L209,Y213}$ transfected cells. Data are representative of n=3.

across GPCR studies, one or more TMs have been frequently implicated in dimer formation and function (107, 128, 137). Given the outward facing orientation of TP-TM5 GxxxGxxxL motif, thus positioned for intermolecular protein interaction, we examined whether homodimerization was modified in the $TP_{L205, L209, Y213}$ mutant. BRET studies were performed, using the optimized protocol outlined in Chapter 2, with TP_{WT} and $TP_{L205, L209, Y213}$ were fused at their C termini to either rLUC (energy donor) or YFP (energy acceptor) and energy transfer quantified as a measure of dimerization. As outlined in Chapter 2 (see Figure 6) in BRET saturation experiments, the donor-tagged receptor is held steady and the acceptor-tagged receptor (whose expression is quantified independently as fold over basal total YFP emission) is gradually increased. A saturable BRET curve indicates a specific interaction of the two protomers to form a dimer while the concentration of acceptor at which the BRET signal reaches 50%, the $BRET_{50}$, reflects the affinity of individual promoters for each other (169).

$TP_{L205, L209, Y213}$ retained the capacity to dimerize, however the $BRET_{50}$ for $TP_{L205, L209, Y213}$ homodimerization was significantly right shifted ($BRET_{50}$ = 1.83 ± 0.1, n=5) compared to the TP_{WT}-TP_{WT} ($BRET_{50}$ = 1.4 ± 0.08, n=4), indicating reduced efficiency in formation of the homodimer when the TM5 GxxxGxxxL motif was disrupted (Figure 24A,B, Figure 25). To confirm impaired homodimerization of the mutant receptor, BRET was measured in HEK 293 cells expressing a fixed ratio of rLuc-TP_{WT} + YFP-TP_{WT} (1:7) and competition by unfused TP_{WT} or $TP_{L205, L209, Y213}$ examined. As expected, TP_{WT} efficiently competed for the interaction of

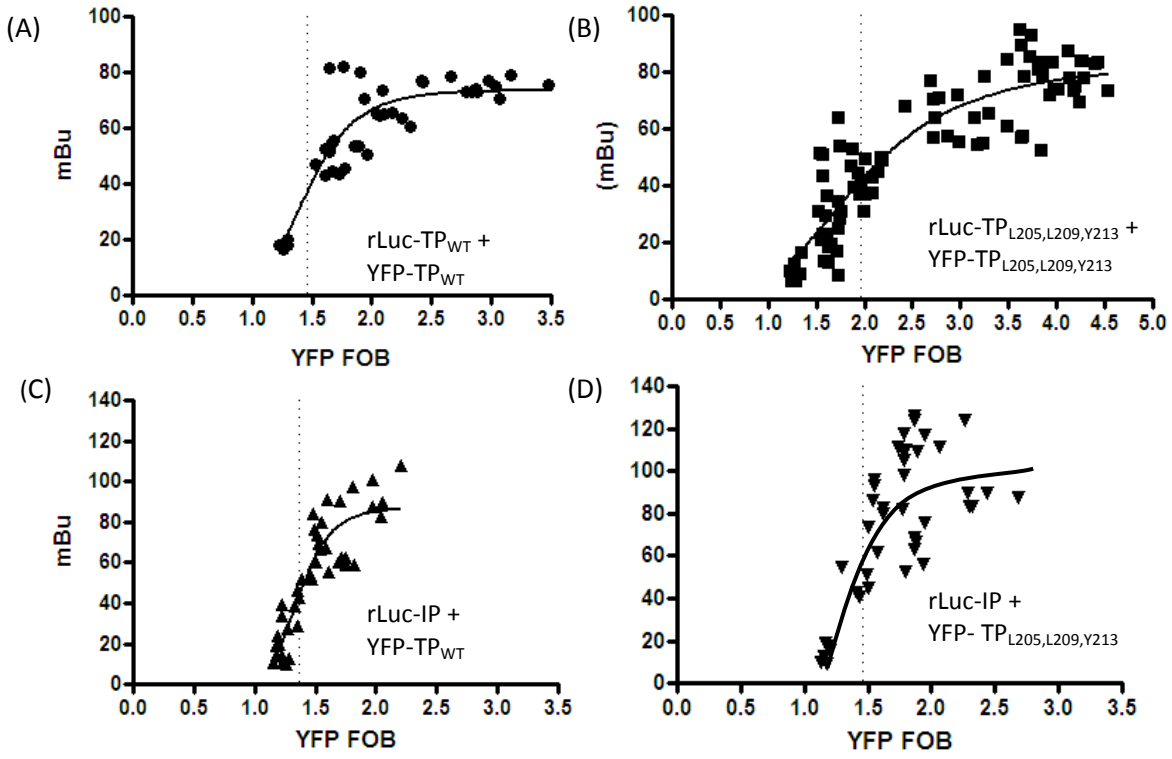

Figure 24: Homo- and hetero- dimerization of TP_{WT} and $TP_{L205,L209,Y213}$ by BRET. Saturable BRET was observed for rLuc- (donor, 0.25µg) + YFP- (acceptor, 0.125µg – 0.75µg) fused pairings of (A) TP_{WT}-TP_{WT}, (B) $TP_{L205,L209,Y213}$-$TP_{L205,L209,Y213}$ (C) IP_{WT} - TP_{WT} or (D) IP_{WT} - $TP_{L205,L209,Y213}$ in transiently transfected HEK 293 cells. Experiments are representative of n=4-6. Data are milli BRET units plotted against fold over basal total YFP emission (a measure of YFP-fused acceptor receptor expression). Individual $BRET_{50}$ values for are indicated by the dotted gray lines.

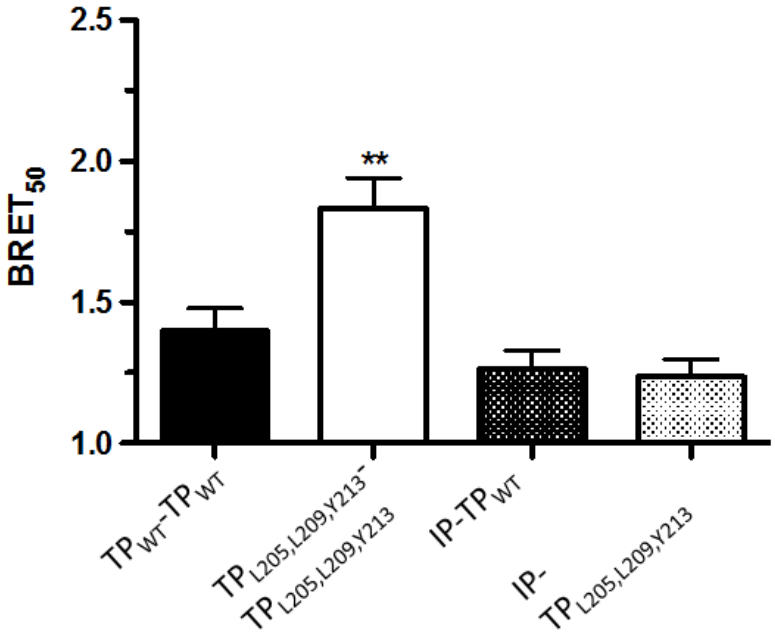

Figure 25: Quantification of homo- and hetero- dimerization of TP_{WT} and $TP_{L205,L209,Y213}$ by BRET. $BRET_{50}$ values were calculated from 4-6 individual BRET saturation experiments (as shown in Figure 24). Data are mean $BRET_{50}$ values ± SEM from n=4-6. **p<0.005 relative to all other data sets.

rLuc-TP_{WT} and YFP-TP_{WT} reducing the BRET signal in a concentration dependent manner. $TP_{L51, L54}$, in which the TP-ICL1 GxxxG motif, $G_{51}ARQG_{55}$, was mutated, was as efficient as the TP_{WT} in competition for rLuc-TP_{WT}-YFP-TP_{WT} interaction while, in contrast, $TP_{L205, L209, Y213}$ did not alter the BRET signal confirming its relative deficiency for dimer formation (Figure 26). Together these data indicate the importance of TP-TM5 GxxxGxxxL for efficient TP homodimerization and suggest that normal homodimerization may be critical for efficient signal transduction.

TM5 GGL domain disruption does not modify TPα-IP heterodimerization or function

The studies thus far indicate that the GxxxGxxxL motif in TM5 of the TPα is important for efficient homodimerization and that its disruption suppresses receptor signaling. As previously described (Chapter 1, Figure 15A), the TP can interact with the IP, a G_s-cAMP coupled receptor, to form a heterodimer (121). When heterodimerized with the IP, the TP's microdomain localization, signal transduction and regulation is markedly altered with reduced "normal" transduction of G_q-inositol phosphate signal in response to TP agonists and a concomitant switch to signal via the G_s-cAMP pathway in an IP-like manner (122). This signaling shift likely contributes to the restraint placed on the TP via the IP and to the increased risk of cardiovascular disease in individuals heterozygous for signaling deficient IP mutants (125).

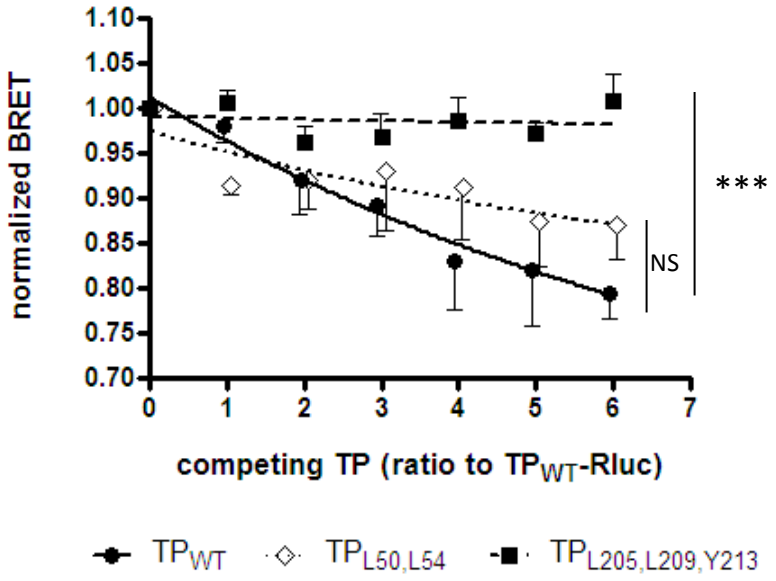

Figure 26: Competition of $TP_{L205,L209,Y213}$, $TP_{L50,L54}$, and TP_{WT} for binding with TP_{WT} by BRET. Competition for BRET in rLUC-TP_{WT} + YFP-TP_{WT} (constant 1:7 ratio) transfected HEK 293 cells by co-transfection with HA-TP_{WT}, HA-$TP_{L205,L209,Y213}$ or HA- $TP_{L51,L54}$. Data are normalized to BRET in rLUC-TP_{WT} + YFP-TP_{WT} transfected cells without co-transfection of a competing receptor (set to 1) and are mean ± sem of n=3-4. ***p<0.0001; ns = non significant.

We next asked whether disruption of the TP TM5 GxxxGxxxL motif modifies TPα-IP heterodimerization and what, if any, functional changes are seen within the paradigm of TP-IP-G_s signaling in response to TP activation. Interestingly, and in stark contrast to the homodimer studies, disruption the TM5 GxxxGxxxL motif did not modify heterodimerization of the TP with the IP – the BRET saturation curves and $BRET_{50}$ for $TP_{L205,\ L209,\ Y213}$-IP (1.24 ± 0.06, n=6) was indistinguishable from the TP_{WT}-IP ($BRET_{50}$ = 1.26 ± 0.06, n=6) (Figure 24C,D, Figure 25). Concordantly, U46619-induced cAMP generation, the signature "switch" in TP signaling from the G_q pathway to the G_s pathways, was not different between TP-IP and $TP_{L206\ L209,Y213}$-IP in transfected HEK 293 cells or MEG-01 cells (Figure 27). Thus, while the TM5 GxxxGxxxL motif appeared critical for efficient TP homodimerization and G_q-signaling, this motif did not contribute to TP-IP heterodimerization or function. These data support the concept that distinct molecular interactions drive the physical association of the TP-TP and TP-IP dimers and their downstream signaling.

A TM GxxxGxxxL motif is found in numerous class A GPCRs

Given that a TM GxxxGxxxL motif was functionally relevant in at least two other GPCRs, the ß2-adrenoreceptor and the α-factor yeast receptor (104, 115), we searched the SwissProt database (http://prosite.expasy.org/scanprosite/) for human GxxxGxxxL-containing GPCRs. Sixty-nine receptors were identified of which, after removal of olfactory (24 hits), taste (2 hits) and orphan (9 hits)

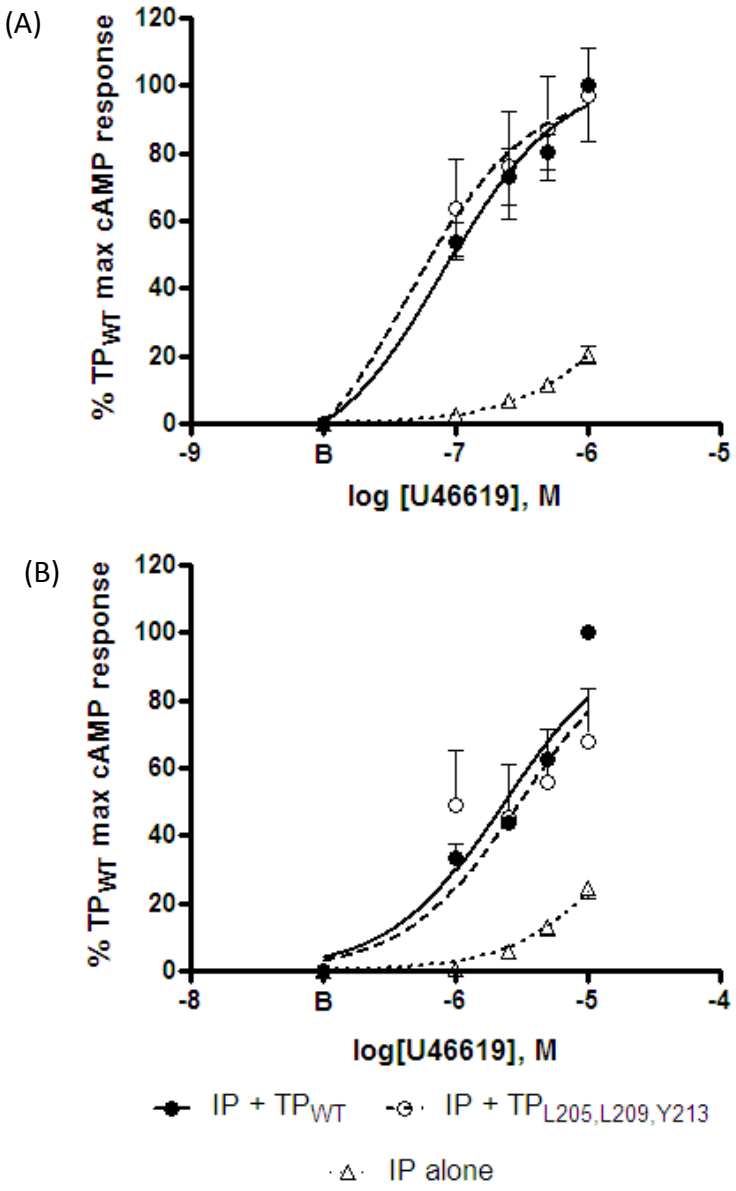

Figure 27: Cyclic AMP Signaling through TP$_{WT}$ or TP$_{L205,L209,Y213}$ heterodimerized with the IP. The TP agonist (U46619) simulated a robust cAMP response in (A) HEK 293 cells or (B) Meg-01 cells co-transfected with IP + TP$_{WT}$ (closed circles) or IP + TP$_{L205,L209,Y213}$ (open circles), compared to cells transfected with IP alone (open triangles). No difference in cAMP signaling was observed between IP+TP$_{WT}$ versus IP + TP$_{L205,L209,Y213}$ transfected cells in either model. Data are % of maximum cAMP response (in IP + TP$_{WT}$ transfectants) and are mean ± SEM of n=3-4.

receptors, 22 GPCRs were identified that contain one or more TM GxxxGxxxL motifs (Table 2). Interestingly, all but one of these 22 was Class A GPCRs suggesting a particular prevalence of this motif among rhodopsin-like GPCRs. The significance of this finding for potential novel therapeutic development is discussed in the following section.

A peptide targeted against a TM GxxxGxxxL motif modifies TP signaling

As previous mentioned, the GxxxGxxxL motif is significant to the function of other membrane proteins. One set of elegant studies explored targeting this TM motif in the αIIbβ3 integrin complex using a Computed Helical Anti-Membrane Protein (CHAMP peptide; Figure 28) intended to mimic the interaction of the individual integrin protomers. Interestingly, this peptide, termed β-CHAMP by its creators, modifies integrin function in transfected cells, micelles, and in platelets (128, 142). We obtained a quantity of this CHAMP and examined the impact on TP signaling. Treatment of HEK 293 cells transiently transfected with TP with 1 mM CHAMP peptide 30 minutes prior to U46619 stimulation led to a significant reduction in maximal signaling capacity (11.8 ± 3 % ($p<0.001$)) compared to control TPα-transfected cells (Figure 29). The small magnitude of the CHAMP effect likely reflects that this peptide was computationally designed to interact with a helical domain of the αII integrin, accounting for surrounding amino acids in the domain, and thus was not optimized to interact with the TP TM5 GxxxGxxxL domain. Despite this caveat, it was possible to pharmacologically

Table 2: Prevalence of the GxxxGxxxL motif in GPCR transmembrane domains. Prosite scan of the UniProt/SwissProt protein database (release 2013_01) for the motif G-x(3)-G-x(3)-L. Filters were set for species = homo sapiens, description = receptor and size >300 and <550.

Receptor	GPCR family	GxxxGxxxL Sequence	Residues	TM
5-hydroxytryptamine receptor 1A	A	**G**IIM**G**TFI**L**	348 - 356	6
5-hydroxytryptamine receptor 1E	A	**G**LIL**G**AFI**L**	294 - 302	6
5-hydroxytryptamine receptor 5A	A	**G**ILI**G**VFV**L**	288 - 296	6
12-(S)-hydroxy-5,8,10,14-eicosatetraenoic acid receptor	A	**G**LEC**G**LGL**L**	22 - 30	1
α1A adrenergic receptor	A	**G**VIL**G**GLI**L**	30 - 38	1
		GIVV**G**CFV**L**	275 - 283	6
α1B adrenergic receptor	A	**G**LVL**G**AFI**L**	49 - 57	1
		GIVV**G**MFI**L**	297 - 305	6
ß1 adrenergic receptor	A	**G**IIM**G**VFT**L**	327 - 335	6
ß2 adrenergic receptor	A	**G**IIM**G**TFT**L**	276 - 284	6
ß3 adrenergic receptor	A	**G**LIM**G**TFT**L**	295 - 303	6
Cannabinoid receptor 2	A	**G**SLA**G**ADF**L**	74 - 82	2
Galanin receptor type 2	A	**G**LIW**G**LSL**L**	147 - 155	4
Glucagon receptor	B	**G**IGW**G**APM**L**	269 - 277	4
Muscarinic acetylcholine receptor M1	A	**G**ITT**G**LLS**L**	29 - 37	1
Muscarinic acetylcholine receptor M5	A	**G**IMI**G**LAW**L**	148 - 156	4
Neuromedin-U receptor 1	A	**G**AVW**G**LAM**L**	183 - 191	4
Neuromedin-U receptor 2	A	**G**IVW**G**FSV**L**	168 - 176	4
Neuropeptide Y receptor type 2	A	**G**LAW**G**ISA**L**	170 - 178	4
Opsin-5	A	**G**FFF**G**CGS**L**	113 - 121	3
Oxoeicosanoid receptor 1	A	**G**LWV**G**ILL**L**	215 - 223	4
P2Y purinoceptor 4	A	**G**LLF**G**VPC**L**	206 - 214	5
Proteinase-activated receptor 4	A	**G**HMY**G**SVL**L**	158 - 166	3
Thromboxane A2 receptor	A	**G**LSV**G**LSF**L**	205 - 213	5

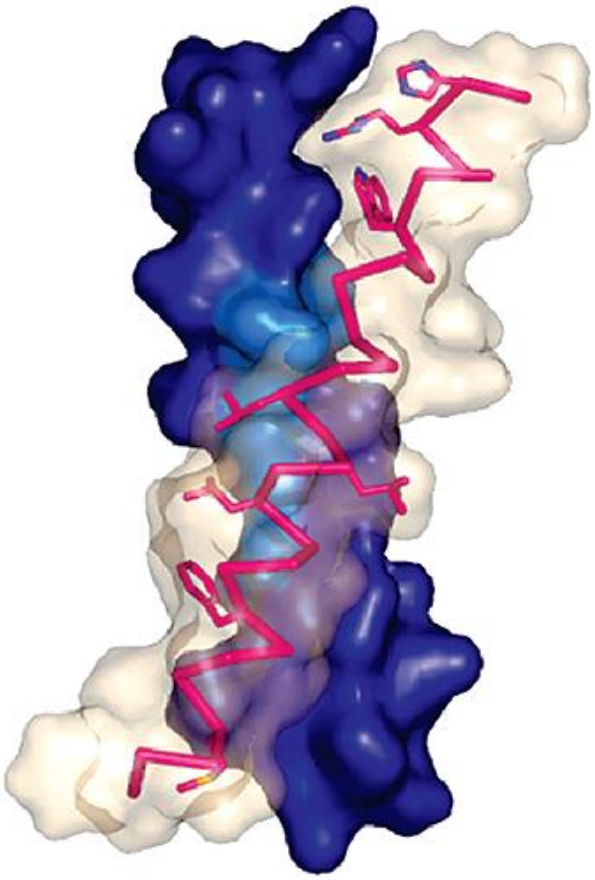

anti-α_{IIb} : NH_2 - KKAYVMLLPFFIGLLLG**LIF**
GGAFWGPARHLKK- $CONH_2$

Figure 28: The β-CHAMP peptide. Sequence of the anti-αIIb CHAMP peptide, and computational model of anti-αIIb bound to the αIIb TM domain. The model predicts that anti-αIIb (red stick: backbone, white: space filling) recognizes the "hot spot" on the αIIb-TM binding surface (light blue) with spatial complementarity at the helix-crossing site of the peptide and integrin. Adapted from: Caputo, G. A., R. I. Litvinov, W. Li, J. S. Bennett, W. F. Degrado, and H. Yin. 2008. Computationally designed peptide inhibitors of protein-protein interactions in membranes. *Biochemistry (Mosc.)*. 47: 8600–6.

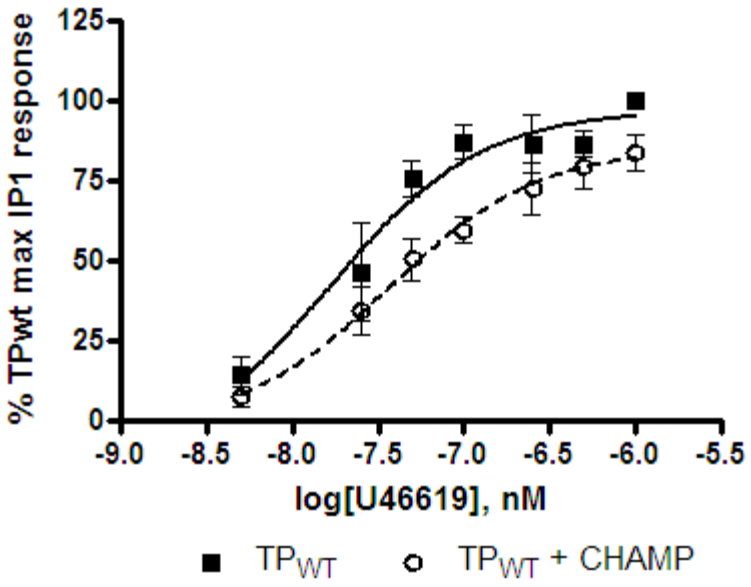

Figure 29: Inositol Phosphate Signaling through TP in presence of the β-CHAMP. Maximal inositol phosphate (InosP) generation was reduced by 11.8 ± 3 % ($p<0.001$) in TP_{WT} transfected HEK 293 cells treated with the CHAMP peptide (open circles) compared to untreated TP_{WT} transfected cells (closed circles) . There was no significant change in EC_{50}. Data are % of maximum response (in TP_{WT}) and are mean ± SEM; n=6.

replicate the signaling deficiency associated with mutation of the TP TM5 GxxxGxxxL, an encouraging result that opens the possibility that a TP TM5 GxxxGxxxL-designed peptide might provide a new approach to antagonize the TP.

Introduction of a peptide derived from the TP TM1 modifies receptor signaling

GPCR dimerization studies report the importance of TM1 for receptor dimerization. For the TP, TM1 was reported as relevant for heterodimerization of the TPα and TPß isoforms (170) although neither homodimer was examined. We developed an approach to examine how interference with TP TM1 can alter receptor function. An expression construct was designed to express the first transmembrane domain of the TP (TM1), comprising residues R_{23} through T_{59} and adding necessary elements to provide for constitutive, stable expression within the cell by virtue of insertion into the pNTAP vector (see Chapter 2, *Constructs, Pages 21-24*; Figure 4). HEK 293 cells were transiently transfected with TP_{WT} either alone or with the TM1 peptide and U46619-induced inositol phosphate signaling examined. Surprisingly, in preliminary studies, there was a significant increase in maximal signaling capacity (62.6%, n=2) when TP-TM1 was co-expressed compared to control (Figure 30), with no change in basal signaling. These early results provide evidence that introduction of a domain-targeted peptide can reduce TP signaling capacity, as with the CHAMP peptide,

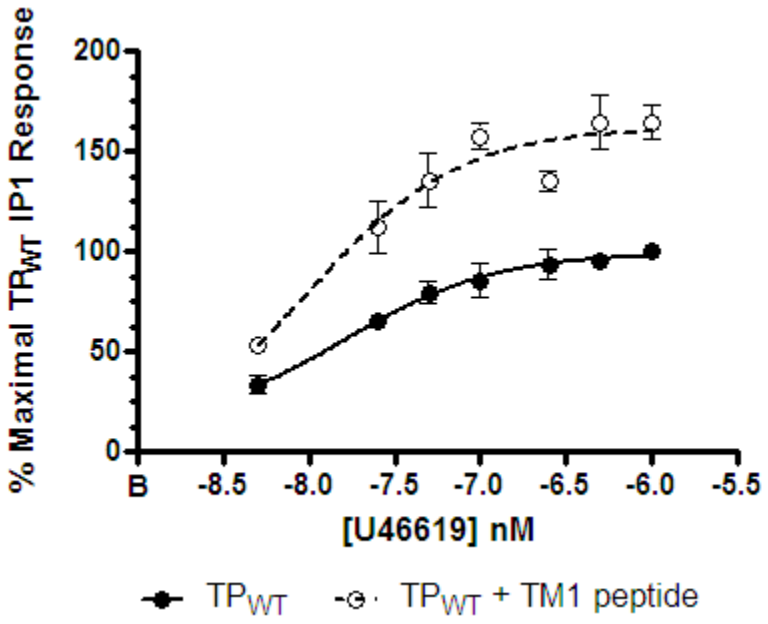

Figure 30: Inositol phosphate signaling through TP in presence of TM1 peptide. Maximal inositol phosphate (InosP) generation was increased in TP_{WT} cotransfected with the TP TM1 peptide (open circles) compared to TP_{WT} (closed circles) in transfected HEK 293 cells. Preliminary studies (n=2) are shown.

but also can positively impact signaling, underscoring the complexity of TP receptor function and the precise functional contribution of distinct receptor domains. Refined understanding of these processes may lead to development of targeted peptides or small molecular that modify receptor function in a precise and highly specific manner to give a desired effect.

CHAPTER 5: DISCUSSION

A role for homodimerization in TP regulation

Having established that there is no significant change in TP mRNA expression levels in response to short term receptor activation (Figure 12, Figure 13), we concluded that increased auto-upregulation of receptor surface expression was likely under post-translational control. We turned to the possibility of receptor homodimerization as a means of controlling receptor trafficking and expression. Reports vary as to the contribution of homodimerization to GPCR function, however there is substantial evidence that homodimerization is necessary for normal receptor surface expression (104, 109, 114, 118, 171, 172) and that a dimeric pair coupled to a single G protein forms the basic signaling unit (100, 108, 173). Dimerization-deficient GPCRs fail to traffic normally to the cell surface, while ER retained GPCRs can force ER retention of their WT counterparts in a dominant negative manner (115).

Given the published evidence for a regulatory role of homodimerization, together with previous work in the lab showing that the TPα appears on western blots of cell lysates at double the expected molecular weight, and that TPα and TPß co-immunoprecipitate in transfected cells (122), we directly assessed whether the TPα formed homodimers. There are significant caveats associated with the analysis of GCPR dimerization in broken cell preparations by immunoprecipitation and western blotting. For example, the use of detergents to disrupt cells can cause dimers to dissociate; however, a gentle disruption

process can allow aggregates to remain giving the appearance of dimeric species on western blot. A review of the many and varied methods used to detect receptor dimerization included such as western blotting, co-immunoprecipitation, cross-linking, FRET (a close relative of BRET but using a fluorescent donor instead of rLuc), yeast two-hybrid analysis, functional complementation, and crystallography (164). This comprehensive review also discussed the dangers of using highly disruptive methods of analysis, and those that did not employ the use of whole, live cells, and noted substantial caveats and limitations associated with many of the methods listed above.

We chose, therefore, to establish a method to examine TP dimerization in living cells by bioluminescence resonance energy transfer (BRET), a minimally invasive method that would generate minimal false positives and negatives derived from artifact. As outlined in Chapter 2 (Figure 8, Figure 10, Figure 11), we rigorously assessed the standard BRET assay for issues of signal stability and quantitative accuracy, ultimately developing a tightly controlled, sensitive BRET experimental platform to assess receptor dimerization in living cells. In advancing the BRET assay we determined that substrate stability, both in solution before addition to the cells and during the lag time while reading an entire 96 well plate, is a critical parameter that should be carefully assessed and controlled. In our hands, resting the substrate for 20 minutes and applying fresh substrate to a small number of wells immediately before collecting light emission markedly improved the internal consistency of the assay and reduced noise

sufficiently to allow precise analysis of dimer formation that may have been lost in the previous iteration of the BRET assay. While this approach still relies on transfection of receptors (fused to a donor or acceptor moiety) in standard cell lines, continuing improvement in antibodies to native receptors and development of labeled ligands is opening avenues to similarly precise assessment of native dimers.

Establishing that BRET occurs in donor/acceptor co-transfected cells is in itself insufficient evidence that physiologically relevant dimers are likely to form. BRET can occur non-specifically when donor and acceptor are co-expressed (so-called bystander BRET), or at such disproportionate levels of one promoter to the other that the physiological interaction is questionable.

Construction of a BRET saturation curve establishes specificity (saturation) and affinity (the $BRET_{50}$). In our work, BRET studies confirmed the formation of specific and saturable interaction of TPα with itself (Figure 14) with a high affinity indicating that the dimer may from in a physiological setting. It is worth noting that although we refer to this interaction as homodimerization, the BRET assay we used does not distinguish between dimers and high order oligomers and it remains an open question whether the number of receptors that associate is two or more and what relevance this may have for receptor regulation and function. We reasoned that, if homodimerization contributed to auto-upregulation of the TP in response to agonist activation, then dimerization would be modified (presumably increased) by agonist. However, analysis of agonist effects on TPα

homodimerization may have been confounded by a limitation of the BRET assay. To propagate signal, agonist binding relies upon changes in receptor conformation and such changes can shift the orientation of the donor and acceptor molecules within the dimer. Thus, a change in distance or orientation of the donor and acceptor can change the nature and magnitude of the resonance energy transfer reaction, confounding the output of the assay in an unpredictable manner. Indeed, although we did not observe changes in TP BRET in response to agonist treatment, significant changes were evident upon addition of antagonist treatment (Figure 17), suggesting that this BRET assay is not a reliable method to define agonist-dependent changes in dimerization. Being that homodimerization is linked to successful signaling, and that signaling is necessary for the auto-upregulation to occur, any successful assay would have to account for this tight intertwining of processes as well. Additionally, the increasing power of molecular modeling could be employed to gain some understanding of the ways in which ligand binding can alter the conformation of a target receptor, as has already been shown for the β(1)- and β(2)-adrenergic receptors (174). This, combined with knowledge of dimerization interfaces determined using molecular methods such as those we employed, could shed light on how ligand binding might influence receptor dimerization.

Thus, while it remains possible that TPα homodimerization contributes to its auto-upregulation in response to agonist, this has not yet been experimentally determined. Such a study could be carried out through the use of different

mutants of the TPα in future studies, including those that are retained in the ER, which might serve as a dominant negative to anchor a wild-type TP, reducing surface expression. However, the confounding effects of disrupted dimerization on agonist-dependent signaling raise substantial challenges for understanding how dimerization impacts ligand-dependent events downstream of the primary signal. Alternative approaches include the use of donor- or acceptor- labeled ligands or antibodies to the native receptors in which energy transfer might not be impacted by conformational changes in either or both receptors

Heterodimeric partners of the TPα and modification of signal transduction

Co-immunoprecipitation of TPα with the IP was reported previously in the lab (123). We also sought to examine, therefore, by BRET, the relative propensity of the TPα to heterodimerize with the IP, as well as other prostanoid receptors, a significant strength of the BRET assay compared to co-immunoprecipitation. We found that TPα forms high affinity heterodimers with the IP (Figure 15), a receptor that is distinct in its sequence (33.6% amino acid homology, FASTA alignment), membrane microdomain localization, regulation and effector signaling (94, 121–123). This highly suggestive evidence for TP-IP heterodimerization complements our previous observation that TP agonists evoke a PGI_2-IP like signal, cAMP generation, through the TP-IP heterodimer (Figure 27), coincident with suppressed canonical TP-inositol phosphate generation (5, 123). In addition, we also observed TP dimerization with the PGD_2 receptor, the DP1, although the

lower affinity for TP-DP1 interaction suggests that this heterodimeric species may form less readily that the TP-IP, given proper physiological conditions (Figure 15). However, it remains possible that TP-DP1 heterodimerization may form more readily in specific contexts including the relative expression levels of the different receptors (e.g. if IP is lower that DP1 or absent) or ligand activation of one of the receptors modifies heterodimerization processes (e.g. if DP1 activation increased its affinity for the TP). Such intricacies of the relative formation of TP containing heterodimers require further in-depth analyses and approaches other than BRET.

Our studies of TP-IP heterodimer signaling, which occurs in transfected and native cells (94, 121, 123), touch upon interesting concepts regarding asymmetrical signaling in dimeric pairs. With receptors like the dopamine D2 receptor (108), $GABA_B$ receptor (175), and the metabotropic glutamate receptor (176), whose basic signaling unit consists of a pair of GPCRs coupled to one G protein, signaling can occur asymmetrically through binding of ligand to the first protomer and subsequent activation of the G protein by the second protomer. This signaling modality would explain the how the TP-IP heterodimer can bind TP agonists (presumably at the TP binding site) while eliciting a G_s-mediated signaling response through asymmetric activation of the IP. While our work with the GxxxGxxL TP mutant supports the paradigm of asymmetric TP-IP signaling (see below), whether the TP homodimer signals asymmetrically remains to be experimentally determined.

Exploration of the role of the GxxxGxxxL motif in TP dimerization and function

Protein-protein interactions are ubiquitous to biological processes and are vital for signaling complex assembly. Compared to cytosolic protein regions, relatively little is known about the interaction of membrane embedded proteins within lipid bilayers, although there is substantial and increasing interest in therapeutic targeting of TM interactions (138). GPCRs are characterized by their 7 transmembrane spanning helical regions, which are capable of intramolecular interactions that define tertiary and quaternary receptor structure and function (177, 178). The GxxxG interaction motif, first described in homodimerization of the single TM sialglycoprotein glycophorin A (GpA), has been identified as a high frequency TM motif across diverse protein families (135, 179). In GpA, as in other transmembrane proteins, residues that neighbor the GxxxG domain appear critical and are thought to provide a three-dimensional structure within the TM helix creating the protein-protein interface. In one particular subclass, termed “glycine zippers”, a small residue (glycine, alanine or serine) is located 3 positions before or after the GxxxG motif (136). More generally, large residues (isoleucine, valine or leucine) are commonly found within 1 or 2 positions of the GxxxG pair (135), forming a groove (the glycines) and ridges (the large residues) arrangement. In the case of the TPα TM5 GxxxGxxxL motif, we determined a similar arrangement with a groove created by $S_{201}G_{205}G_{209}$ and a ridge created

leucines 203, 206, 210 and 213 (see Figure 31). The positioning of Leu_{213} three residues after the GxxxG pair serves to align the GGL triplet along the same α-helix face (see Figure 3) and was observed in multiple other Class A human GPCRs (Table 2), as well as α integrins (142).

To define its contribution to TPα function, we mutated the small-small-big arrangement of $G_{205}xxxG_{209}xxxL_{213}$ motif to $L_{205}xxxL_{209}xxxY_{213}$, similar to other studies of this specific motif (115, 139, 141, 142), an approach designed to disrupt the grove and ridge alignment along the outer-side of TM5 (see Figure 3, Figure 31). As outlined in Chapter 4, signaling of the $TP_{L205,L209,Y213}$ via the G_q-inositol phosphate cascade was markedly reduced in both transfected HEK 293 cells and Meg-01 platelet-like cells. Given the role of GxxxG motifs in helical packing (135), we considered that this loss of function might be due to improper processing of the correctly folded receptor at the cell surface. However, comparable cell surface expression of the wild type and TM5 GxxxGxxxL mutant receptor was evident by flow cytometry in both *in vitro* models (Figure 20) and no alteration in processing of the fully glycosylated receptor was evident by fluorescence microscopy (Figure 19) or immunoblotting (Figure 23). Further, displacement analysis using a range of TP ligands revealed no difference in the ligand binding properties of $TP_{L205,L209,213}$ compared TP_{WT} and both the mutant and WT receptor displayed high agonist affinity (Figure 21), consistent with normal G protein association and the comparable levels of G_q that accompanied the wild type or mutant receptor in co-immunoprecipitation experiments

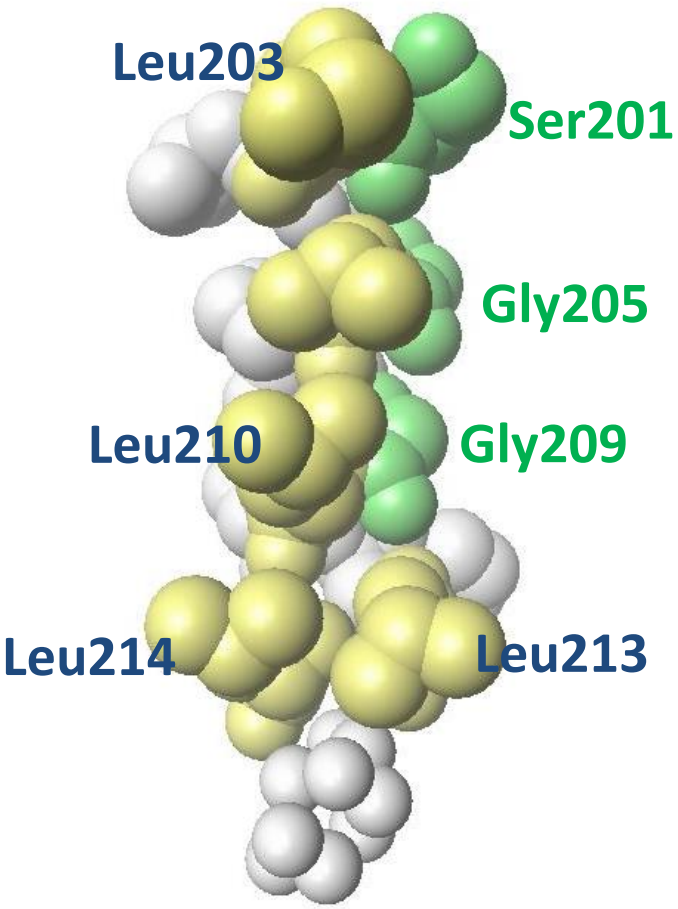

Figure 31: Modeling of the "groove and ridge" structure of the GxxxGxxxL motif. Modeling of the TPα TM5 highlighting the leucines that neighbor G_{205} and G_{209} and L_{213}. By analogy with glycophorin A, the small residues, S_{201}, G_{205} and G_{209}, align to create a groove (green), while the large residues L_{203}, L_{206}, L_{210} and L_{213} form an adjacent ridge (yellow). (Credit: Scott Gleim/Hwa Lab, Yale University School of Medicine)

(Figure 23). Together these analyses clearly indicate no major role for the TM5 GxxxGxxL motif in processing of the TPα to form a high affinity receptor-G_q complex at the cell surface.

Homodimerization of GPCRs appears universal across the superfamily (102, 119, 165). Given the established contribution of GxxxG motifs to helix-helix interactions, the extensive evidence that TMs are critical for GPCR homodimerization and the outward facing orientation of the $G_{205}xxxG_{209}xxxL_{213}$ triplet in TPα TM5 we considered whether this motif contributes to TPα homodimer formation. We found that while saturable BRET was achieved, the $BRET_{50}$ for $TP_{L205,L209,Y213}$ homodimerization was significantly right-shifted compared to TP_{WT} (Figure 24,Figure 25). Thus, while $TP_{L205L209Y213}$ protomers can dimerize, they do so with a reduced affinity. Importantly, we confirmed independently that $TP_{L205,L209,Y213}$ was unable to compete for TP_{WT}-TP_{WT} interaction, confirming the mutant's dimerization deficiency (Figure 26). Thus, similar to the ß2-AR (115, 130) and yeast α-factor (104, 180) receptors, a TM motif GxxxGxxxL is necessary for normal efficient TPα homodimerization.

In the case of ß2 adrenergic receptor, disruption of the TM6 GxxxGxxxL motif right shifted the $BRET_{50}$ for homodimerization coincident with reduced cell surface receptor expression (115). Our data showing normal processing (Figure 19), cell surface expression (Figure 20) and G protein association of $TP_{L205,L209,Y213}$ (Figure 23) despite impaired dimerization suggests that for the TPα the two processes, homodimerization and cell surface expression, are

independent. Alternatively, it may be that the level of $TP_{L205,L209,Y213}$ homodimerizes sufficiently to traffic to the cell surface but that the reduced protomer affinity significantly modifies the efficiency with which signal is transduced. Our data does not reveal how activation of G_q via $TP_{L205L209Y213}$ is reduced but one possibility is the formation of a suboptimal conformation of the $TP_{L205L209Y213}$ homodimer, impacting the receptor dimer's ability to undergo the necessary conformational shift to fully activate G_q.

Having determined that the $G_{205}xxxG_{209}xxxL_{213}$ motif does in fact play a significant role in TP homodimer formation and function, we also were interested in evaluating the effects of mutation of this motif on the TP/IP heterodimer. Interestingly, mutation of the $G_{205}xxxG_{209}xxxL_{213}$ motif did not impact either heterodimerization with the IP, or TP agonist-induced cAMP generation through the heterodimer. BRET assays showed no significant change in $BRET_{50}$ for the TP-IP heterodimer upon substitution of $TP_{L205,L209,213}$ for TP_{WT}, and the mutant TPα allowed for activation along the TPα-IP-G_s pathway in response to TP agaonist with no changes in maximal signaling or EC_{50}. Thus, it appears that the TPα TM5 GxxxGxxxL motif contributes selectively to homodimerization and that distinct receptor regions direct formation of the TPα-IP heterodimer. Further, the normal TP-agonist-cAMP signal propagated by the $TP_{L205,L209,213}$-IP heterodimer supports the concept of asymmetric signaling (see below).

Promise of the GGL as a target for future therapeutics

It has been over a decade since the GPCR dimerization was first reported (181–183). Since that time, much has been learned about the molecular mechanisms of GPCR dimerization and the biological relevance for receptor function. The most well established model of GPCR dimerization holds that two receptors couple to one G protein (108, 173). In heterodimers, one promoter typically dominates the downstream signal transduced, and hence the biological outcome (108). For example, in heterodimers of the B2 receptor for the vasorelaxant bradykinin and the AT1 receptor for the vasoconstrictor angiotensin II, the latter dominates leading to enhanced AT1-Gq signaling and vasoconstriction (105, 165). It remains unclear whether ligation of one or both protomers is optimal and to what extent G protein activation is symmetrical (the agonist activates the protomer that is directly associated with the G protein) or asymmetrical (the agonist indirectly activates the G protein through the non-G protein associated protomer) (103, 173). In the case of the serotonin type 4 receptor homodimer, evidence supports asymmetrical G protein activation through one ligand binding to its protomer but activating signaling via the companion protomer (173). For the TPα-IP, we established that the IP dominates the heterodimer's signaling through the G_s-cAMP cascade but that agonists for either protomer could activate the complex (123). Our observations that the TM5 GxxxGxxxL mutant did not support normal G_q-inositol phosphate signaling in the homodimer but was fully capable of propagating a normal cAMP response to TP agonist in the IPTPα heterodimer, provides further support for the 2-receptors-1-G-protein model and

for asymmetrical G protein activation through one protomer in a dimeric complex (in this case agonism of the TPα led to activation of the IP-associated Gs in the TPα-IP heterodimer).

We reported that the shift in TPα function to G_s signaling when dimerized with the IP likely contributes to the restraint placed by the PGI_2-IP system and the TXA_2-TP system in vivo (102, 115, 124). It is, therefore, very promising to uncover a molecular region the selectively reduces TP homodimer function without altering activation and signaling of TPα-IP heterodimer. Efforts to antagonize the TP have proved clinically disappointing (12, 147), perhaps because TP antagonists block activation of the TP in both its TP-TP homodimeric (G_q-coupled) and TP-IP heterodimeric (G_s-coupled) complexes (102). Our work opens novel avenues to biased interference with the TP-TP homodimer while sparing the function of the TP-IP heterodimer and its beneficial cardiovascular biological effects. Arguably, such an approach should be superior to inhibitors of thromboxane synthase, and even selective inhibition of platelet COX-1 with low dose aspirin, because the endogenous ligand acting at the TP-IP heterodimer would be spared.

Recently, computationally designed peptides directed at the GxxxGxxxL motif that mediates interaction of the αIIbβ3 integrins were reported to modify integrin function in platelets (128, 142). We propose that such a peptide targeted at TP TM5 GxxxGxxxL domain may provide a novel approach to biased TP antagonism. Conceivably, such selective targeting of the TP homodimer would allow us to modify signaling in cell types with high TP-TP expression, such as

platelets, while largely preserving the function of cells that have a higher TP-IP dimer population, such as macrophages (125).

It is also worth considering the promise of the GxxxGxxxL domain in light of our examination of the motif's presence in other GPCRs (Table 2). In our analysis of 114 GPRCs, a TM GxxxGxxxL motif was identified in 22 receptors including the TPα. The conservation of this sequence within the transmembrane domains of other receptors underscores its likely importance as a specialized interaction motif, as does the lack of incidence of SNPs appearing within this motif in the TP, in contrast to the large number of coding SNPs reported elsewhere in the receptor (184). This motif may play a similar role in dimerization of other protein-protein interaction for the 21 other receptors identified, a topic for future studies. It may be that this motif provides a "druggable" target for the development of a new class of precisely tailored therapeutics for specific receptor dimers. The prevalence of the motif suggests that it is common enough to be worth pursuing, while uncommon enough to limit off-target effects with rationale design of the targeted peptide or molecule. Indeed, exciting advances in computational design of peptides to precisely target the TM domains (128) open the possibility of design novel reagents that can selectively target the TP TM5 GxxxGxxxL domain, and by extension other TM domains in GPCRs of interest, while minimizing the effects of such interference in nearby receptors that also contain the functional domain. Such precise tools may allow assessment of native GPCR dimers in relevant normal cells, without the need for addition of an energy donor

or acceptor moiety and expression in a non-native cell line, and in animal models of normal and disease receptor function. Perhaps more importantly, precise targeting of a specific receptor domain, modifying one signaling arm, may allow development of a novel class of therapeutics designed to bias receptor function toward a desired beneficial outcome.

BIBLIOGRAPHY

1. Simmons, D. L., R. M. Botting, and T. Hla. 2004. Cyclooxygenase isozymes: the biology of prostaglandin synthesis and inhibition. *Pharmacol Rev*. **56**: 387–437.

2. Smith, W. L., and R. Langenbach. 2001. Why there are two cyclooxygenase isozymes. *J Clin Invest*. **107**: 1491–5.

3. Smyth, E. M., and G. A. FitzGerald. 2009. *In* Handbook of Cell Signaling. Second Edition (Bradshaw, R. A., and Dennis, E. A., eds.). pp. 1219–1228. , Academic Press, UK.

4. Hamberg, M., J. Svensson, and B. Samuelsson. 1975. Thromboxanes: a new group of biologically active compounds derived from prostaglandin endoperoxides. *Proc. Natl. Acad. Sci. U. S. A.* **72**: 2994–2998.

5. Rocca, B., P. Secchiero, G. Ciabattoni, F. O. Ranelletti, L. Catani, L. Guidotti, E. Melloni, N. Maggiano, G. Zauli, and C. Patrono. 2002. Cyclooxygenase-2 expression is induced during human megakaryopoiesis and characterizes newly formed platelets. *Proc Natl Acad Sci U S*. **99**: 7634–9.

6. McAdam, B. F., I. A. Mardini, A. Habib, A. Burke, J. A. Lawson, S. Kapoor, and G. A. FitzGerald. 2000. Effect of regulated expression of human cyclooxygenase isoforms on eicosanoid and isoeicosanoid production in inflammation. *J Clin Invest*. **105**: 1473–82.

7. Ding, X., and P. A. Murray. 2005. Cellular mechanisms of thromboxane A2-mediated contraction in pulmonary veins. *Am J Physiol Lung Cell Mol Physiol*. **289**: L825–33.

8. Kobayashi, T., Y. Tahara, M. Matsumoto, M. Iguchi, H. Sano, T. Murayama, H. Arai, H. Oida, T. Yurugi-Kobayashi, J. K. Yamashita, H. Katagiri, M. Majima, M. Yokode, T. Kita, and S. Narumiya. 2004. Roles of thromboxane A(2) and prostacyclin in the development of atherosclerosis in apoE-deficient mice. *J Clin Invest*. **114**: 784–94.

9. Winn, R., J. Harlan, B. Nadir, L. Harker, and J. Hildebrandt. 1983. Thromboxane A2 mediates lung vasoconstriction but not permeability after endotoxin. *J. Clin. Invest.* **72**: 911–918.

10. Ishizuka, T., M. Kawakami, T. Hidaka, Y. Matsuki, M. Takamizawa, K. Suzuki, A. Kurita, and H. Nakamura. 1998. Stimulation with thromboxane A2 (TXA2) receptor

agonist enhances ICAM-1, VCAM-1 or ELAM-1 expression by human vascular endothelial cells. *Clin Exp Immunol*. **112**: 464–70.

11. Nie, D., M. Lamberti, A. Zacharek, L. Li, K. Szekeres, K. Tang, Y. Chen, and K. V. Honn. 2000. Thromboxane A(2) regulation of endothelial cell migration, angiogenesis, and tumor metastasis. *Biochem Biophys Res Commun*. **267**: 245–51.

12. Smyth, E. M. 2010. Thromboxane and the thromboxane receptor in cardiovascular disease. *Clin Lipidol*. **5**: 209–219.

13. FitzGerald, G. A. 1991. Mechanisms of platelet activation: thromboxane A2 as an amplifying signal for other agonists. *Am J Cardiol*. **68**: 11B–15B.

14. Katugampola, S. D., and A. P. Davenport. 2001. Thromboxane receptor density is increased in human cardiovascular disease with evidence for inhibition at therapeutic concentrations by the AT(1) receptor antagonist losartan. *Br J Pharmacol*. **134**: 1385–92.

15. Dorn, G. W., N. Liel, J. L. Trask, D. E. Mais, M. E. Assey, and P. V. Halushka. 1990. Increased platelet thromboxane A2/prostaglandin H2 receptors in patients with acute myocardial infarction. *Circulation*. **81**: 212–8.

16. FitzGerald, G. A., J. Tigges, P. Barry, and J. A. Lawson. 1997. Markers of platelet activation and oxidant stress in atherothrombotic disease. *Thromb Haemost*. **78**: 280–4.

17. Ridker, P. M., N. R. Cook, I. M. Lee, D. Gordon, J. M. Gaziano, J. E. Manson, C. H. Hennekens, and J. E. Buring. 2005. A randomized trial of low-dose aspirin in the primary prevention of cardiovascular disease in women. *N Engl J Med*. **352**: 1293–304.

18. Sanmuganathan, P. S., P. Ghahramani, P. R. Jackson, E. J. Wallis, and L. E. Ramsay. 2001. Aspirin for primary prevention of coronary heart disease: safety and absolute benefit related to coronary risk derived from meta-analysis of randomised trials. *Heart*. **85**: 265–71.

19. Collaborative meta-analysis of randomised trials of antiplatelet therapy for prevention of death, myocardial infarction, and stroke in high risk patients. 2002. *BMJ*. **324**: 71–86.

20. Collaborative overview of randomised trials of antiplatelet therapy--I: Prevention of death, myocardial infarction, and stroke by prolonged antiplatelet therapy in

various categories of patients. Antiplatelet Trialists' Collaboration. 1994. *BMJ*. **308**: 81–106.

21. Cheng, Y., S. C. Austin, B. Rocca, B. H. Koller, T. M. Coffman, T. Grosser, J. A. Lawson, and G. A. FitzGerald. 2002. Role of prostacyclin in the cardiovascular response to thromboxane A2. *Science*. **296**: 539–41.

22. Rudic, R. D., D. Brinster, Y. Cheng, S. Fries, W. L. Song, S. Austin, T. M. Coffman, and G. A. FitzGerald. 2005. COX-2-derived prostacyclin modulates vascular remodeling. *Circ Res*. **96**: 1240–7.

23. Egan, K. M., M. Wang, S. Fries, M. B. Lucitt, A. M. Zukas, E. Pure, J. A. Lawson, and G. A. FitzGerald. 2005. Cyclooxygenases, thromboxane, and atherosclerosis: plaque destabilization by cyclooxygenase-2 inhibition combined with thromboxane receptor antagonism. *Circulation*. **111**: 334–42.

24. Audoly, L. P., B. Rocca, J. E. Fabre, B. H. Koller, D. Thomas, A. L. Loeb, T. M. Coffman, and G. A. FitzGerald. 2000. Cardiovascular responses to the isoprostanes iPF(2alpha)-III and iPE(2)-III are mediated via the thromboxane A(2) receptor in vivo. *Circulation*. **101**: 2833–40.

25. Smyth, S. S., D. S. Woulfe, J. I. Weitz, C. Gachet, P. B. Conley, S. G. Goodman, M. T. Roe, A. Kuliopulos, D. J. Moliterno, P. A. French, S. R. Steinhubl, and R. C. Becker. 2009. G-protein-coupled receptors as signaling targets for antiplatelet therapy. *Arter. Thromb Vasc Biol*. **29**: 449–57.

26. Vilahur, G., L. Casani, and L. Badimon. 2007. A thromboxane A2/prostaglandin H2 receptor antagonist (S18886) shows high antithrombotic efficacy in an experimental model of stent-induced thrombosis. *Thromb Haemost*. **98**: 662–9.

27. Bal Dit Sollier, C., I. Crassard, G. Simoneau, J. F. Bergmann, M. G. Bousser, and L. Drouet. 2009. Effect of the thromboxane prostaglandin receptor antagonist terutroban on arterial thrombogenesis after repeated administration in patients treated for the prevention of ischemic stroke. *Cerebrovasc Dis*. **28**: 505–13.

28. Blackman, S. C., G. Dawson, K. Antonakis, and G. C. Le Breton. 1998. The identification and characterization of oligodendrocyte thromboxane A2 receptors. *J. Biol. Chem.* **273**: 475–483.

29. Obara, Y., H. Kurose, and N. Nakahata. 2005. Thromboxane A2 promotes interleukin-6 biosynthesis mediated by an activation of cyclic AMP-response element-

binding protein in 1321N1 human astrocytoma cells. *Mol. Pharmacol.* **68**: 670–679.

30. Yalcin, M., S. Cavun, M. S. Yilmaz, and V. Savci. 2006. Activation of the central cholinergic system mediates the reversal of hypotension by centrally administrated U-46619, a thromboxane A2 analog, in hemorrhaged rats. *Brain Res.* **1118**: 43–51.

31. Honma, S., M. Saika, S. Ohkubo, H. Kurose, and N. Nakahata. 2006. Thromboxane A2 receptor-mediated G12/13-dependent glial morphological change. *Eur. J. Pharmacol.* **545**: 100–108.

32. Kitiyakara, C., W. J. Welch, J. G. Verbalis, and C. S. Wilcox. 2002. Role of thromboxane receptors in the dipsogenic response to central angiotensin II. *Am. J. Physiol. Regul. Integr. Comp. Physiol.* **282**: R865–869.

33. Orr, J. A., M. Ernst, J. Carrithers, and H. W. Shirer. 1990. Cardiopulmonary responses to HCl infusion are mediated by thromboxane A2 but not by serotonin. *Respir. Physiol.* **80**: 203–217.

34. Karla, W., H. Shams, J. A. Orr, and P. Scheid. 1992. Effects of the thromboxane A2 mimetic, U46,619, on pulmonary vagal afferents in the cat. *Respir. Physiol.* **87**: 383–396.

35. Kenagy, J., J. VanCleave, L. Pazdernik, and J. A. Orr. 1997. Stimulation of group III and IV afferent nerves from the hindlimb by thromboxane A2. *Brain Res.* **744**: 175–178.

36. Minami, K., and C. Kamei. 2004. A chronic model for evaluating the itching associated with allergic conjunctivitis in rats. *Int. Immunopharmacol.* **4**: 101–108.

37. Spurney, R. F., J. J. Onorato, F. J. Albers, and T. M. Coffman. 1993. Thromboxane binding and signal transduction in rat glomerular mesangial cells. *Am. J. Physiol.* **264**: F292–299.

38. Bruggeman, L. A., E. A. Horigan, S. Horikoshi, P. E. Ray, and P. E. Klotman. 1991. Thromboxane stimulates synthesis of extracellular matrix proteins in vitro. *Am. J. Physiol.* **261**: F488–494.

39. Mené, P., G. R. Dubyak, A. Scarpa, and M. J. Dunn. 1991. Regulation of cytosolic pH of cultured mesangial cells by prostaglandin F2 alpha and thromboxane A2. *Am. J. Physiol.* **260**: C159–166.

40. Spurney, R. F., P. Y. Fan, P. Ruiz, F. Sanfilippo, D. S. Pisetsky, and T. M. Coffman. 1992. Thromboxane receptor blockade reduces renal injury in murine lupus nephritis. *Kidney Int.* **41**: 973–982.

41. Kobayashi, T., J. Suzuki, M. Watanabe, S. Suzuki, K. Yoshida, K. Kume, and H. Suzuki. 1997. Changes in platelet calcium concentration by thromboxane A2 stimulation in patients with nephrotic syndrome of childhood. *Nephron*. **77**: 309–314.

42. Ushikubi, F., Y. Aiba, K. Nakamura, T. Namba, M. Hirata, O. Mazda, Y. Katsura, and S. Narumiya. 1993. Thromboxane A2 receptor is highly expressed in mouse immature thymocytes and mediates DNA fragmentation and apoptosis. *J. Exp. Med.* **178**: 1825–1830.

43. Kabashima, K., T. Murata, H. Tanaka, T. Matsuoka, D. Sakata, N. Yoshida, K. Katagiri, T. Kinashi, T. Tanaka, M. Miyasaka, H. Nagai, F. Ushikubi, and S. Narumiya. 2003. Thromboxane A2 modulates interaction of dendritic cells and T cells and regulates acquired immunity. *Nat. Immunol.* **4**: 694–701.

44. Martin, C., S. Uhlig, and V. Ullrich. 2001. Cytokine-induced bronchoconstriction in precision-cut lung slices is dependent upon cyclooxygenase-2 and thromboxane receptor activation. *Am. J. Respir. Cell Mol. Biol.* **24**: 139–145.

45. Takayama, K., K. Yuhki, K. Ono, T. Fujino, A. Hara, T. Yamada, S. Kuriyama, H. Karibe, Y. Okada, O. Takahata, T. Taniguchi, T. Iijima, H. Iwasaki, S. Narumiya, and F. Ushikubi. 2005. Thromboxane A2 and prostaglandin F2alpha mediate inflammatory tachycardia. *Nat. Med.* **11**: 562–566.

46. Miller, A. M., M. Masrorpour, C. Klaus, and J. X. Zhang. 2007. LPS exacerbates endothelin-1 induced activation of cytosolic phospholipase A2 and thromboxane A2 production from Kupffer cells of the prefibrotic rat liver. *J. Hepatol.* **46**: 276–285.

47. Nagai, H., H. Teramachi, and T. Tuchiya. 2006. Recent advances in the development of anti-allergic drugs. *Allergol. Int. Off. J. Jpn. Soc. Allergol.* **55**: 35–42.

48. Tanaka, K., M. H. Roberts, N. Yamamoto, H. Sugiura, M. Uehara, X.-Q. Mao, T. Shirakawa, and J. M. Hopkin. 2002. Genetic variants of the receptors for thromboxane A2 and IL-4 in atopic dermatitis. *Biochem. Biophys. Res. Commun.* **292**: 776–780.

49. Shirasaki, H., M. Kikuchi, N. Seki, E. Kanaizumi, K. Watanabe, and T. Himi. 2007. Expression and localization of the thromboxane A2 receptor in human nasal mucosa. *Prostaglandins Leukot. Essent. Fatty Acids*. **76**: 315–320.

50. Michel, F., J.-S. Silvestre, L. Waeckel, S. Corda, T. Verbeuren, J. P. Vilaine, M. Clergue, M. Duriez, and B. I. Levy. 2006. Thromboxane A2/prostaglandin H2 receptor activation mediates angiotensin II-induced postischemic neovascularization. *Arterioscler. Thromb. Vasc. Biol.* **26**: 488–493.

51. Nakahata, N. 2008. Thromboxane A2: physiology/pathophysiology, cellular signal transduction and pharmacology. *Pharmacol Ther*. **118**: 18–35.

52. Coyle, A. T., S. M. Miggin, and B. T. Kinsella. 2002. Characterization of the 5' untranslated region of alpha and beta isoforms of the human thromboxane A2 receptor (TP). Differential promoter utilization by the TP isoforms. *Eur. J. Biochem. FEBS*. **269**: 4058–4073.

53. Coyle, A. T., and B. T. Kinsella. 2005. Characterization of promoter 3 of the human thromboxane A receptor gene. A functional AP-1 and octamer motif are required for basal promoter activity. *FEBS J.* **272**: 1036–1053.

54. Parent, J. L., P. Labrecque, M. Driss Rochdi, and J. L. Benovic. 2001. Role of the differentially spliced carboxyl terminus in thromboxane A2 receptor trafficking: identification of a distinct motif for tonic internalization. *J Biol Chem*. **276**: 7079–85.

55. Vezza, R., A. Habib, and G. A. FitzGerald. 1999. Differential signaling by the thromboxane receptor isoforms via the novel GTP-binding protein, Gh. *J. Biol. Chem.* **274**: 12774–12779.

56. Hirata, T., F. Ushikubi, A. Kakizuka, M. Okuma, and S. Narumiya. 1996. Two thromboxane A2 receptor isoforms in human platelets. Opposite coupling to adenylyl cyclase with different sensitivity to Arg60 to Leu mutation. *J. Clin. Invest.* **97**: 949–956.

57. Hamelin, E., C. Thériault, G. Laroche, and J.-L. Parent. 2005. The intracellular trafficking of the G protein-coupled receptor TPbeta depends on a direct interaction with Rab11. *J. Biol. Chem.* **280**: 36195–36205.

58. Reid, H. M., and B. T. Kinsella. 2003. The alpha, but not the beta, isoform of the human thromboxane A2 receptor is a target for nitric oxide-mediated desensitization. Independent modulation of Tp alpha signaling by nitric oxide and prostacyclin. *J. Biol. Chem.* **278**: 51190–51202.

59. Miggin, S. M., and B. T. Kinsella. 2002. Regulation of extracellular signal-regulated kinase cascades by alpha- and beta-isoforms of the human thromboxane A(2) receptor. *Mol. Pharmacol.* **61**: 817–831.

60. Ashton, A. W., and J. A. Ware. 2004. Thromboxane A2 receptor signaling inhibits vascular endothelial growth factor-induced endothelial cell differentiation and migration. *Circ. Res.* **95**: 372–379.

61. Ashton, A. W., Y. Cheng, A. Helisch, and J. A. Ware. 2004. Thromboxane A2 receptor agonists antagonize the proangiogenic effects of fibroblast growth factor-2: role of receptor internalization, thrombospondin-1, and alpha(v)beta3. *Circ. Res.* **94**: 735–742.

62. Benndorf, R. A., E. Schwedhelm, A. Gnann, R. Taheri, G. Kom, M. Didié, A. Steenpass, S. Ergün, and R. H. Böger. 2008. Isoprostanes inhibit vascular endothelial growth factor-induced endothelial cell migration, tube formation, and cardiac vessel sprouting in vitro, as well as angiogenesis in vivo via activation of the thromboxane A(2) receptor: a potential link between oxidative stress and impaired angiogenesis. *Circ. Res.* **103**: 1037–1046.

63. Daniel, T. O., H. Liu, J. D. Morrow, B. C. Crews, and L. J. Marnett. 1999. Thromboxane A2 is a mediator of cyclooxygenase-2-dependent endothelial migration and angiogenesis. *Cancer Res.* **59**: 4574–4577.

64. Namba, T., Y. Sugimoto, M. Hirata, Y. Hayashi, A. Honda, A. Watabe, M. Negishi, A. Ichikawa, and S. Narumiya. 1992. Mouse thromboxane A2 receptor: cDNA cloning, expression and northern blot analysis. *Biochem Biophys Res Commun*. **184**: 1197–203.

65. Armstrong, R. A. 1996. Platelet prostanoid receptors. *Pharmacol Ther*. **72**: 171–91.

66. Norel, X. 2007. Prostanoid receptors in the human vascular wall. *ScientificWorldJournal*. **7**: 1359–1374.

67. Miggin, S. M., and B. T. Kinsella. 1998. Expression and tissue distribution of the mRNAs encoding the human thromboxane A2 receptor (TP) alpha and beta isoforms. *Biochim. Biophys. Acta*. **1425**: 543–559.

68. Miggin, S. M., and B. T. Kinsella. 2001. Thromboxane A(2) receptor mediated activation of the mitogen activated protein kinase cascades in human uterine smooth muscle cells. *Biochim. Biophys. Acta*. **1539**: 147–162.

69. Habib, A., R. Vezza, C. Creminon, J. Maclouf, and G. A. FitzGerald. 1997. Rapid, agonist-dependent phosphorylation in vivo of human thromboxane receptor

isoforms. Minimal involvement of protein kinase C. *J Biol Chem*. **272**: 7191–200.

70. Wilson, S. J., C. C. Cavanagh, A. M. Lesher, A. J. Frey, S. E. Russell, and E. M. Smyth. 2009. Activation-dependent stabilization of the human thromboxane receptor: role of reactive oxygen species. *J Lipid Res*. **50**: 1047–56.

71. Kelley, L. P., and B. T. Kinsella. 2003. The role of N-linked glycosylation in determining the surface expression, G protein interaction and effector coupling of the alpha (alpha) isoform of the human thromboxane A(2) receptor. *Biochim Biophys Acta*. **1621**: 192–203.

72. Hirata, M., Y. Hayashi, F. Ushikubi, Y. Yokota, R. Kageyama, S. Nakanishi, and S. Narumiya. 1991. Cloning and expression of cDNA for a human thromboxane A2 receptor. *Nature*. **349**: 617–20.

73. Zhang, L., C. DiLizio, D. Kim, E. M. Smyth, and D. R. Manning. 2006. The G12 family of G proteins as a reporter of thromboxane A2 receptor activity. *Mol Pharmacol*. **69**: 1433–40.

74. Moers, A., N. Wettschureck, S. Gruner, B. Nieswandt, and S. Offermanns. 2004. Unresponsiveness of platelets lacking both Galpha(q) and Galpha(13). Implications for collagen-induced platelet activation. *J Biol Chem*. **279**: 45354–9.

75. Shenker, A., P. Goldsmith, C. G. Unson, and A. M. Spiegel. 1991. The G protein coupled to the thromboxane A2 receptor in human platelets is a member of the novel Gq family. *J. Biol. Chem.* **266**: 9309–9313.

76. Berridge, M. J., and R. F. Irvine. 1984. Inositol trisphosphate, a novel second messenger in cellular signal transduction. *Nature*. **312**: 315–321.

77. Nishizuka, Y. 1984. Turnover of inositol phospholipids and signal transduction. *Science*. **225**: 1365–1370.

78. Houslay, M. D., D. Bojanic, and A. Wilson. 1986. Platelet activating factor and U44069 stimulate a GTPase activity in human platelets which is distinct from the guanine nucleotide regulatory proteins, Ns and Ni. *Biochem. J.* **234**: 737–740.

79. Kozasa, T., X. Jiang, M. J. Hart, P. M. Sternweis, W. D. Singer, A. G. Gilman, G. Bollag, and P. C. Sternweis. 1998. p115 RhoGEF, a GTPase activating protein for Galpha12 and Galpha13. *Science*. **280**: 2109–2111.

80. Offermanns, S. 2006. Activation of platelet function through G protein-coupled receptors. *Circ Res*. **99**: 1293–304.

81. Ohkubo, S., N. Nakahata, and Y. Ohizumi. 1996. Thromboxane A2-mediated shape change: independent of Gq-phospholipase C--Ca2+ pathway in rabbit platelets. *Br. J. Pharmacol.* **117**: 1095–1104.

82. Maier, U., A. Babich, N. Macrez, D. Leopoldt, P. Gierschik, D. Illenberger, and B. Nurnberg. 2000. Gbeta 5gamma 2 is a highly selective activator of phospholipid-dependent enzymes. *J. Biol. Chem.* **275**: 13746–13754.

83. Murray, R., E. Shipp, and G. A. FitzGerald. 1990. Prostaglandin endoperoxide/thromboxane A2 receptor desensitization. Cross-talk with adenylate cyclase in human platelets. *J. Biol. Chem.* **265**: 21670–21675.

84. Dorn, G. W., 2nd. 1992. Regulation of response to thromboxane A2 in CHRF-288 megakaryocytic cells. *Am. J. Physiol.* **262**: C991–999.

85. Sakai, K., N. Nakahata, H. Ono, T. Yamamoto, and Y. Ohizumi. 1996. Homologous desensitization of thromboxane A2 receptor in 1321N1 human astrocytoma cells. *J. Pharmacol. Exp. Ther.* **276**: 829–836.

86. Walsh, M. T., J. F. Foley, and B. T. Kinsella. 2000. The alpha, but not the beta, isoform of the human thromboxane A2 receptor is a target for prostacyclin-mediated desensitization. *J. Biol. Chem.* **275**: 20412–20423.

87. Kelley-Hickie, L. P., and B. T. Kinsella. 2006. Homologous desensitization of signalling by the beta (beta) isoform of the human thromboxane A2 receptor. *Biochim. Biophys. Acta*. **1761**: 1114–1131.

88. Parent, J. L., P. Labrecque, M. J. Orsini, and J. L. Benovic. 1999. Internalization of the TXA2 receptor alpha and beta isoforms. Role of the differentially spliced cooh terminus in agonist-promoted receptor internalization. *J. Biol. Chem.* **274**: 8941–8948.

89. Ahn, S., C. D. Nelson, T. R. Garrison, W. E. Miller, and R. J. Lefkowitz. 2003. Desensitization, internalization, and signaling functions of beta-arrestins demonstrated by RNA interference. *Proc. Natl. Acad. Sci. U. S. A.* **100**: 1740–1744.

90. Sasaki, M., J. Sukegawa, K. Miyosawa, T. Yanagisawa, S. Ohkubo, and N. Nakahata. 2007. Low expression of cell-surface thromboxane A2 receptor beta-isoform through the negative regulation of its membrane traffic by proteasomes. *Prostaglandins Other Lipid Mediat.* **83**: 237–249.

91. Rochdi, M. D., G. Laroche, E. Dupré, P. Giguère, A. Lebel, V. Watier, E. Hamelin, M.-C. Lépine, G. Dupuis, and J.-L. Parent. 2004. Nm23-H2 interacts with a G protein-coupled receptor to regulate its endocytosis through an Rac1-dependent mechanism. *J. Biol. Chem.* **279**: 18981–18989.

92. Laroche, G., M. D. Rochdi, S. A. Laporte, and J.-L. Parent. 2005. Involvement of actin in agonist-induced endocytosis of the G protein-coupled receptor for thromboxane A2: overcoming of actin disruption by arrestin-3 but not arrestin-2. *J. Biol. Chem.* **280**: 23215–23224.

93. Thériault, C., M. D. Rochdi, and J.-L. Parent. 2004. Role of the Rab11-associated intracellular pool of receptors formed by constitutive endocytosis of the beta isoform of the thromboxane A2 receptor (TP beta). *Biochemistry (Mosc.)*. **43**: 5600–5607.

94. Wilson, S. J., J. K. Dowling, L. Zhao, E. Carnish, and E. M. Smyth. 2007. Regulation of thromboxane receptor trafficking through the prostacyclin receptor in vascular smooth muscle cells: role of receptor heterodimerization. *Arter. Thromb Vasc Biol*. **27**: 290–6.

95. Chiang, N., and H. H. Tai. 1998. The role of N-glycosylation of human thromboxane A2 receptor in ligand binding. *Arch. Biochem. Biophys.* **352**: 207–213.

96. Walsh, M. T., J. F. Foley, and B. T. Kinsella. 1998. Characterization of the role of N-linked glycosylation on the cell signaling and expression of the human thromboxane A2 receptor alpha and beta isoforms. *J. Pharmacol. Exp. Ther.* **286**: 1026–1036.

97. Grosser, T., S. Fries, and G. A. FitzGerald. 2006. Biological basis for the cardiovascular consequences of COX-2 inhibition: therapeutic challenges and opportunities. *J Clin Invest*. **116**: 4–15.

98. Smyth, E. M. and F. 2003. *In* Handbook of Cell Signaling (Bradshaw, R. D., ed.). pp. 265–273. , E. Academic Press, San Diego, CA.

99. Yu, Y., Y. Cheng, J. Fan, X. S. Chen, A. Klein-Szanto, G. A. Fitzgerald, and C. D. Funk. 2005. Differential impact of prostaglandin H synthase 1 knockdown on platelets and parturition. *J Clin Invest*. **115**: 986–95.

100. Bulenger, S., S. Marullo, and M. Bouvier. 2005. Emerging role of homo- and heterodimerization in G-protein-coupled receptor biosynthesis and maturation. *Trends Pharmacol Sci*. **26**: 131–7.

101. Filizola, M. 2009. Increasingly accurate dynamic molecular models of G-protein coupled receptor oligomers: Panacea or Pandora's box for novel drug discovery? *Life Sci*. [online] http://www.ncbi.nlm.nih.gov/entrez/query.fcgi?cmd=Retrieve&db=PubMed&dopt=Citation&list_uids=19465029.

102. Baneres, J. L., and J. Parello. 2003. Structure-based analysis of GPCR function: evidence for a novel pentameric assembly between the dimeric leukotriene B4 receptor BLT1 and the G-protein. *J Mol Biol*. **329**: 815–29.

103. Lee, S. P., B. F. O'Dowd, R. D. Rajaram, T. Nguyen, and S. R. George. 2003. D2 dopamine receptor homodimerization is mediated by multiple sites of interaction, including an intermolecular interaction involving transmembrane domain 4. *Biochemistry (Mosc.)*. **42**: 11023–31.

104. Overton, M. C., S. L. Chinault, and K. J. Blumer. 2003. Oligomerization, biogenesis, and signaling is promoted by a glycophorin A-like dimerization motif in transmembrane domain 1 of a yeast G protein-coupled receptor. *J Biol Chem*. **278**: 49369–77.

105. AbdAlla, S., H. Lother, A. M. Abdel-tawab, and U. Quitterer. 2001. The angiotensin II AT2 receptor is an AT1 receptor antagonist. *J Biol Chem*. **276**: 39721–6.

106. Maurel, D., L. Comps-Agrar, C. Brock, M. L. Rives, E. Bourrier, M. A. Ayoub, H. Bazin, N. Tinel, T. Durroux, L. Prezeau, E. Trinquet, and J. P. Pin. 2008. Cell-surface protein-protein interaction analysis with time-resolved FRET and snap-tag technologies: application to GPCR oligomerization. *Nat Methods*. **5**: 561–7.

107. Agnati, L. F., S. Ferre, C. Lluis, R. Franco, and K. Fuxe. 2003. Molecular mechanisms and therapeutical implications of intramembrane receptor/receptor interactions among heptahelical receptors with examples from the striatopallidal GABA neurons. *Pharmacol Rev*. **55**: 509–50.

108. Han, Y., I. S. Moreira, E. Urizar, H. Weinstein, and J. A. Javitch. 2009. Allosteric communication between protomers of dopamine class A GPCR dimers modulates activation. *Nat Chem Biol*. **5**: 688–95.

109. Gomes, I., B. A. Jordan, A. Gupta, C. Rios, N. Trapaidze, and L. A. Devi. 2001. G protein coupled receptor dimerization: implications in modulating receptor function. *J Mol Med Berl*. **79**: 226–42.

110. Breit, A., M. Lagacé, and M. Bouvier. 2004. Hetero-oligomerization between beta2- and beta3-adrenergic receptors generates a beta-adrenergic signaling unit with distinct functional properties. *J. Biol. Chem.* **279**: 28756–28765.

111. Kroeger, K. M., K. D. G. Pfleger, and K. A. Eidne. 2003. G-protein coupled receptor oligomerization in neuroendocrine pathways. *Front. Neuroendocrinol.* **24**: 254–278.

112. Terrillon, S., T. Durroux, B. Mouillac, A. Breit, M. A. Ayoub, M. Taulan, R. Jockers, C. Barberis, and M. Bouvier. 2003. Oxytocin and vasopressin V1a and V2 receptors form constitutive homo- and heterodimers during biosynthesis. *Mol Endocrinol*. **17**: 677–91.

113. Issafras, H., S. Angers, S. Bulenger, C. Blanpain, M. Parmentier, C. Labbe-Jullie, M. Bouvier, and S. Marullo. 2002. Constitutive agonist-independent CCR5 oligomerization and antibody-mediated clustering occurring at physiological levels of receptors. *J Biol Chem*. **277**: 34666–73.

114. Hague, C., M. A. Uberti, Z. Chen, R. A. Hall, and K. P. Minneman. 2004. Cell surface expression of alpha1D-adrenergic receptors is controlled by heterodimerization with alpha1B-adrenergic receptors. *J Biol Chem*. **279**: 15541–9.

115. Salahpour, A., S. Angers, J. F. Mercier, M. Lagace, S. Marullo, and M. Bouvier. 2004. Homodimerization of the beta2-adrenergic receptor as a prerequisite for cell surface targeting. *J Biol Chem*. **279**: 33390–7.

116. Benkirane, M., D. Y. Jin, R. F. Chun, R. A. Koup, and K. T. Jeang. 1997. Mechanism of transdominant inhibition of CCR5-mediated HIV-1 infection by ccr5delta32. *J Biol Chem*. **272**: 30603–6.

117. Kaykas, A., J. Yang-Snyder, M. Heroux, K. V. Shah, M. Bouvier, and R. T. Moon. 2004. Mutant Frizzled 4 associated with vitreoretinopathy traps wild-type Frizzled in the endoplasmic reticulum by oligomerization. *Nat Cell Biol*. **6**: 52–8.

118. Devi, L. A. 2001. Heterodimerization of G-protein-coupled receptors: pharmacology, signaling and trafficking. *Trends Pharmacol Sci*. **22**: 532–7.

119. Breitwieser, G. E. 2004. G protein-coupled receptor oligomerization: implications for G protein activation and cell signaling. *Circ Res*. **94**: 17–27.

120. Panetta, R., and M. T. Greenwood. 2008. Physiological relevance of GPCR oligomerization and its impact on drug discovery. *Drug Discov Today*. **13**: 1059–66.

121. Ibrahim, S., A. McCartney, N. Markosyan, and E. M. Smyth. 2013. Heterodimerization with the prostacyclin receptor triggers thromboxane receptor relocation to lipid rafts. *Arter. Thromb Vasc Biol*. **33**: 60–6.

122. Wilson, S. J., K. McGinley, A. J. Huang, and E. M. Smyth. 2007. Heterodimerization of the alpha and beta isoforms of the human thromboxane receptor enhances isoprostane signaling. *Biochem Biophys Res Commun*. **352**: 397–403.

123. Wilson, S. J., A. M. Roche, E. Kostetskaia, and E. M. Smyth. 2004. Dimerization of the human receptors for prostacyclin and thromboxane facilitates thromboxane receptor-mediated cAMP generation. *J Biol Chem*. **279**: 53036–47.

124. Yu, Y., J. Stubbe, S. Ibrahim, W. L. Song, E. M. Smyth, C. D. Funk, and G. A. FitzGerald. 2010. Cyclooxygenase-2-dependent prostacyclin formation and blood pressure homeostasis: targeted exchange of cyclooxygenase isoforms in mice. *Circ Res*. **106**: 337–45.

125. Ibrahim, S., M. Tetruashvily, A. J. Frey, S. J. Wilson, J. Stitham, J. Hwa, and E. M. Smyth. 2010. Dominant negative actions of human prostacyclin receptor variant through dimerization: implications for cardiovascular disease. *Arter. Thromb Vasc Biol*. **30**: 1802–9.

126. Fink, A., N. Sal-Man, D. Gerber, and Y. Shai. 2012. Transmembrane domains interactions within the membrane milieu: Principles, advances and challenges. *Biochim Biophys Acta*. **1818**: 974–83.

127. Senes, A., D. E. Engel, and W. F. DeGrado. 2004. Folding of helical membrane proteins: the role of polar, GxxxG-like and proline motifs. *Curr Opin Struct Biol*. **14**: 465–79.

128. Caputo, G. A., R. I. Litvinov, W. Li, J. S. Bennett, W. F. Degrado, and H. Yin. 2008. Computationally designed peptide inhibitors of protein-protein interactions in membranes. *Biochemistry (Mosc.)*. **47**: 8600–6.

129. Blazer, L. L., and R. R. Neubig. 2009. Small molecule protein-protein interaction inhibitors as CNS therapeutic agents: current progress and future hurdles. *Neuropsychopharmacology*. **34**: 126–41.

130. Hebert, T. E., S. Moffett, J. P. Morello, T. P. Loisel, D. G. Bichet, C. Barret, and M. Bouvier. 1996. A peptide derived from a beta2-adrenergic receptor transmembrane domain inhibits both receptor dimerization and activation. *J Biol Chem*. **271**: 16384–92.

131. Kaczor, A. A., and J. Selent. 2011. Oligomerization of G protein-coupled receptors: biochemical and biophysical methods. *Curr. Med. Chem.* **18**: 4606–4634.

132. Taddese, B., L. M. Simpson, I. D. Wall, F. E. Blaney, and C. A. Reynolds. 2013. Modeling active GPCR conformations. *Methods Enzymol.* **522**: 21–35.

133. Taddese, B., L. M. Simpson, I. D. Wall, F. E. Blaney, N. J. Kidley, H. S. X. Clark, R. E. Smith, G. J. G. Upton, P. R. Gouldson, G. Psaroudakis, R. P. Bywater, and C. A. Reynolds. 2012. G-protein-coupled receptor dynamics: dimerization and activation models compared with experiment. *Biochem. Soc. Trans.* **40**: 394–399.

134. Latek, D., A. Modzelewska, B. Trzaskowski, K. Palczewski, and S. Filipek. 2012. G protein-coupled receptors--recent advances. *Acta Biochim. Pol.* **59**: 515–529.

135. Senes, A., M. Gerstein, and D. M. Engelman. 2000. Statistical analysis of amino acid patterns in transmembrane helices: the GxxxG motif occurs frequently and in association with beta-branched residues at neighboring positions. *J Mol Biol*. **296**: 921–36.

136. Kim, S., T. J. Jeon, A. Oberai, D. Yang, J. J. Schmidt, and J. U. Bowie. 2005. Transmembrane glycine zippers: physiological and pathological roles in membrane proteins. *Proc Natl Acad Sci U S*. **102**: 14278–83.

137. Arselin, G., M. F. Giraud, A. Dautant, J. Vaillier, D. Brethes, B. Coulary-Salin, J. Schaeffer, and J. Velours. 2003. The GxxxG motif of the transmembrane domain of subunit e is involved in the dimerization/oligomerization of the yeast ATP synthase complex in the mitochondrial membrane. *Eur J Biochem*. **270**: 1875–84.

138. Moore, D. T., B. W. Berger, and W. F. DeGrado. 2008. Protein-protein interactions in the membrane: sequence, structural, and biological motifs. *Structure*. **16**: 991–1001.

139. Lemmon, M. A., J. M. Flanagan, J. F. Hunt, B. D. Adair, B. J. Bormann, C. E. Dempsey, and D. M. Engelman. 1992. Glycophorin A dimerization is driven by specific interactions between transmembrane alpha-helices. *J Biol Chem*. **267**: 7683–9.

140. Lemmon, M. A., H. R. Treutlein, P. D. Adams, A. T. Brunger, and D. M. Engelman. 1994. A dimerization motif for transmembrane alpha-helices. *Nat Struct Biol*. **1**: 157–63.

141. George, S. R., S. P. Lee, G. Varghese, P. R. Zeman, P. Seeman, G. Y. Ng, and B. F. O'Dowd. 1998. A transmembrane domain-derived peptide inhibits D1 dopamine receptor function without affecting receptor oligomerization. *J Biol Chem*. **273**: 30244–8.

142. Berger, B. W., D. W. Kulp, L. M. Span, J. L. DeGrado, P. C. Billings, A. Senes, J. S. Bennett, and W. F. DeGrado. 2010. Consensus motif for integrin transmembrane helix association. *Proc Natl Acad Sci U S*. **107**: 703–8.

143. Grosser, T., S. Fries, J. A. Lawson, S. C. Kapoor, G. R. Grant, and G. A. FitzGerald. 2013. Drug resistance and pseudoresistance: an unintended consequence of enteric coating aspirin. *Circulation*. **127**: 377–385.

144. Poredos, P., and M. K. Jezovnik. 2013. Is aspirin still the drug of choice for management of patients with peripheral arterial disease? *VASA Z. Für Gefässkrankheiten*. **42**: 88–95.

145. Tang, W. H., J. Stitham, S. Gleim, C. Di Febbo, E. Porreca, C. Fava, S. Tacconelli, M. Capone, V. Evangelista, G. Levantesi, L. Wen, K. Martin, P. Minuz, J. Rade, P. Patrignani, and J. Hwa. 2011. Glucose and collagen regulate human platelet activity through aldose reductase induction of thromboxane. *J. Clin. Invest.* **121**: 4462–4476.

146. Hennekens, C. H., and J. E. Dalen. 2013. Aspirin in the treatment and prevention of cardiovascular disease: past and current perspectives and future directions. *Am. J. Med.* **126**: 373–378.

147. Bousser, M. G., P. Amarenco, A. Chamorro, M. Fisher, I. Ford, K. M. Fox, M. G. Hennerici, H. P. Mattle, P. M. Rothwell, A. de Cordoue, and M. D. Fratacci. 2011. Terutroban versus aspirin in patients with cerebral ischaemic events (PERFORM): a randomised, double-blind, parallel-group trial. *Lancet*. **377**: 2013–22.

148. Rosenfeld, L., G. J. Grover, and C. T. Stier Jr. 2001. Ifetroban sodium: an effective TxA2/PGH2 receptor antagonist. *Cardiovasc. Drug Rev.* **19**: 97–115.

149. Fukuoka, T., S. Miyake, T. Umino, N. Inase, N. Tojo, and Y. Yoshizawa. 2003. The effect of seratrodast on eosinophil cationic protein and symptoms in asthmatics. *J. Asthma Off. J. Assoc. Care Asthma*. **40**: 257–264.

150. Lonsdale, R. J., S. Heptinstall, J. C. Westby, D. C. Berridge, P. W. Wenham, B. R. Hopkinson, and G. S. Makin. 1993. A study of the use of the thromboxane A2 antagonist, sulotroban, in combination with streptokinase for local thrombolysis in patients with recent peripheral arterial occlusions: clinical effects, platelet function and fibrinolytic parameters. *Thromb. Haemost.* **69**: 103–111, 123.

151. Li, X., G. Zhou, X. Zhou, and S. Zhou. 2013. The efficacy and safety of aspirin plus dipyridamole versus aspirin in secondary prevention following TIA or stroke: A meta-analysis of randomized controlled trials. *J. Neurol. Sci.*

152. Celestini, A., and F. Violi. 2007. A review of picotamide in the reduction of cardiovascular events in diabetic patients. *Vasc. Heal. Risk Manag.* **3**: 93–98.

153. Tytgat, G. N. J., L. Van Nueten, I. Van De Velde, A. Joslyn, and S. B. Hanauer. 2002. Efficacy and safety of oral ridogrel in the treatment of ulcerative colitis: two multicentre, randomized, double-blind studies. *Aliment. Pharmacol. Ther.* **16**: 87–99.

154. Carty, E., D. S. Rampton, H. Schneider, P. Rutgeerts, and J. P. Wright. 2001. Lack of efficacy of ridogrel, a thromboxane synthase inhibitor, in a placebo-controlled, double-blind, multi-centre clinical trial in active Crohn's disease. *Aliment. Pharmacol. Ther.* **15**: 1323–1329.

155. Hirenallur-S, D. K., N. D. Detweiler, S. T. Haworth, J. T. Leming, J. B. Gordon, and N. J. Rusch. 2012. Furegrelate, a thromboxane synthase inhibitor, blunts the development of pulmonary arterial hypertension in neonatal piglets. *Pulm. Circ.* **2**: 193–200.

156. Zhang, J., J. Yang, X. Chang, C. Zhang, H. Zhou, and M. Liu. 2012. Ozagrel for acute ischemic stroke: a meta-analysis of data from randomized controlled trials. *Neurol. Res.* **34**: 346–353.

157. Smyth, E. M., S. C. Austin, M. P. Reilly, and G. A. FitzGerald. 2000. Internalization and sequestration of the human prostacyclin receptor. *J Biol Chem*. **275**: 32037–45.

158. Gould, S., and R. C. Scott. 2005. 2-Hydroxypropyl-beta-cyclodextrin (HP-beta-CD): a toxicology review. *Food Chem. Toxicol. Int. J. Publ. Br. Ind. Biol. Res. Assoc.* **43**: 1451–1459.

159. Biotinylated Gaussia Luciferase. [online] www.interchim.fr/ft/B/BS8190.pdf (Accessed July 9, 2013).

160. Livak, K. J., and T. D. Schmittgen. 2001. Analysis of relative gene expression data using real-time quantitative PCR and the 2(-Delta Delta C(T)) Method. *Methods San Diego Calif*. **25**: 402–408.

161. Mount, D. W. 2008. Comparison of the PAM and BLOSUM Amino Acid Substitution Matrices. *CSH Protoc.* **2008**: pdb.ip59.

162. Teller, D. C., T. Okada, C. A. Behnke, K. Palczewski, and R. E. Stenkamp. 2001. Advances in determination of a high-resolution three-dimensional structure of rhodopsin, a model of G-protein-coupled receptors (GPCRs). *Biochemistry (Mosc.)*. **40**: 7761–72.

163. Phillips, J. C., R. Braun, W. Wang, J. Gumbart, E. Tajkhorshid, E. Villa, C. Chipot, R. D. Skeel, L. Kalé, and K. Schulten. 2005. Scalable molecular dynamics with NAMD. *J. Comput. Chem.* **26**: 1781–1802.

164. Bai, M. 2004. Dimerization of G-protein-coupled receptors: roles in signal transduction. *Cell. Signal.* **16**: 175–186.

165. AbdAlla, S., H. Lother, A. el Missiry, P. Sergeev, A. Langer, Y. el Faramawy, and U. Quitterer. 2009. Dominant negative AT2 receptor oligomers induce G-protein arrest and symptoms of neurodegeneration. *J Biol Chem*. **284**: 6566–74.

166. MEG-01 ATCC ® CRL-2021™ Homo sapiens bone marrow chronic mye. [online] http://www.atcc.org/products/all/CRL-2021.aspx (Accessed August 1, 2013).

167. Maudsley, S., B. Martin, and L. M. Luttrell. 2005. The origins of diversity and specificity in g protein-coupled receptor signaling. *J. Pharmacol. Exp. Ther.* **314**: 485–494.

168. Maudsley, S., S. A. Patel, S.-S. Park, L. M. Luttrell, and B. Martin. 2012. Functional signaling biases in G protein-coupled receptors: Game Theory and receptor dynamics. *Mini Rev. Med. Chem.* **12**: 831–840.

169. James, J. R., M. I. Oliveira, A. M. Carmo, A. Iaboni, and S. J. Davis. 2006. A rigorous experimental framework for detecting protein oligomerization using bioluminescence resonance energy transfer. *Nat Methods*. **3**: 1001–6.

170. Fanelli, F., M. Mauri, V. Capra, F. Raimondi, F. Guzzi, M. Ambrosio, G. Enrico Rovati, and M. Parenti. 2011. Light on the structure of thromboxane A(2) receptor heterodimers. *Cell Mol Life Sci*. [online] http://www.ncbi.nlm.nih.gov/entrez/query.fcgi?cmd=Retrieve&db=PubMed&dopt=Citation&list_uids=21213014.

171. Canals, M., J. F. Lopez-Gimenez, and G. Milligan. 2009. Cell surface delivery and structural re-organization by pharmacological chaperones of an oligomerization-defective alpha(1b)-adrenoceptor mutant demonstrates membrane targeting of GPCR oligomers. *Biochem J*. **417**: 161–72.

172. Jordan, B. A., N. Trapaidze, I. Gomes, R. Nivarthi, and L. A. Devi. 2001. Oligomerization of opioid receptors with beta 2-adrenergic receptors: a role in trafficking and mitogen-activated protein kinase activation. *Proc Natl Acad Sci U S*. **98**: 343–8.

173. Pellissier, L. P., G. Barthet, F. Gaven, E. Cassier, E. Trinquet, J. P. Pin, P. Marin, A. Dumuis, J. Bockaert, J. L. Baneres, and S. Claeysen. 2011. G protein activation by serotonin type 4 receptor dimers: evidence that turning on two protomers is more efficient. *J Biol Chem*. **286**: 9985–97.

174. Dror, R. O., A. C. Pan, D. H. Arlow, D. W. Borhani, P. Maragakis, Y. Shan, H. Xu, and D. E. Shaw. 2011. Pathway and mechanism of drug binding to G-protein-coupled receptors. *Proc. Natl. Acad. Sci. U. S. A.* **108**: 13118–13123.

175. Pin, J.-P., T. Galvez, and L. Prézeau. 2003. Evolution, structure, and activation mechanism of family 3/C G-protein-coupled receptors. *Pharmacol. Ther.* **98**: 325–354.

176. Brock, C., N. Oueslati, S. Soler, L. Boudier, P. Rondard, and J.-P. Pin. 2007. Activation of a dimeric metabotropic glutamate receptor by intersubunit rearrangement. *J. Biol. Chem.* **282**: 33000–33008.

177. Bécu, J.-M., J. Pelé, P. Rodien, H. Abdi, and M. Chabbert. 2013. Structural evolution of G-protein-coupled receptors: a sequence space approach. *Methods Enzymol.* **520**: 49–66.

178. Lebon, G., T. Warne, and C. G. Tate. 2012. Agonist-bound structures of G protein-coupled receptors. *Curr. Opin. Struct. Biol.* **22**: 482–490.

179. Fink, A. K., R. R. German, M. Heron, S. L. Stewart, C. J. Johnson, J. L. Finch, D. Yin, and P. E. Schaeffer. 2012. Impact of using multiple causes of death codes to compute site-specific, death certificate-based cancer mortality statistics in the United States. *Cancer Epidemiol*. **36**: 22–8.

180. Overton, M. C., and K. J. Blumer. 2002. The extracellular N-terminal domain and transmembrane domains 1 and 2 mediate oligomerization of a yeast G protein-coupled receptor. *J Biol Chem*. **277**: 41463–72.

181. Devi, L. A., and L. S. Brady. 2000. Dimerization of G-protein coupled receptors. *Neuropsychopharmacol. Off. Publ. Am. Coll. Neuropsychopharmacol.* **23**: S3–4.

182. Gouldson, P. R., C. Higgs, R. E. Smith, M. K. Dean, G. V. Gkoutos, and C. A. Reynolds. 2000. Dimerization and domain swapping in G-protein-coupled receptors: a computational study. *Neuropsychopharmacol. Off. Publ. Am. Coll. Neuropsychopharmacol.* **23**: S60–77.

183. Tallman, J. 2000. Dimerization of G-protein-coupled receptors: implications for drug design and signaling. *Neuropsychopharmacol. Off. Publ. Am. Coll. Neuropsychopharmacol.* **23**: S1–2.

184. Gleim, S., J. Stitham, W. H. Tang, H. Li, K. Douville, P. Chelikani, J. J Rade, K. A. Martin, and J. Hwa. 2013. Human thromboxane A2 receptor genetic variants: in silico, in vitro and “in platelet” analysis. *PloS One*. **8**: e67314.